공학박사 학위논문

# Development of a Multi-Level Approach for the Evaluation of Parametric Roll and its Application to Modern Commercial Ships

## 파라메트릭 롤 평가를 위한 단계별 해석기법 개발 및 실선 적용

2013년 2월

서울대학교 대학원

공과대학 조선해양공학과

송 강 현

# Development of a Multi-Level Approach for the Evaluation of Parametric Roll and its Application to Modern Commercial Ships

지도 교수 김 용 환

이 논문을 공학박사 학위논문으로 제출함
2013년 2월

서울대학교 대학원
공과대학 조선해양공학과
송 강 현

송강현의 박사 학위논문을 인준함
2013년 2월

위 원 장 _____ (인)

부위원장 _____ (인)

위 원 _____ (인)

위 원 _____ (인)

위 원 _____ (인)

## Abstract

# Development of a Multi-Level Approach for the Evaluation of Parametric Roll and its Application to Modern Commercial Ships

Kanghyun Song

Department of Naval Architecture and Ocean Engineering

Seoul National University

A multi-level approach for the quantitative evaluation of parametric roll is developed and its application results to modern commercial ships are presented and reviewed in this thesis.

Despite many previous studies, it is still a challenging issue to quantify the vulnerability of a ship to parametric roll occurrence on sea-going vessels. Therefore, occurrence mechanism and physical and stochastic characteristics of parametric roll are investigated in depth and this thesis presents a new numerical form for quantitatively analyzing the susceptibility of a ship to parametric roll in random sea ways based on the study. Due to the non-ergodic characteristics of parametric roll motion, numerous direct time-domain simulations are needed to obtain a stable long-term distribution of parametric rolls. To avoid such heavy computational demand and to accelerate numerical

simulations, a 1.5-DOF computational model for parametric roll prediction is developed for both regular- and irregular-wave excitations, adopting the approximated GZ curve. In this model, the concept of transfer functions is introduced for the mean and the first harmonic component of GM, which is introduced to approximate GM fluctuation. The simulation results obtained by using this model are compared to those of a three-dimensional weakly nonlinear simulation program. The sensitivities of the simulation results to the initial value, time window and number of simulations are investigated by applying Monte-Carlo simulation, and their proper values are proposed.

This thesis also introduces several numerical approaches to analyze parametric roll from simple Mathieu equation to advanced numerical tools based on IRF method and Rankine panel method. Using advantages of various approaches including 1.5-DOF GM-GZ approximation method, a multi-level approach is developed to evaluate the vulnerability of a ship to parametric roll quantitatively. It consists of $1^{st}$ level check by Mathieu equation, $2^{nd}$ level check for regular wave, $3^{rd}$ level check for irregular wave and operational guidance by IRF method. Most advanced tool based on Rankine panel method is used to verify each numerical tool.

This multi-level approach is applied to several modern commercial ships including 4 post-Panamax container ships, 3 PCTCs (Pure Car and Truck Carrier), 3 Passenger ships, VLCC and S175 based on North Atlantic wave data. Based on the simulation results, the vulnerability of each ship to

parametric roll is evaluated, and the influences of still water GM, roll damping coefficient and ship speed are reviewed and discussed. It is confirmed that each level provides consistent results and the results give very useful information of the vulnerability to parametric roll for each ship type and ship length.

As a powerful and effective countermeasure against parametric roll, operational guidance is very important to support crew's decision making in harsh environmental condition. In this thesis, the procedure for operational guidance development based on IRF method is proposed and it is applied to 8,000 TEU container ship. All the application results are provided and summarized with easy instruction to help ship crew's efficient decision making and to avoid severe parametric roll.

The contribution of this study on ship design, dynamic stability criteria are discussed and future works to reinforce the current approach and numerical scheme are proposed

**Keywords: Parametric roll, Multi-level approach, Quantitative analysis, 1.5-DOF GM-GZ approximation, 2nd Generation of dynamic stability criteria, Operational guidance**

**Student Number: 2006-30809**

# Contents

# List of Tables

# List of Figures

# Chapter 1. Introduction

## 1.1 Background

Parametric roll is a phenomenon of large unstable roll motion in head or following sea. Due to the acceleration induced by severe roll angle, ships suffer from the loss of cargos and lives, machinery failures, structural damages and even capsize. More than 100 years ago, Froude [17] observed that ships have unexpected roll when the natural frequency in pitch is twice the natural roll frequency and this phenomenon has been studied by naval architects for over than fifty years. In recent years, parametric roll has been observed in large seagoing vessels, particularly, container ships, PCTC (Pure Car and Truck Carrier) and passenger ships which have low GM and large flare angle or long transom stern. A significant casualty occurred in late October 1998 when a post-Panamax container ship of APL China encountered with a strong storm during the voyage from Kaohsiung to Seattle in the North Pacific Ocean [16]. The ship experienced a large roll motion with up to 30 ~ 35 degrees accompanied with significant heave and pitch motion in head sea. As consequences, almost 1,300 deck containers, one-third of whole cargos had been lost overboard and another one-third were damaged or destructed as shown in Figure 1.1. The total loss amounted to fifty million dollars. This kind of casualty induced by parametric roll frequently occurred since post-

Panamax container ships and large PCTCs started to be constructed and operated. These dynamic stability issues attracted IMO's attention and IMO [23-28] has launched working group for 'Development of 2nd generation Intact stability criteria in 2009 and has discussed this issue.


Figure 1.1 Casualty of post-Panamax container ship due to parametric roll

Ship operators and designers know that parametric roll phenomenon is very dangerous and should be avoided in harsh environmental conditions. However, despite the many previous studies, the question of 'How dangerous it is' has not been fully investigated, even when the quantitative analysis of this phenomenon is essential for the design of hull form, roll damping device, cargo securing system, machinery system and structural strength. The primary difficulty in quantifying parametric roll lies in the fact that this phenomenon is a highly non-ergodic process with nonlinear damping, nonlinear stiffness and nonlinear self-excitation [5, 6]. When a process is not ergodic, the temporal average obtained from one realization cannot be substituted for the ensemble average or statistical expectation. It means that each numerical computation or experimental test gives different statistical parameters such as mean and standard deviation. Therefore, enough number of realizations must be collected to get a stable probabilistic distribution. More number of realizations leads more stable results and the proper number of realizations depends on the degree of non-ergodicity and the confidence level. Considering many sea states in a wave scatter diagram, the total number of realizations for a stable long-term prediction would be enormously large. This large number means that not only the accuracy of each data but also computation speed become very important in a highly non-ergodic process. Therefore, for quantitative analysis of this phenomenon, a very fast and effective numerical tool should be developed in use of combination with some simplifications of real physics.

Parametric roll is a threshold phenomenon. If some conditions for generation of parametric roll are satisfied, it will occur. If not, it never occurs. For example, tankers or bulk carriers hardly encounter parametric roll because they have small flare angle and large GM while post-Panamax container ships and PCTCs are known to be vulnerable to parametric roll. For passenger ships, the vulnerability is not clear. Therefore, systematic procedure is necessary to evaluate the vulnerability to parametric roll [1]. The procedure should include simple way to disregard ships which not vulnerable definitely to complex way to identify the vulnerability precisely. The best way to evaluate the vulnerability of parametric roll is to carry out direct ship motion analysis using state-of-art numerical tools. However, it is too time consuming and the computation is very expensive. It is not necessary to carry out direct motion analysis for tankers or bulk carriers because we know already they are not vulnerable to this phenomenon. Therefore, multi-level approach to evaluate the vulnerability of parametric roll is necessary in the view of practical sense. At first, simple check to confirm the vulnerability to parametric roll is necessary. If a ship doesn't pass the first simple check, the ship is regarded as unconventional type and the ship may be or may not be vulnerable to parametric roll the accuracy of $1^{st}$ level check is not enough. The role of $1^{st}$ check is to disregard ships which are not vulnerable to parametric roll definitely. Then, second check is to be performed to confirm the vulnerability, before requiring the direct stability assessment. It means that the purpose of

second check or intermediate assessment is to provide justification for application of the direct stability assessment, if necessary. If a ship is found to be vulnerable by the second check, direct stability assessment with performance-based criteria will be applied. If a ship doesn't satisfy direct stability criteria ($3^{rd}$ level check) the vulnerability should be reduced by revision of ship design, installation of roll damping devices or provision of operational guidance.

Parametric roll may be avoided by the ship design change fundamentally or ship operation. However, ship design change such as increase of GM, decrease of flare angle or installing a roll damping devices is not preferable to ship owner or ship builder because it needs reduction of cargo capacity on deck or more building expense. For the economical and practical reasons, the operational guidance can be a best countermeasure. By choosing a proper course and speed under given loading condition and environmental condition, the crew can avoid severe roll response with the help of operational guidance. According to conventional operation customs, the crew is expected to keep the course in head sea in harsh environmental condition. However, this custom may lead very dangerous situation for ships which are vulnerable to parametric roll because parametric roll is maximized in longitudinal sea. Therefore, development of operational guidance is essential for the safety of a ship against parametric roll.

To improve the safety of ships against parametric roll, it is very challenging issues to develop numerical tolls for quantitative analysis, multi-level evaluation procedure and operational guidance.

## 1.2 State of the arts

A 1-DOF model for a regular wave has been traditionally used to investigate influencing parameters of parametric roll and Pauling [37] and Shin et al [40] showed that the stability region can be analyzed by adopting the Mathieu equation in this model. This model is very useful to check parametric resonance. However, this model is not proper for quantitative analysis because it cannot account for the nonlinear restoring moment coupled with heave and pitch.

Parametric roll is mainly caused by a variation of roll righting moment induced by roll, heave and pitch. Therefore, a 3-DOF nonlinear roll model was tried by Neves [34, 35] and Holden [18]. This model is much simpler than a 6-DOF model but it still requires a considerable amount of computation to analyze excitation forces and to solve a coupled motion.

Oh et al [36] tried 1-DOF model with a coupled term of heave and pitch, which are assumed as harmonic functions, and a righting moment approximated by a third-order polynomial function. Bulian [11] proposed a 1.5-DOF numerical model for a regular wave. In this quasi-static method, the

half DOF accounts for the coupling of heave and pitch. He approximated GZ curves with respect to wave height and crest position by fitting to polynomial functions and Fourier series for a regular wave. He also proposed the use of Grim's effective wave to find the GZ curve for irregular waves. It is very effective to use Grim's effective wave concept for an irregular wave, although the use of this concept yields very conservative results [45]. Dunwoody [13, 14] proved mathematically that the difference between a time-varying meta-centric height and a calm water meta-centric height is linear to the wave height and showed that the spectrum of GM for parametric roll could be used for parametric roll analysis analytically.

All these approaches have pros and cons, so it is still needed to find a very effective numerical model which can give enough number of numerical realizations by the Monte Carlo simulation to overcome the non-ergodicity of the parametric roll phenomenon in practically reasonable time [6, 45]. In this context, it is essential to develop a very fast numerical model which can be used for a stable long-term prediction of parametric roll.

The number of DOF and the GZ approximation method are the most critical for the reduction in computation time. Considering that the influence of roll on heave and pitch is not significant, a fully coupled heave-roll-pitch equation does not need to be solved if 1-DOF roll motion with the heave and pitch effect is considered [11, 36].

The restoring moment can be directly obtained by integration of the external pressure acting on wetted surface [47], but it is to be excluded when a huge number of numerical realizations need to be carried out. A GZ curve fitted by a fifth-order non-linear function of roll [28, 46] can be a good alternative to replace direct pressure integration but the curve's shape of the current post-Panamax container ship has several curvatures so that it is difficult to fit this kind of curve with a polynomial function. To solve this problem, several GZ curves for regular waves are calculated for a typical post-Panamax container ship in this thesis. Based on the observation of these results, the fluctuation of the curves for the wave is approximated by the combination of the still water GZ curve and meta-centric height fluctuations. The spectrum of GM is calculated considering heave, pitch and wave elevation and it is used to obtain the fluctuation for irregular waves. Based on this concept, a 1-DOF computational model for parametric roll prediction is developed with the spectrum of meta-centric height including the heave and pitch coupling term and the GZ curves approximated by the still water curve. The computation speed is fast enough to overcome non-ergodicity of parametric roll.

If a ship design does not meet the standard of parametric roll corresponding to a certain safety level or vulnerability criteria, the ship should avoid a severe parametric roll during operation by proper operational guidance. Guidance should be developed using state-of-the-art tools as much as possible to support ship crew's proper decision making in an urgent situation [26].

However, a large number of realizations for each sea state do not need to be carried out by the state-of-the-art tools. Moreover, the purpose of operational guidance is not to give exact roll angles but to indicate the degree of danger qualitatively. Therefore, qualitative operational guidance should be developed.

In the computational approach, many of the time-domain simulation codes for nonlinear motion analysis are applicable for parametric roll prediction. The three-dimensional panel method, widely used for direct nonlinear ship motion calculation, is still time-consuming. The impulse-response-function (IRF) approach formulated by Cummins [12] can be a good candidate for the compromise between accuracy and efficiency of a numerical computation. This approach solves the equation of ship motion by using pre-computed hydrodynamic coefficients. Considering the nonlinear restoring force on an instantaneous wetted surface in the IRF method, Spanos [41] and Kim et al [32] applied this method in the parametric roll analysis of a fishing vessel.

There are many numerical tools to analyze parametric roll. ABS (American Bureau of Shipping) developed guidance for the assessment of parametric roll resonance in the design of container ships in 2004 [1]. It consists of susceptibility check, severity check and numerical simulations and operational guidance. However, it considers just one design wave and doesn’t provide quantitative evaluation step to overcome non-ergodicity. Hong [19] pointed out that the design wave of which length is equal to ship length doesn’t give

always worst scenario and proposed an improved susceptibility check formula to consider hydrostatic balance.

## 1.3 Objective and work of scope

The main targets of this thesis are as follows

- Development of new numerical tool for quantitative analysis
- Development of multi-level approach for evaluation of vulnerability to parametric roll
- Application of the approach to modern commercial ships

The procedure or criteria cannot be validated without tools for quantitative analysis. Therefore, the first target is essential for the other development and application. For this purpose, the physical and stochastic characteristics of parametric roll were studied in the regular wave and irregular waves. By numerical studies and observation, new tools for quantitative analysis are developed.

Second target is to develop procedure for evaluation of vulnerability to parametric roll based on multi-level approach. The procedure includes simple resonance check, simplified intermediate check for regular wave, performance based direct stability check for irregular waves and finally operational guidance.

For each level, proper numerical tools are proposed considering computation expense, degree of accuracy and safety margin.

The last target of this thesis is application of the approach to modern commercial ships. Sample ships cover 4 container ships, 3 PCTCs and 3 passenger ships which are known to vulnerable to parametric roll and also a VLCC and S175 which are known to be safe from this phenomenon for reference. Development of operational guidance including procedure is included in this subject.

Not only development of new tools and procedure but also the results of application to real ship cases are important parts in this thesis. Review and observation of quantitative analysis for various ship types and sizes will improve ship designers' and operators' understanding of this phenomenon.

## 1.4 Outline of thesis

Background of thesis and historical review of state of the arts are introduced in Chapter 1. This chapter also shows main targets and related work scope. In Chapter 2, the characteristics of parametric roll are studied. This study will improve understanding of this phenomenon and will be used for development of new numerical tool introduced in Chapter 3. The occurrence mechanism of parametric roll is introduced in the beginning. The characteristics are categorized in two parts. First part is for physical characteristics and second

part is for stochastic characteristics. As introduced in background, main difficulty of quantitative analysis is that numerous computations should be carried out to get stable long-term expectation. Therefore, in Chapter 2.3, stochastic characteristics including non-ergodicity are studied, giving the necessity of development of very efficiency numerical tool for quantitative analysis. The physical characteristics are studied in Chapter 2.2 and the study of GM fluctuation and GZ variation in waves are numerically obtained and used for development of very efficiency numerical tool.

In Chapter 3, theoretical backgrounds of several numerical tools are described. At first, simple Mathieu equation is introduced. Then, 1.5-DOF GM-GZ approximation method is developed as an efficient numerical tool for quantitative analysis in this thesis. Numerical tool using IRF called SNU-PARAROLL is also introduced and the advantage of the tool in developing operational guidance is discussed. The most advanced tool based on Rankine panel method called WISH is introduced as a verification tool. Comparison of the numerical results between the tools is carried out and the computation speed of each tool is compared. Finally, the pro and cons are analyzed and the appropriate role in multi-level approaches are recommended.

In Chapter 4, multi-level approach to evaluate the vulnerability to parametric roll is developed. Environmental condition is defined in the beginning based on North Atlantic Sea. Multi-level approach consists of simple resonance

check (1st level), regular wave check (2nd level check) and irregular wave check (3rd level) and operational guidance.

In Chapter 5, the approach is applied to various modern ships including container ships, passenger ships, PCTCs and VLCC. Development of operational guidance for a post-Panamax container ship is also introduced separately because it should be dealt in operation phase while other levels are used for criteria. The results of real ship application are reviewed in the view of ship's vulnerability and operation.

Conclusions and discussion for all contents of this thesis are included in Chapter 6 and Chapter 7 respectively.

# Chapter 2. Characteristics of Parametric Roll

## 2.1 Occurrence mechanism of parametric roll

### 2.1.1 Basic mechanism

When a ship encounters longitudinal sea, she will experience wave crest and trough regularly in waves. If she has long parallel mid body, large flare angle in for body and long transom stern like container ship, the water plane area gets very large when the wave trough is amidships and become small when the wave crest is amidships shown in Figure 2.1 and Figure 2.2.

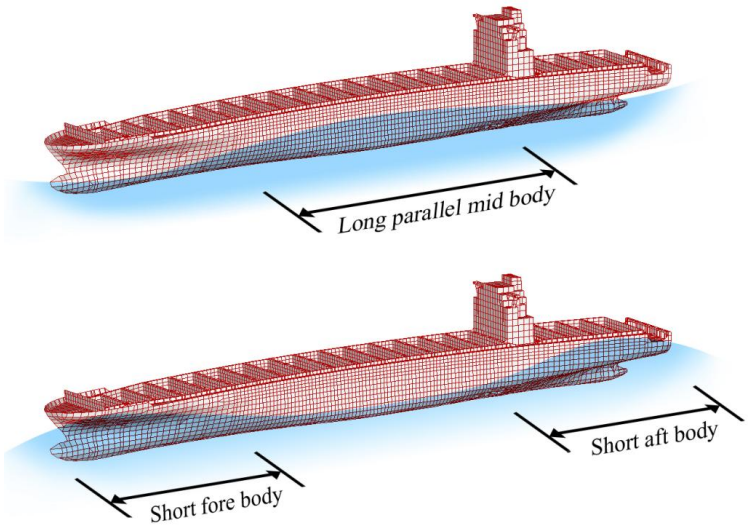


Figure 2.1 Wetted surface according to the position of wave crest

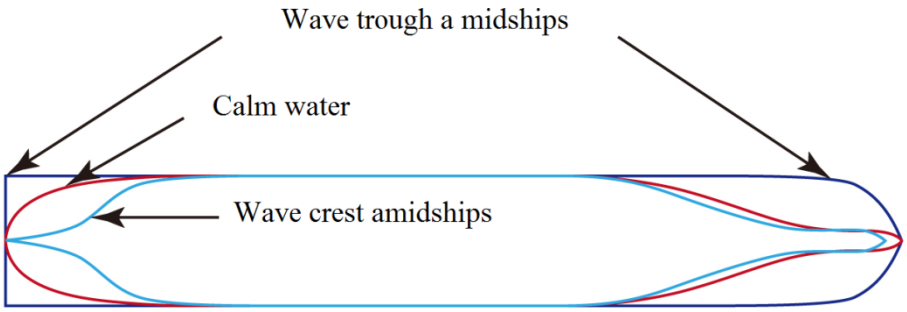


Figure 2.2 Change of water plane area in a wave

Increased water plane area results in increase of GM and restoring moment. If this oscillatory change in stability occurs at approximately twice the natural roll period, roll motions may increase to a significant angle, possibly unacceptable, as a result of parametric roll resonance.

If a ship sails on a course exactly perpendicular to the crests of head or following seas, there would be no wave–induced heeling moment. However, the ship may experience a very small roll disturbance from some external or internal cause (It always happens by wind or slightly oblique waves). When the ship rolls, the hydrostatic restoring moment acts to return it to the upright position. At this point, if the wave trough is amidships, the restoring moment is maximized and larger than calm water. Therefore, the ship goes to upright position faster than calm water. Once upright, there is no restoring moment and the ship keeps rolling to opposite side due to inertia. Near this point, if the wave crest is located amidships, the restoring moment is minimized and less than calm water. Therefore, it accelerates the roll motion easier than calm

water. After the ship passes upright position the restoring moment works against further motion and it stops at some roll angle. At this point, the wave trough is located amidships again and the ship is ready to bounce back by excessive righting moment. During the one cycle of wave elevation, the roll goes for half cycle and in this self exciting mechanism, the ship gains energy from each roll motion and the roll becomes larger and larger. If there is no damping, the roll will be increased infinitely. However, it is limited by the change of roll resonance frequency induced by nonlinear GZ curve. Figure 2.3 shows this mechanism.

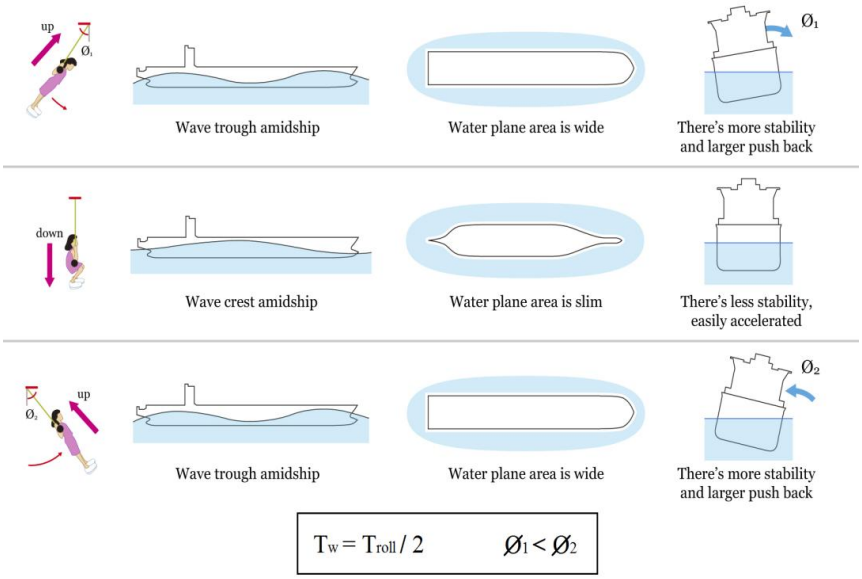


Figure 2.3 Mechanism of parametric roll

In this mechanism, the wave energy is not used to generate exciting moment directly but used to increase and decrease the restoring moment. During each roll cycle, parametric roll gains energy more and more until it reaches to steady state angle. Therefore, parametric roll is occurred by its own instability in motion equation or self-excited motion.

On the contrary, synchronized roll is generated by external forces induced by wave. The water plane area is almost same to the calm water and the roll angle reaches to its steady state when the external heeling moment is balanced to the restoring moment. Figure 2.4 shows this mechanism.

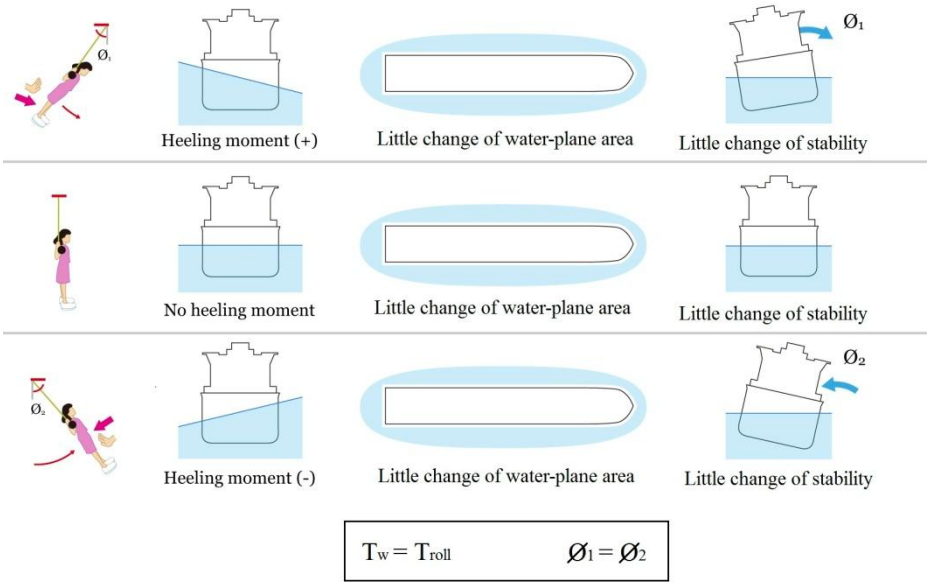


Figure 2.4 Mechanism of synchronized roll

### 2.1.2 Ship motion and wave effects

The water plane area is changed by wave and vertical motion or roll, heave and pitch. GM is meta-centric height when the roll is zero and it has not affected by roll motion. Then, the water plane area variation by wave, heave and pitch is main source of parametric roll occurrence.

## 2.2 Physical characteristic

Figure 2.5 shows phases of parametric roll motion from initiation to steady state and associated GM variation in head sea. Parametric roll is started with initial roll disturbance of 5 degree. The roll amplitude is not decreased and slightly increased from the former amplitude in the beginning. Then roll amplitude starts to grow rapidly until it reaches to steady state. Between growth stage and steady state, roll amplitude is decreased from its maximum value in transient region. When roll reaches its peak, GM in wave is larger than in calm water. On the contrary, GM in wave is smaller than in calm water when roll is near zero angle. The roll period is twice of wave period.

### 2.2.1 Initiation stage

The roll starts with initial disturbance in numerical simulation. If there is no disturbance, the roll never occurs in longitudinal seas for a ship which shape is symmetric. However, there is always small disturbance from wind, swell and directional waves in real seas.

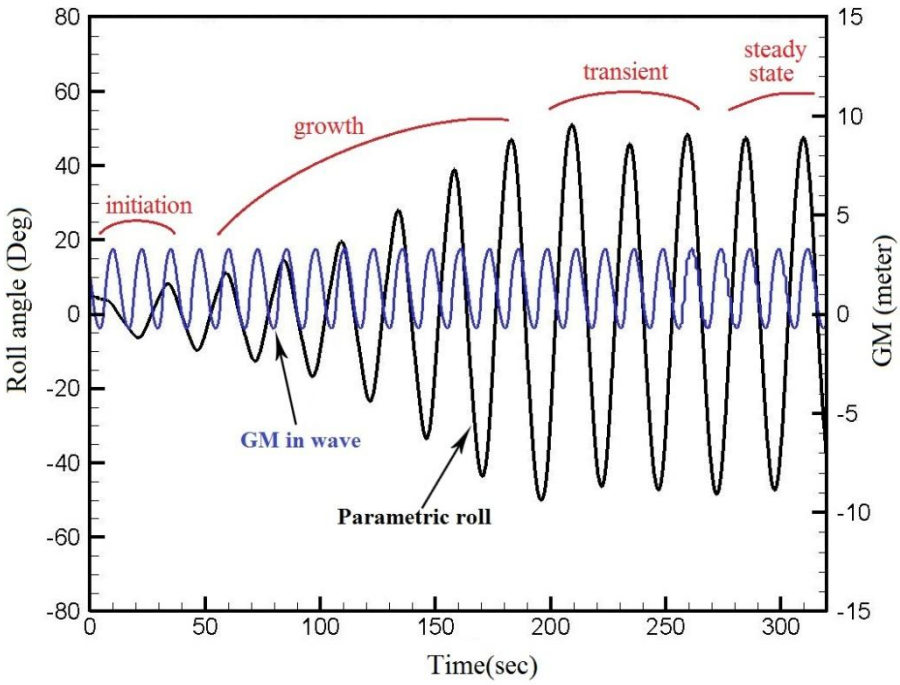


Figure 2.5 Phases of parametric roll motion and associated GM variation (10,000 TEU Container ship, $\lambda / L = 1.0,\ ka = 0.1$)

After roll is initiated by this small disturbance, parametric roll starts to grow if two essential conditions of parametric roll generation are satisfied. The first

condition is that roll period is to be near the twice of wave period and the second condition is that the energy gain should be larger than energy loss due to damping. Therefore this is a threshold phenomenon.

Figure 2.6 shows several simulations of parametric roll starting from different initial roll angles. The growth stage, transient stage and steady state keep almost same shape for different initial values. Large initial value shortens the time to reach steady state. It means that the growth rate and steady state roll angel are determined by wave and GM value and are independent from initial values.

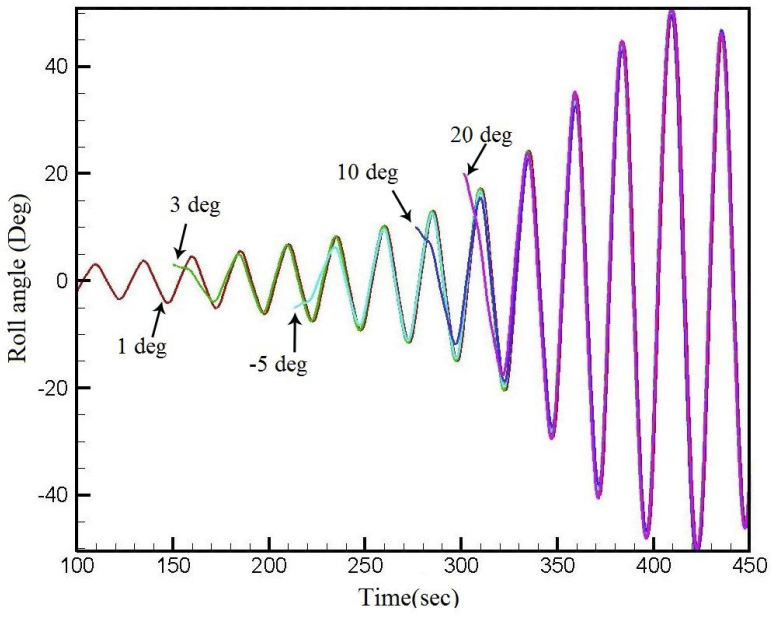


Figure 2.6 Parametric roll simulations according to different initiation angles (10,000 TEU Container ship, $\lambda / L = 1.0,\ ka = 0.1$)

### 2.2.2 Development and steady state

If the two conditions are satisfied, the roll keeps on growing. Figure 2.7 shows energy gain by changing of restoring moment. The restoring moment in wave is larger than calm water in way of roll peaks and less than calm water in way of upright position. In this stage, roll amplitude grows rapidly.

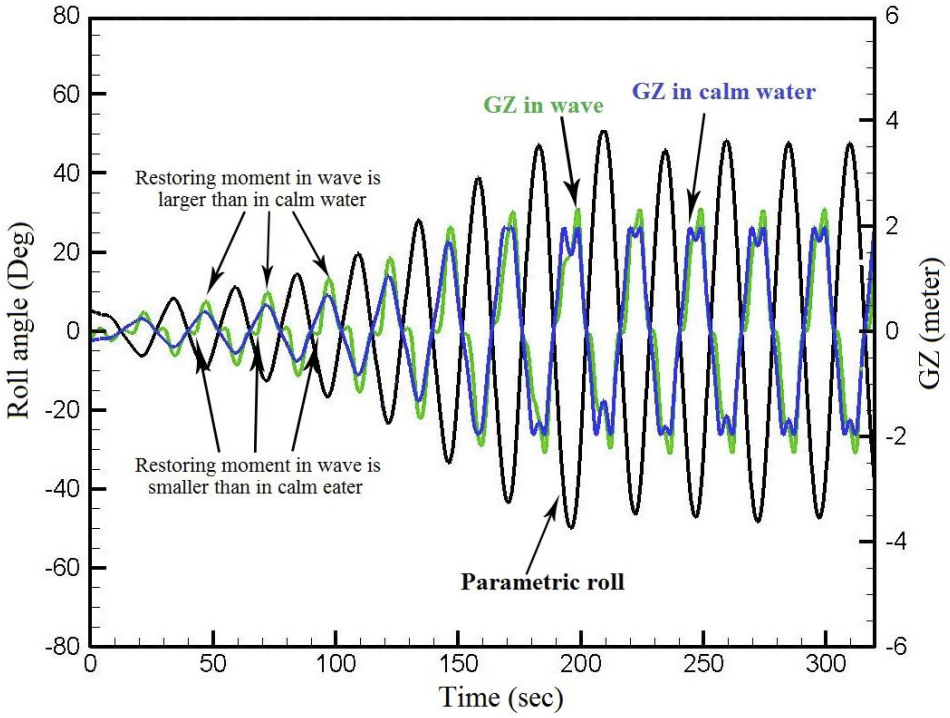


Figure 2.7 Restoring moment in wave and calm water
(10,000 TEU Container ship, $\lambda / L = 1.0,\ ka = 0.1$)

After roll grows more than 40 degrees, the roll is bounded to steady state angle because the energy gain is not increased any more. It means that the

whole energy gain through each roll cycle is balanced to energy loss by roll damping. The slope of GZ curve keeps almost constant within 30 degrees and decreases nonlinearly after 40 degrees. Therefore, when the roll is relatively small, the GM increase results in increase of GZ value or larger push-back moment. While, when the roll is larger than 40 degrees, the push back moment is slightly larger than calm water and there is a little energy gain shown in Figure 2.8. Therefore total energy gain is bounded to certain value and it is balanced to the steady state roll angle. If GZ curve were linear, parametric roll would be always diverged because larger energy gain is obtained in larger roll angle.

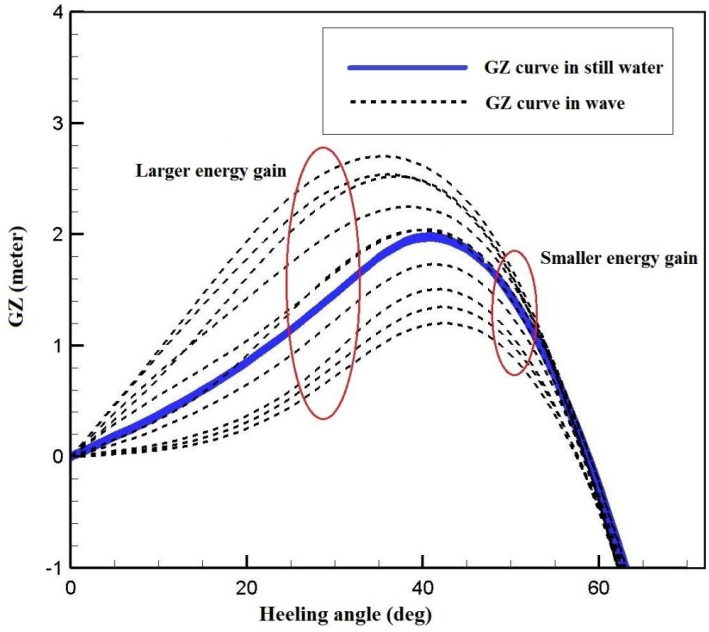


Figure 2.8 Energy gain by restoring moment change in wave
(10,000 TEU Container ship, $\lambda / L = 1.0,\ ka = 0.1$)

### 2.2.3 Roll damping effect

The roll damping takes an important role in parametric roll development. Figure 2.9 shows parametric roll for different damping coefficients.

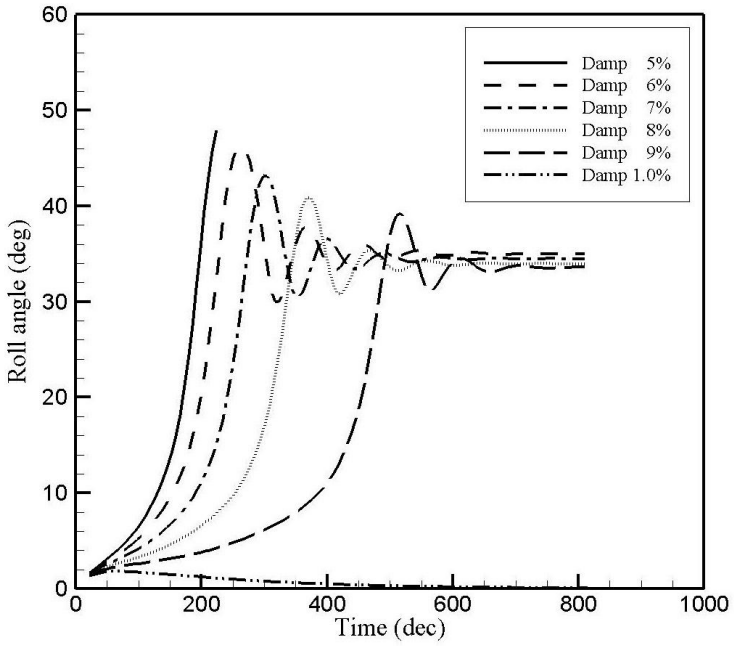


Figure 2.9 Damping effect on parametric roll
(10,000 TEU Container ship, $\lambda / L = 1.0,\ ka = 0.1$)

Under lower roll damping, parametric roll grows faster. If the damping is smaller than 0.5%, parametric roll is diverged. It's because the inertia induced by lager push-back moment results in 45 degrees and the restoring moment is too small to make the roll bounce back. However, if the damping is smaller

than the threshold value for convergence, parametric roll reaches to steady state. Larger damping makes the roll converge faster.

It's interesting that the steady state roll angles are almost same values regardless of roll damping. It means that the steady state roll angle is not determined by roll damping but wave and GZ curve and the total energy gain is limited as explained above. Even if roll damping is larger and the energy gain is smaller, the energy is accumulated slowly until it is bounded to steady state angle by nonlinear GZ curve.

If the roll damping is larger than certain threshold value, the roll dies away because the energy gain is smaller than energy loss due to roll damping

### 2.2.4 GM fluctuation

The most important source of parametric roll is the change of GM in waves. The GM fluctuates according to the variation of the water-plane area. The water-plane area also varies according to the interaction between the wave, heave, pitch, and hull shape. Figure 2.10 shows an example of GM variation when the wave length is equal to the ship length in head sea for a 10,000 TEU container ship. The graph is flat and lower than the still water GM when the wave crest is near the mid-ship region, while the graph is steep and larger when wave crest is near the bow and stern. This is because a typical container ship has a long parallel mid body, large bow flare angle and overhanging transom in short fore and aft body. From the above observations, it is expected

that the mean value of GM will be shifted from still water GM to normally positive side, and nonlinear components will exist. Therefore, GM fluctuation may be useful to be decomposed into Fourier series to analyze its characteristics.

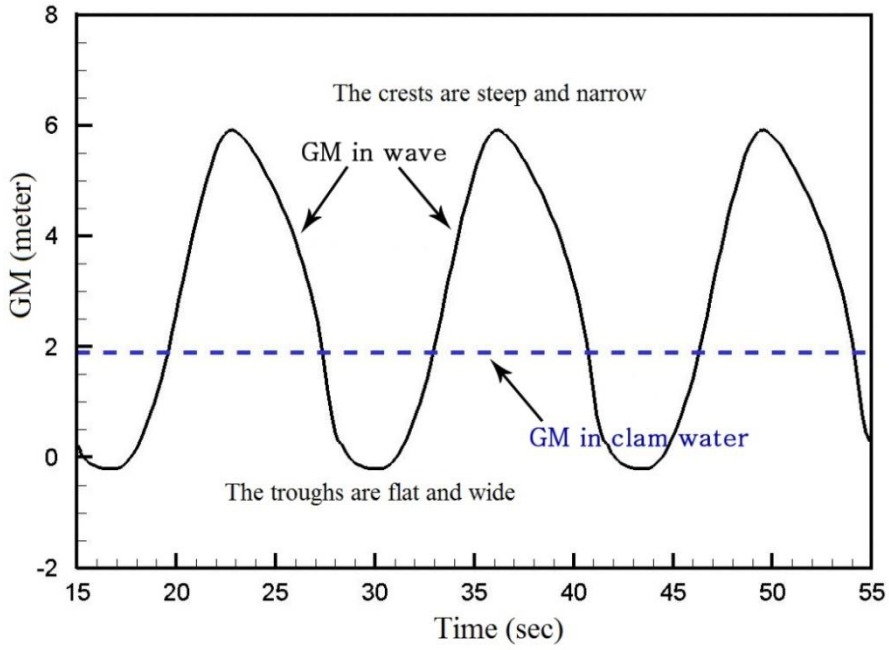


Figure 2.10 GM fluctuation
(10,000 TEU Container ship, $\lambda / L = 1.0,\ ka = 0.1$)

$GM(t)$ can be decomposed into a fluctuation term $GM_f(t)$ and a still water term $GM_{still}$ and $GM_f(t)$ can be also expressed by a Fourier series as follows

$$GM(t) = GM_f(t) + GM_{still} \tag{1}$$

$$GM_f(t) = GM_0 + \sum_{n=1}^{\infty} GM_n \cos(n\omega t + \alpha_n) \quad (2)$$

Figure 2.11 to Figure 2.13 show the transfer functions of $GM_0$, $GM_1$ and $GM_2$, which denote the mean value, the first and second harmonic components, respectively, for typical post-Panamax container ships and a VLCC. The main dimensions of the ships are shown in Table 2.1. The heave and pitch are calculated by a 3D linear potential code.

Table 2.1 Main dimension of typical container ships and a VLCC

| | 5500 TEU | 6500 TEU | 8000 TEU | 10000 TEU | VLCC |
|---|---|---|---|---|---|
| Length(m) | 263.0 | 286.3 | 309.2 | 334.0 | 322.0 |
| Breadth(m) | 40.0 | 40.0 | 42.8 | 45.6 | 59.6 |
| Depth(m) | 24.2 | 24.2 | 24.6 | 27.3 | 30.5 |
| Design Draft(m) | 12.0 | 12.0 | 13.0 | 13.0 | 21.0 |

$GM_0$ is always positive, as expected. The positive $GM_0$ will increase the actual $GM$ and that normally will make the roll resonance frequency shift to higher one and mitigate parametric roll in general. Considering that a modern post-Panamax container ship is operated with a still water $GM$ about 1 or 2 meters, the shift of $GM_0$ should not be neglected.

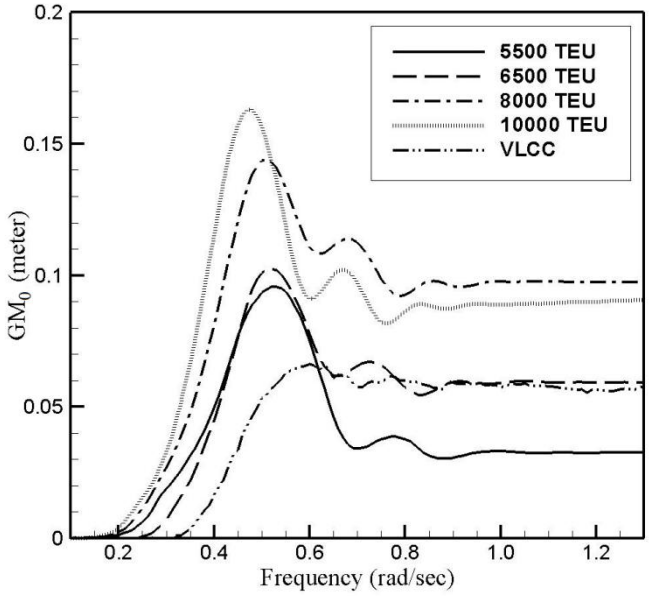


Figure 2.11 Transfer functions of $GM_0$

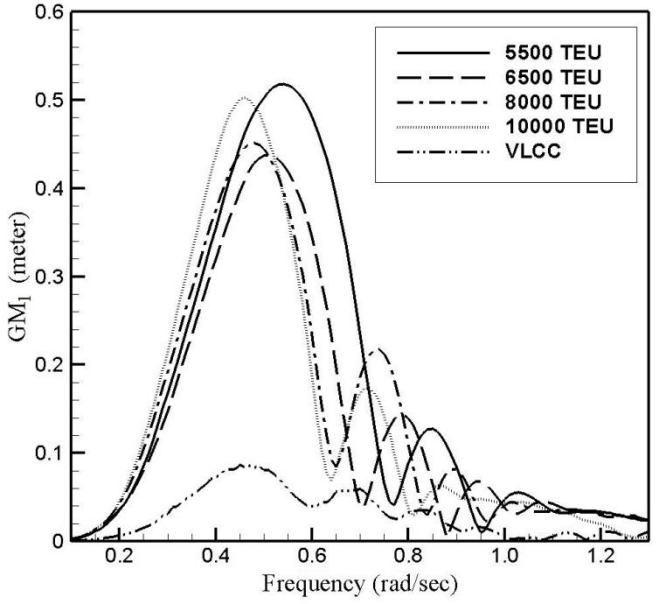


Figure 2.12 Transfer functions of $GM_1$

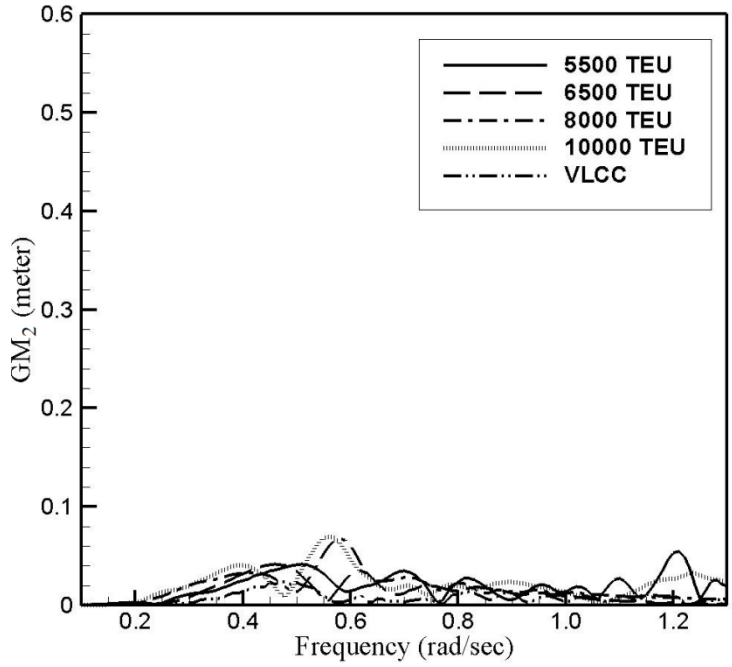


Figure 2.13 Transfer functions of $GM_2$

The maximum $GM_1$ occurs when the wave length is near 0.8L for container ships and occurs when it is the same as the ship length for a VLCC. Interestingly, the water plane area coefficients $C_W$ of container ships and oil tankers are near 0.8 and 1.0 respectively, which means that the effective wave length $L_{EF}$ which maximizes the $GM$ fluctuation can be obtained as the water plane area $S_{WL}$ divided by the breadth $B$.

$$L_{EF} = S_{WL} / B = C_W L \tag{3}$$

Compared to container ships, a VLCC has a very small $GM_1$ because of its slight geometrical nonlinearity. .

There are several clear hollows and humps in the $GM_1$ curves. The hollows occur when the wave length equals $1/n$ -th of $L_{EF}$ and the humps occurs when the wavelength equals $1/(1+n)$ -th of $L_{EF}$ .

$GM_2$ is much smaller than $GM_1$ for all ships, and is too small to generate parametric roll. $GM_0$ and $GM_1$ are used to check the vulnerability of a ship to parametric roll by means of the Mathieu equation. Even though $GM_0$ and $GM_1$ are induced by geometrical nonlinearity, Figure 2.14 to Figure 2.15 show that both values are linear up to a very high wave amplitude before the deck is immersed. This linearity was proven by Dunwoody. Considering the severe geometrical nonlinearity of container ships, this assumption may be valid for most ship types in general.

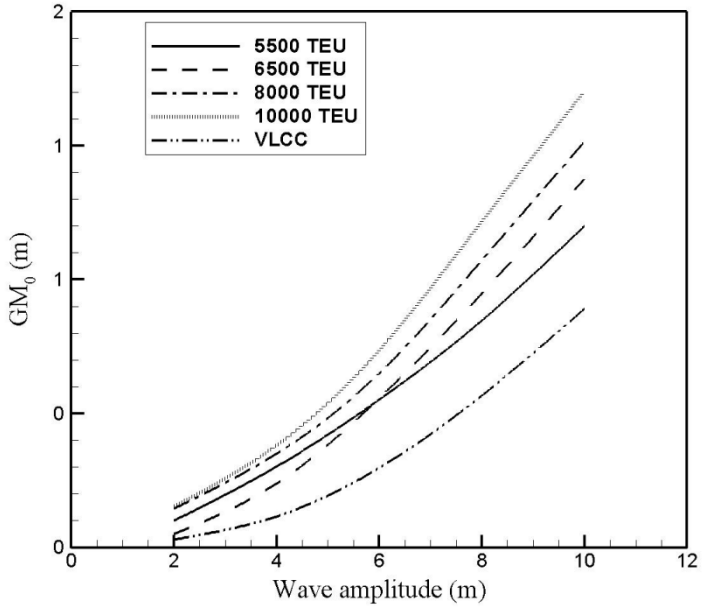


Figure 2.14 Variations of $GM_0$ according to wave amplitude

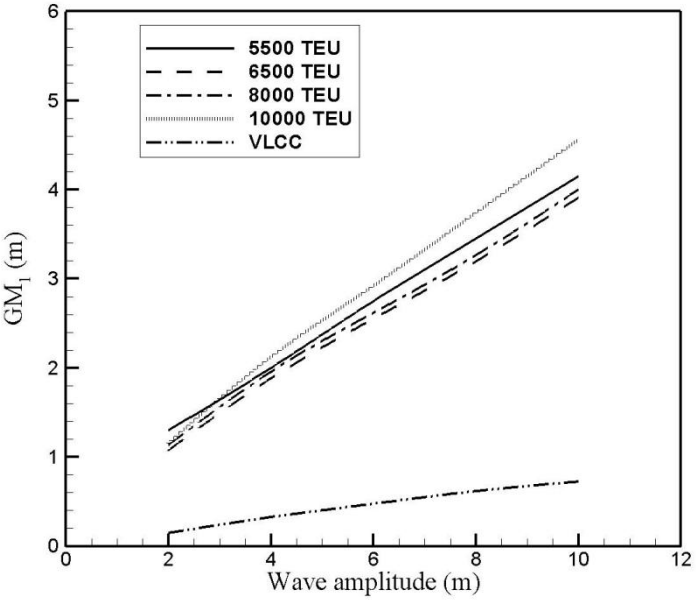


Figure 2.15 Variations of $GM_1$ according to wave amplitude

The assumption of $GM_1$ linearity for container ships can be tested for irregular waves. If $GM_1$ is linear, the spectrum of $GM_1$, $S(GM_1, \omega)$, can be obtained from the product of the transfer function of $GM_1$, $RAO(GM_1, \omega)$, and the wave spectrum $S(\omega)$ as follows.

$$S(GM_1, \omega) = RAO(GM_1, \omega)^2 S(\omega) \tag{4}$$

Figure 2.16 shows the comparison between the response spectrum from equation (4) and the Fourier transform results of numerical time simulation of GM variation for a 10,000 TEU container ship in irregular waves. The significant wave height, $H_s$, is 6 meters and the modal frequency, $\omega_m$, is 0.43 rad/sec. Except the very small or large wave frequencies, the analytical approach based on linear $GM_1$ assumption seems valid for irregular waves.

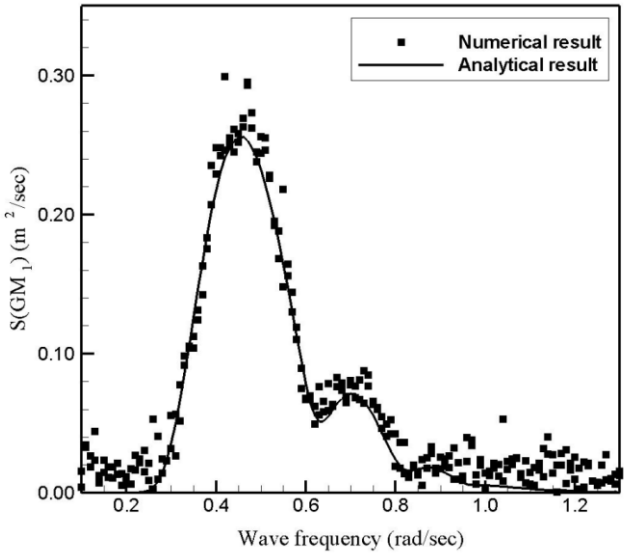


Figure 2.16 Comparison of spectrums $GM_1$ from numerical simulation and analytical approach ( $Hs = 6m, \lambda_{modal} / L = 1.0$ )

Figure 2.17 shows also the temporal means of GM variations, which were obtained from several numerical tests. The temporal means of GM variation asymptotically converge to a certain value, which is always positive like that of a regular wave case. If we assume $GM_0$ is linear with respect to wave height, the mean value for a sea state with significant wave height $Hs$ and zero crossing period $Tz$ can be obtained by the equation (5) using the area of response spectrum $m_0$.

$$\begin{aligned} m_0 &= \int S(\omega) RAO^2(GM_0, \omega) d\omega \\ GM_0(Hs, Tz) &= \sqrt{m_0} \end{aligned} \tag{5}$$

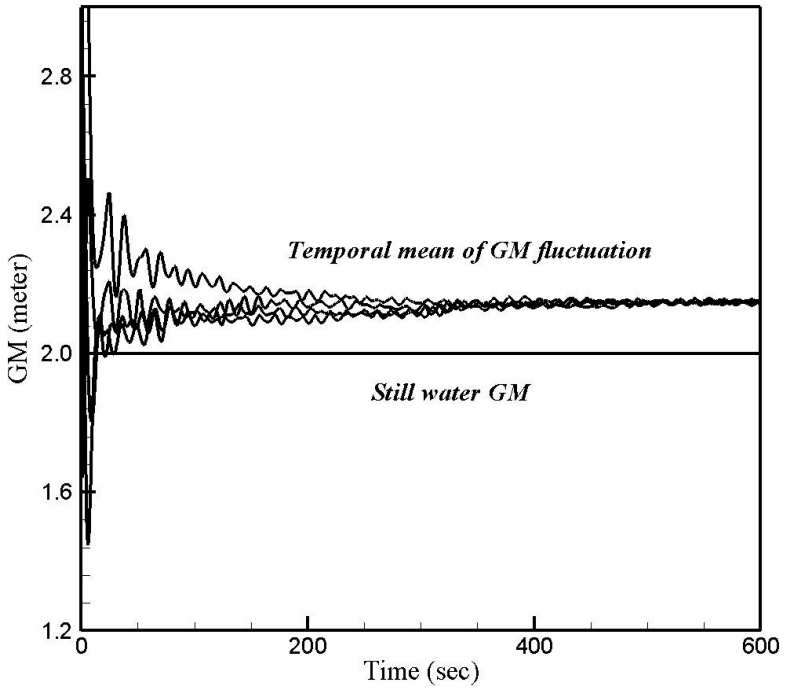


Figure 2.17 Temporal mean of $GM$ fluctuation for irregular waves

( $Hs = 6m, \lambda_{modal} / L = 1.0$ )

Figure 2.18 shows the comparison between the response spectrum from equation (4) and the Fourier transform results of numerical time simulation of GM variation for 5,500 TEU, 6,500 TEU and 8,000 TEU container ships in irregular waves which assume that the linearity if $GM_1$ can be quite valid in general.

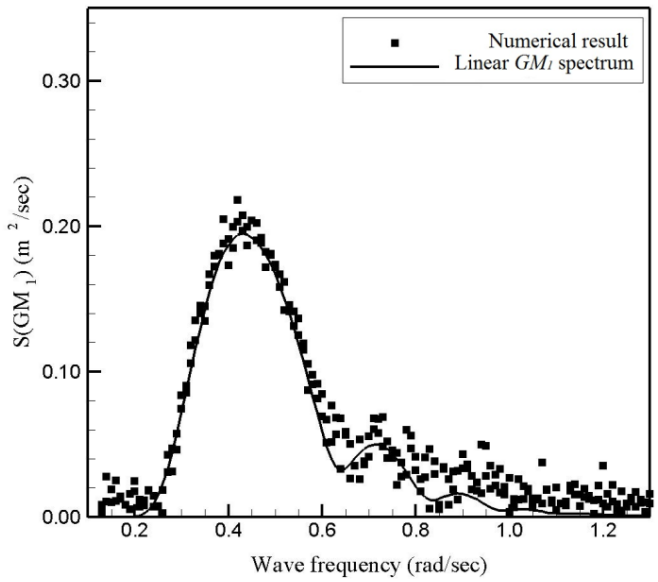


(a) 5,500 TEU

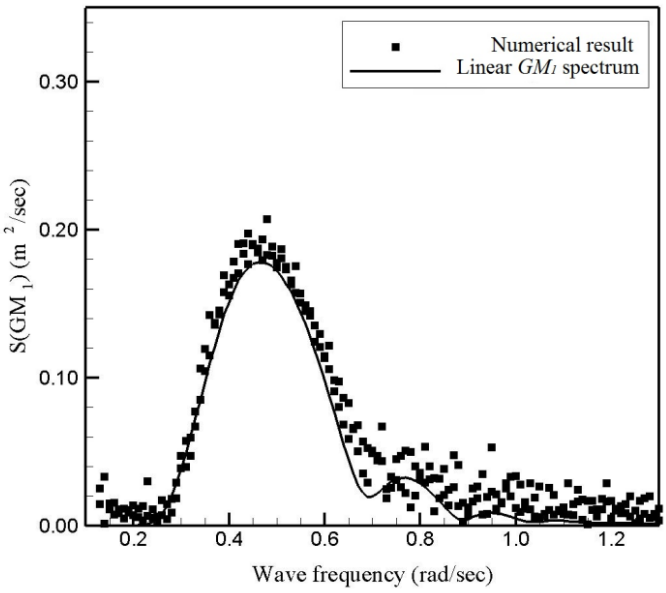


(b) 6,500 TEU

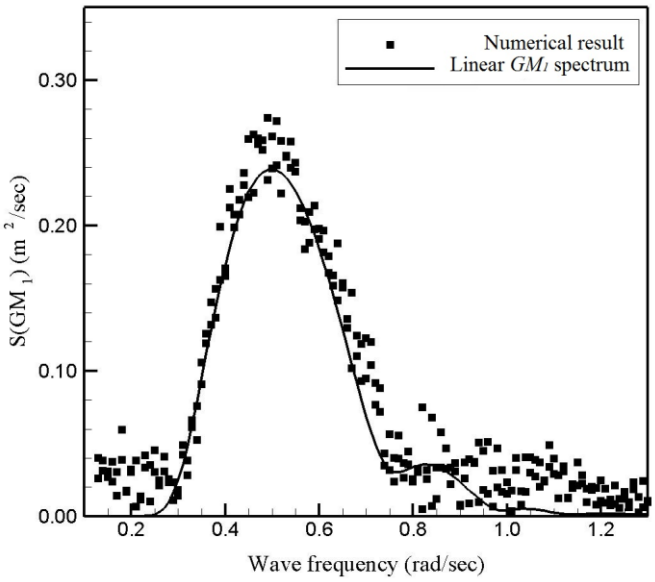


(c) 8,000 TEU

Figure 2.18 Comparison of spectrums $GM_1$ from numerical simulation and analytical approach for 5,500 TEU, 6,500 TEU and 8,000 TEU ( $Hs = 6m, \lambda_{modal} / L = 1.0$ )

### 2.2.5 GZ fluctuation

The shape of the GZ curve for still water is highly influenced by GM, which governs the slope of the curve for the upright condition or the zero roll angle. For many ship types, the GZ curve is linear up to a certain roll angle before the side of a ship's deck is immersed into water. The linear region of the GZ curve reaches up to almost 30 degrees for container ships and to even larger degrees for tankers. This fact is still true for ships under motions in waves.

Figure 2.19 shows the fluctuations of actual GZ curves of a 10,000 TEU container ship when wave crests move the ship forward in head sea. Still water $GM$ is 2 m. Figure 2.19 (a), (b) and (c) show the GZ curves for wave lengths $\lambda$ of 2L, L and L/2, respectively where L means the ship length. The wave slope, $ka$, is fixed to 0.1. The bold line stands for the still water GZ curve and the slopes of the GZ curves at the zero heeling angle means GM. Figure 2.19 shows that the GZ curves move up and down from the still water GZ curve according to wave condition, and the fluctuations are governed by the slope of the linear region. The amplitude of the slope or the GM variation is maximized when the ship length is equal to the wave length. It also shows that the angles of the zero restoring moment are focused on a narrow range of angles where the still water GZ curve is zero regardless of the wave position or wave length.

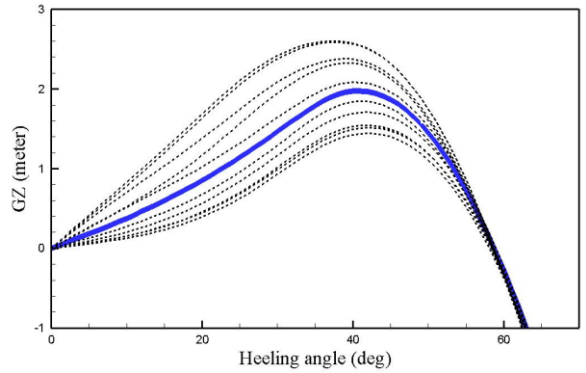


(a) $\lambda = 2L$

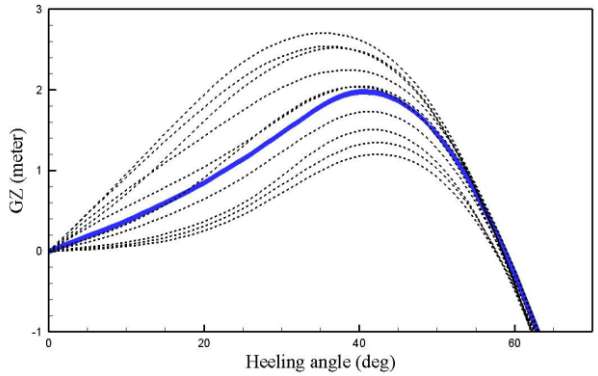


(b) $\lambda = L$

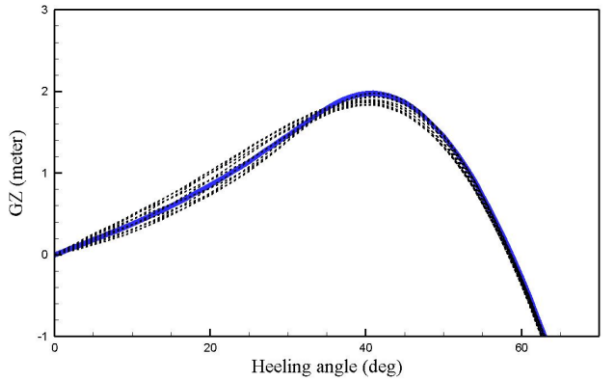


(c) $\lambda = L/2$

Figure 2.19 Actual $GZ$ curves for different wave lengths ( $ka = 0.1$ )

## 2.3 Stochastic characteristics

### 2.3.1 Non-ergocity

A process is said to be ergodic when its statistical property such as mean and variance can be estimated from one single realization with infinite time length. Assumption of ergodic process is very useful in present seakeeping tests because the probabilistic qualities of ship motions are usually estimated by means of temporal averages. In linear ship motion theory, ship motions are proven to be Gaussian and ergodic driven by the zero mean Gaussian sea elevation.

When pitch and heave are of concern in a longitudinal sea, the assumption can be considered quite good and ergodicity of motion can be assumed. However, when roll is of concern, non-linear effects come into play in both restoring and damping. Moreover, if we consider parametric roll, the roll motion is built up due to a self excitation, that is a time variation of the restoring capability. In this condition, the roll response is far from a Gaussian process. To check these stochastic characteristics, ship motions of 10,000 TEU container ship are analyzed. Significant wave height is 6 meter and modal wave length is equal to ship length except roll motion. For roll motion, modal period of 15 sec is used and wave direction is 90 degree. Figure 2.20 to Figure 2.22 show that wave elevation, heave and pitch follow Gaussian distribution well. However, Figure 2.23 shows synchronized roll is quite different from

Gaussian distribution and Figure 2.24 shows parametric roll is far from Gaussian distribution. In parametric roll, the value near zero has sharp peak because parametric roll does not occur at all in some condition while wave elevation, for example, continuously occurs in any condition.

The shape of tales for parametric roll is thicker than Gaussian distribution because parametric roll occurs consecutively if the condition is satisfied. Wave elevation, however, occurs almost randomly.

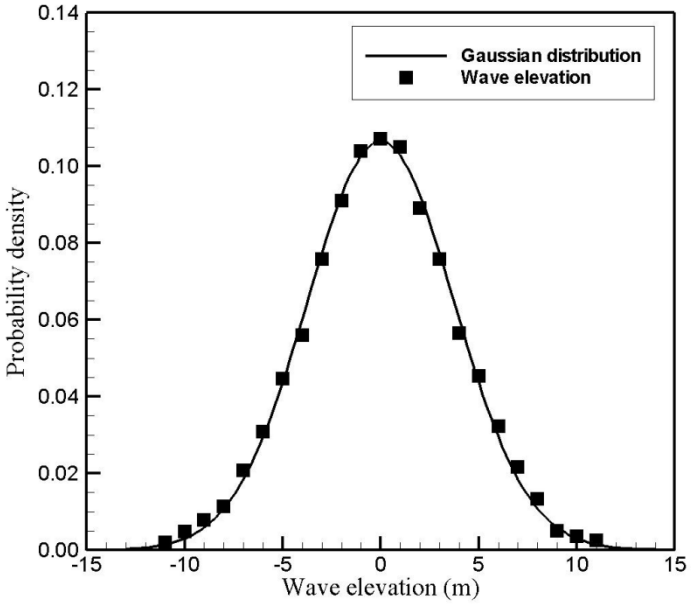


Figure 2.20 Comparison of Gaussian distribution and wave elevation

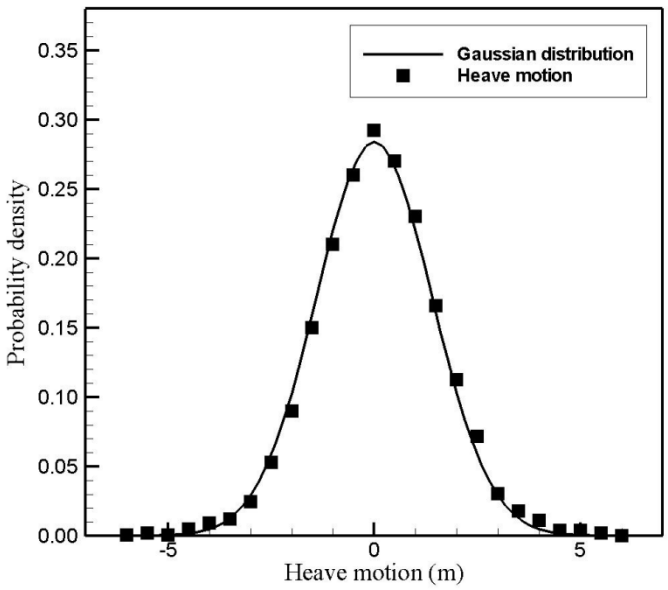


Figure 2.21 Comparison of Gaussian distribution and heave motion

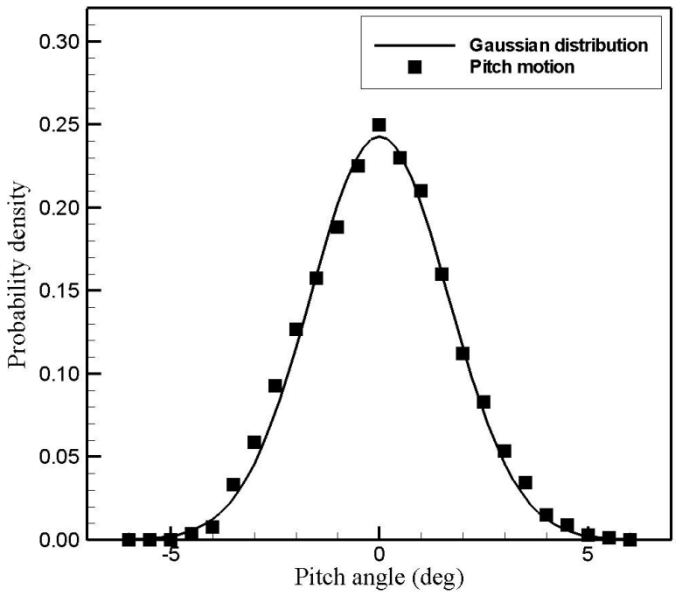


Figure 2.22 Comparison of Gaussian distribution and pitch motion

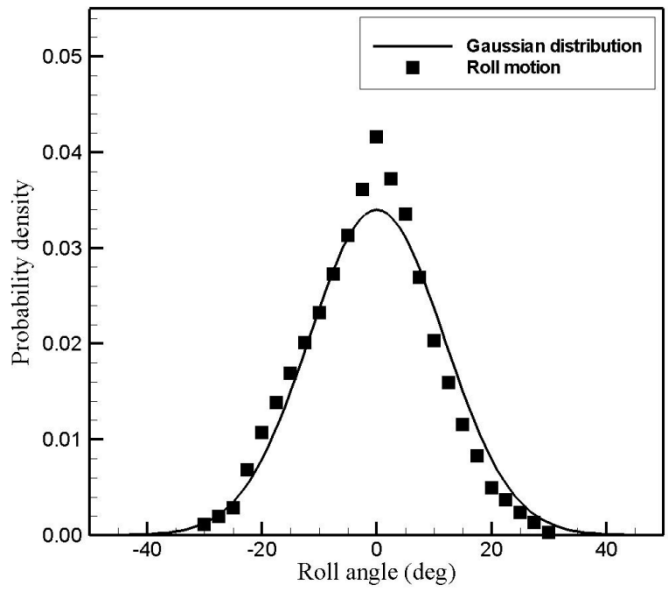


Figure 2.23 Comparison of Gaussian distribution and roll motion

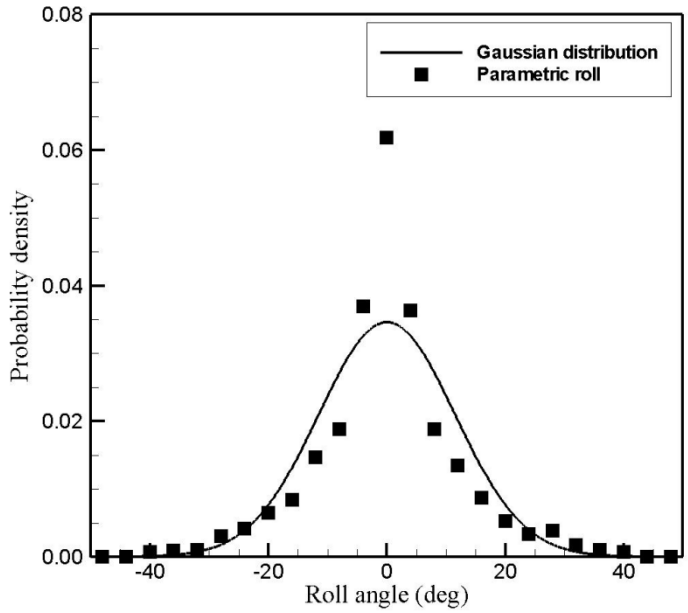


Figure 2.24 Comparison of Gaussian distribution and parametric roll

If a process is assumed to be ergodic, it should be stationary or statistical parameters are independent from the time.

Figure 2.25 to Figure 2.29 show temporal variations of wave elevation, heave, pitch, synchronized roll and parametric roll obtained from 5 times realization. Temporal variations of wave elevation, heave and pitch are converged into specific values but those of synchronized roll and parametric roll don't converge but vary in some regions. Especially, the variances of parametric roll are spread significantly.

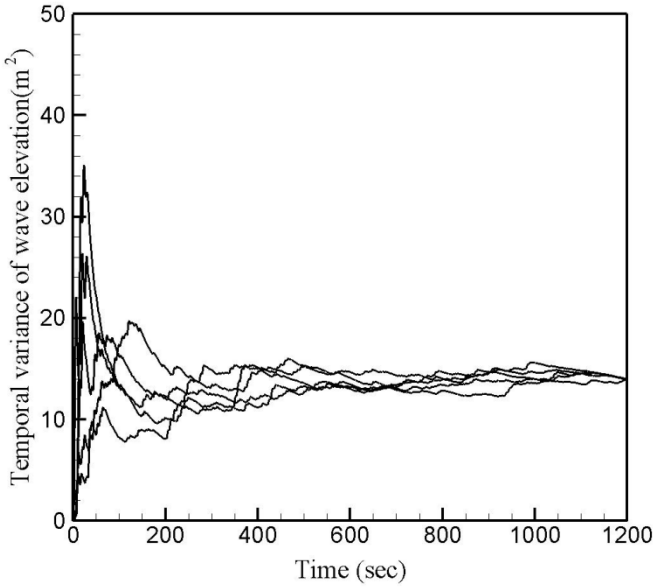


Figure 2.25 Temporal variance of wave elevation

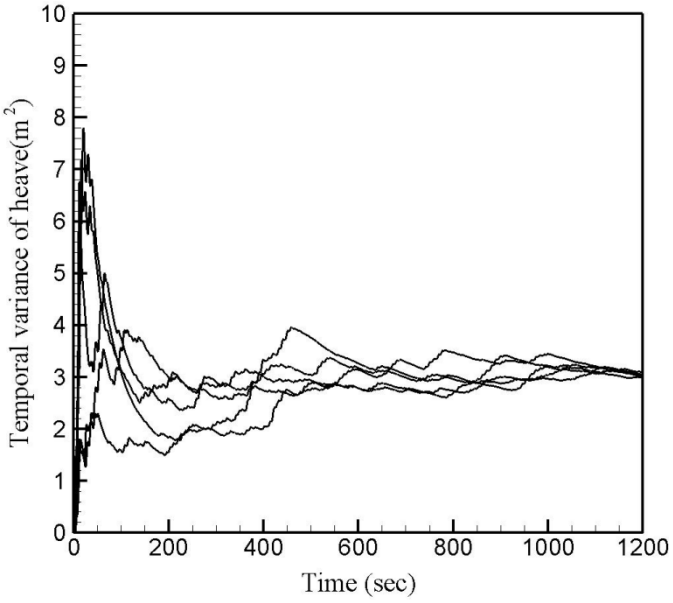


Figure 2.26 Temporal variance of heave motion

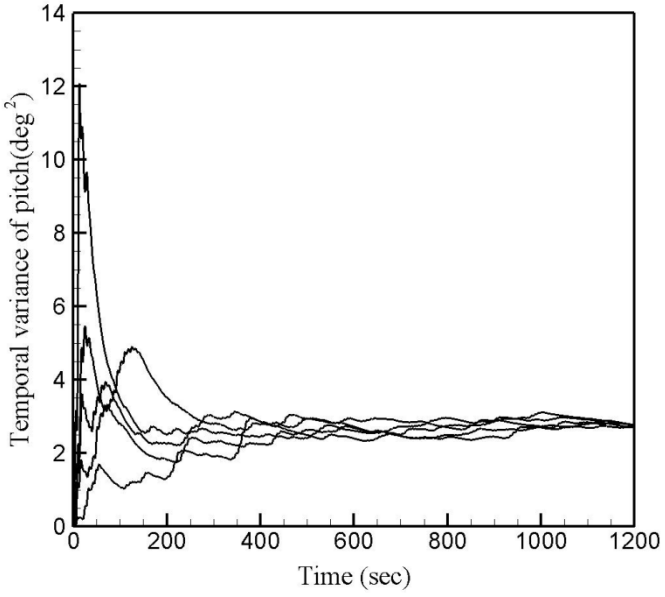


Figure 2.27 Temporal variance of pitch motion

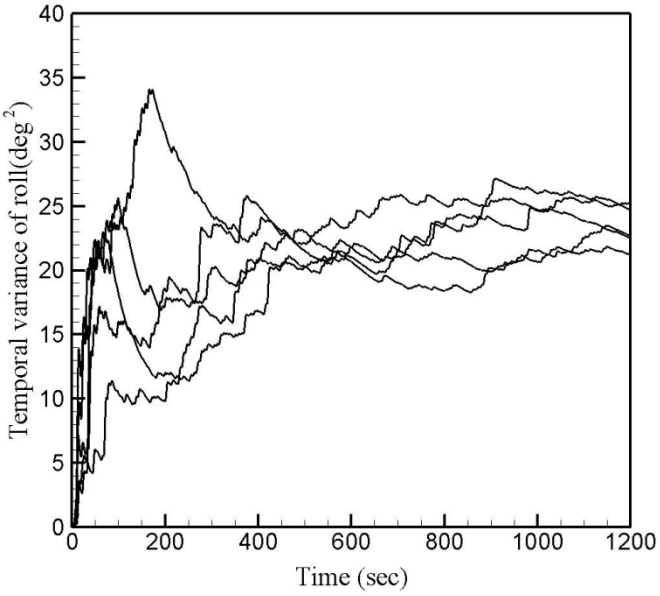


Figure 2.28 Temporal variance of roll motion

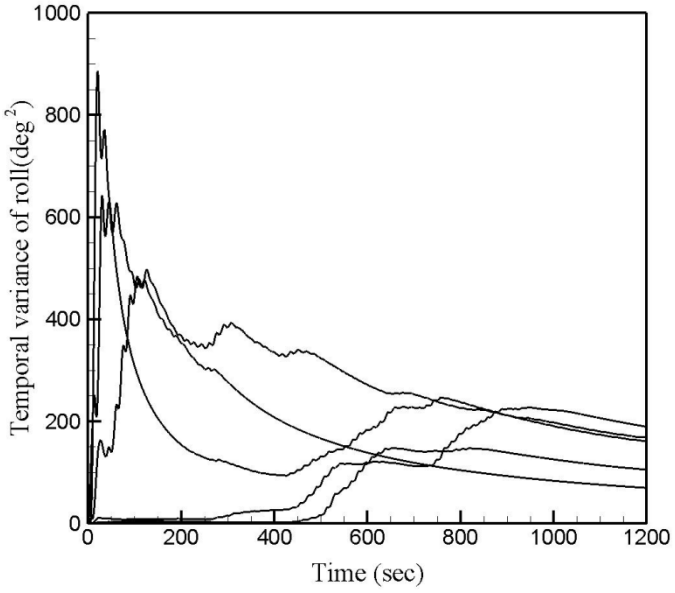


Figure 2.29 Temporal variance of parametric roll

### 2.3.2 Occurrence in irregular seas

Figure 2.30 shows several parametric roll simulations for a given significant wave height $H_S$ of 5.5m and $\lambda_{modal}/L$ is equal to 1.0. It shows that the variances of parametric roll for same sea state diverge critically. The variances of parametric roll in each numerical test seem almost random variable. For example, simulation 3 never shows parametric roll occurrence and simulation 4 shows very large roll angle occurs and fades away suddenly. Simulation 1, simulation 2 and simulation 5 show similar tendency but different variance. Simply to say, each realization will give different statistical prediction.

Therefore, it is impossible to predict expectation of parametric roll using mean and auto-correlation function by just one realization with limited time duration.

Figure 2.30 shows clearly that the variance of variances randomly changes. When the irregular waves are grouped into several successive regular waves with resonance frequency, the energy is easily gained and accumulated and parametric roll is developed to quite large amplitude. However, if those kinds of successive grouping are failed, parametric roll cannot grow, even never occurs like Figure 2.30 (c).

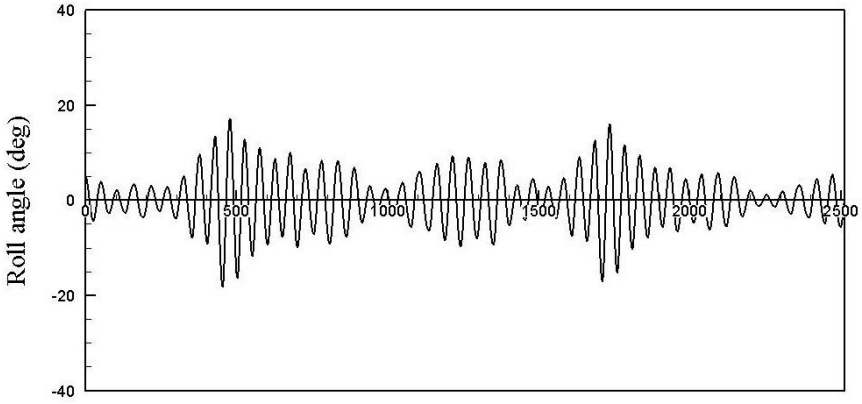


(a) Simulation 1

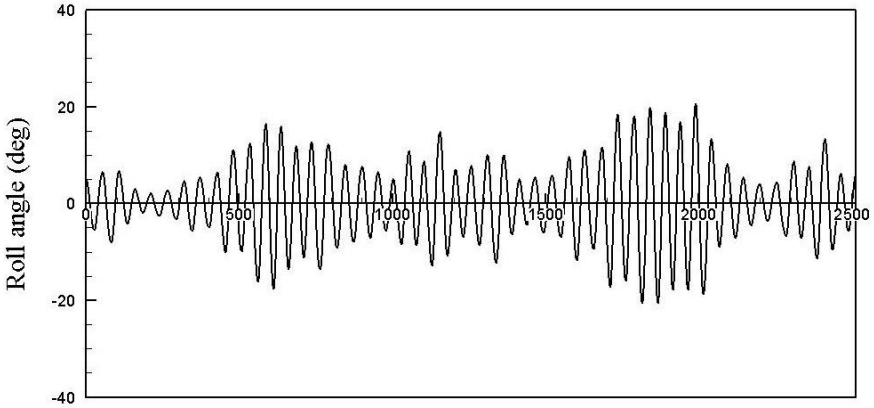


(b) Simulation 2

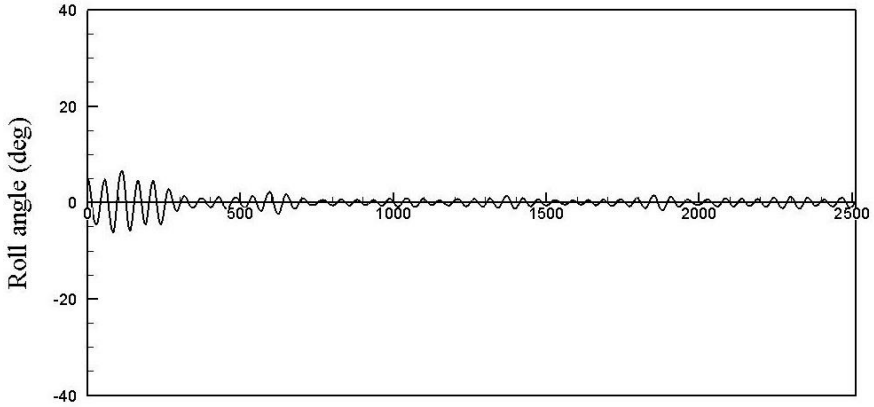


(c) Simulation 3

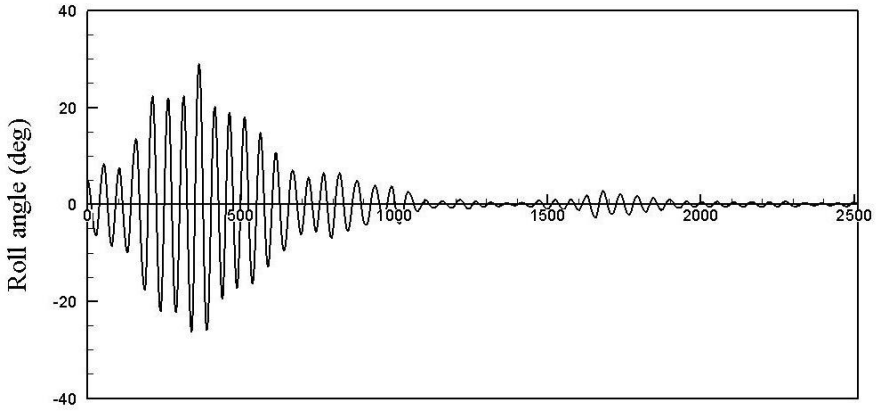


(d) Simulation 4

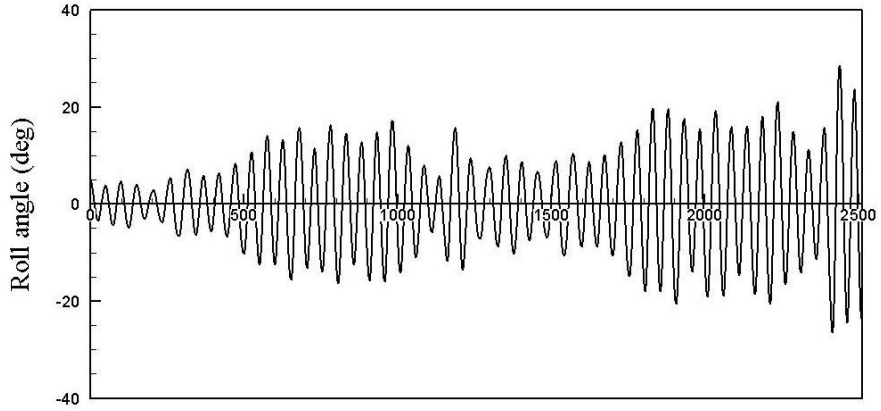


(e) Simulation 5

Figure 2.30 Various parametric roll responses for same sea states

( $Hs = 5.5m$ , $\lambda_{\mathrm{mod}al} / L = 1.0$ )

To show this kind of occurrence rate, hundreds of numerical tests should be performed for each irregular sea state. Figure 2.31 (a) shows the number of parametric roll occurrence contour during 500 numerical realizations for each irregular sea state and Figure 2.31 (b) shows the response spectrum for specific sea states for a 10,000 TEU container ship when the still water $GM$ is 1 meter. A parametric roll never occurs in sea states A and C and always occurs in sea state B, as shown in Figure 2.31 (a).

The response spectrum is affected by both wave spectrum and transfer function $GM_1$. For this reason, the two peaks in the C response spectrum correspond to the peak of transfer function $GM_1$ and the modal wave frequency of the wave spectrum. At point B, the modal frequencies of the $GM_1$ transfer function and wave spectrum are similar and very close to the resonance frequency of 0.43 rad/sec. The spectra are wide and low at points A and C, where the modal frequency of wave spectrum is apart from that of transfer function $GM_1$ and the resonance frequency. This means that the area of response spectrum of $GM_1$ near the resonance frequency is maximized when the resonance frequency and the two modal frequencies are close to each other and can be a good index indicating parametric roll occurrence in irregular waves.

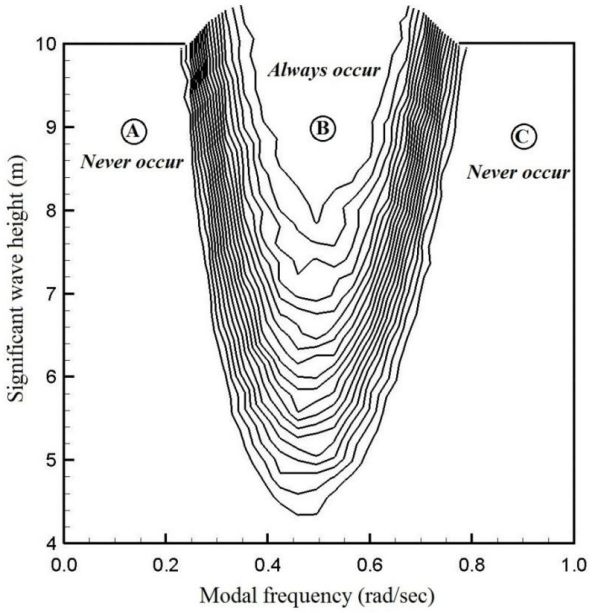


(a) Parametric roll occurrence contour

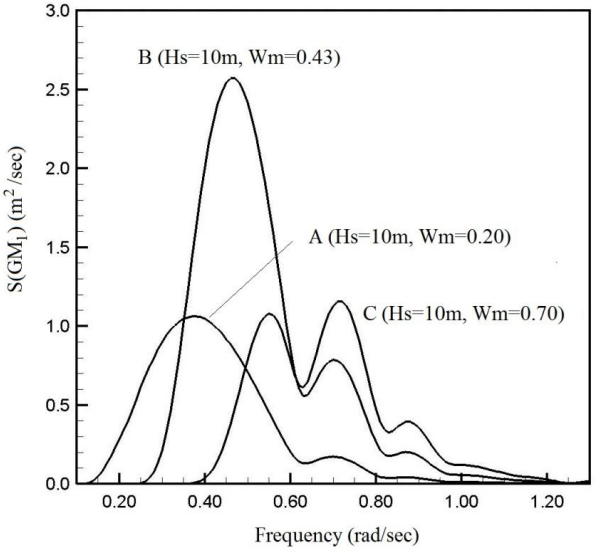


(b) Response spectrum

Figure 2.31 Parametric roll occurrence contours for irregular waves and response spectrum of $GM_1$

### 2.3.3 Probability density function

To get a stable probability density function of parametric roll, the only possible way is to collect enough sample data by a lot of numerical tests, so called Monte-Carlo simulation. In this approach, several parameters such as the initial values, run lengths and number of realizations should be carefully chosen. If we assume that the standard deviations of each realization are random, their values will follow a Gaussian distribution on the basis of the central limit theorem. Then, the sample size for a given confidence level and the error bound limit can be obtained. For example, equation (6) yields sample size $n$ for 99% confidence level and 1 deg. of error limit from the standard deviation $\sigma$ of sufficient number of realizations.

$$n = \left( \frac{2.57 \cdot \sigma}{1.0} \right)^2 \tag{6}$$

Table 2.2 shows the sample size needed to satisfy each error bound at 99% confidence level for different significant wave heights under resonance frequency and also show the occurrence ratio at the North Atlantic Sea for a 10,000 TEU container ship.

Table 2.2 Number of realizations for given error bounds

| | $Hs = 6m$ | $Hs = 7m$ | $Hs = 8m$ | $Hs = 9m$ |
|---|---|---|---|---|
| $\sigma(\deg)$ | 0.23 | 1.70 | 4.75 | 6.00 |
| $n$ ; $\pm 0.1\deg$ | 36 | 1910 | 14,912 | 23,776 |
| $n$ ; $\pm 0.2\deg$ | 9 | 478 | 3,728 | 5,944 |
| $n$ ; $\pm 0.3\deg$ | 4 | 212 | 1,657 | 2,642 |
| $n$ ; $\pm 0.4\deg$ | 2 | 119 | 932 | 1,486 |
| $n$ ; $\pm 0.5\deg$ | 1 | 76 | 596 | 951 |
| Occurrence | 1.3% | 1.1% | 0.8% | 0.3% |

Above table shows that more realizations are needed when a more severe parametric roll occurs, even when a relatively high occurrence ratio is assumed for lower sea states. . For example, about 1,000 samples should be collected to get a stable distribution function when $Hs$ is 8m and error bound is 0.4 deg., when the standard deviations are assumed to follow a Gaussian distribution.

Figure 2.32 shows that the degree of convergence depends on the number of realizations. Each graph in Figure 2.32 shows several exceedance probability curves of parametric roll obtained from summing the results of 10, 100, and 1000 numerical tests, respectively. Each realization is carried out for 20 minutes. All calculations were done for the significant wave heights of 7m

and 9m at resonance frequency. Evidently, more number of realizations gives more converged distributions and the convergence becomes faster for less severe sea states, as expected. Although state-of-the-art tools that can solve 6-DOF problems can simulate the ship motions exactly, they take too much time to carry out 1000 numerical tests for each sea state. If each test takes 20 minutes to complete, long-term predictions based on the North Atlantic wave data would take several years. Therefore, calculation speed seems to be more important than accuracy of numerical code in highly non-ergodic cases.

Another issue is the initial condition. Parametric roll should be triggered by the initial roll angle. Figure 2.33 shows the exceedance probability curves for different initial roll angles. One realization takes 40 min and the first 20 min results are cut off to eliminate transient results. However, in the figure, the initial value greatly affects the exceedance probability, meaning that the initial value is correlated to the overall parametric roll process. If the initial value is greater than 15 degree, the curves have small differences. Therefore, the initial value should be large enough to yield a fully developed parametric roll distribution.

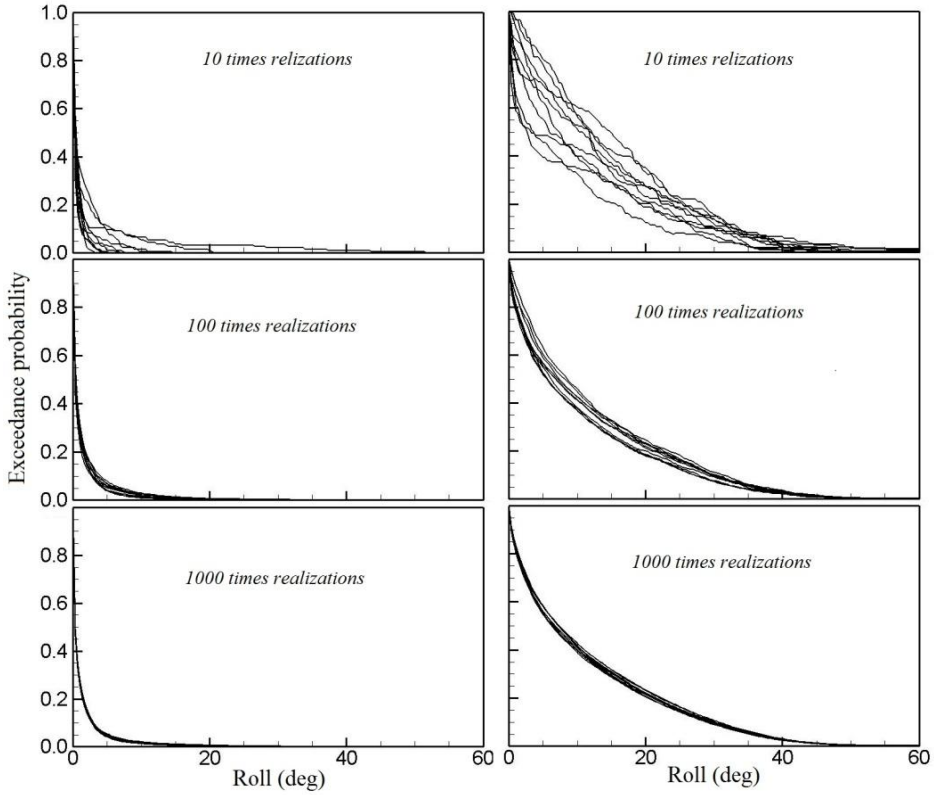


Figure 2.32 Exceedance probability for different numbers of realizations

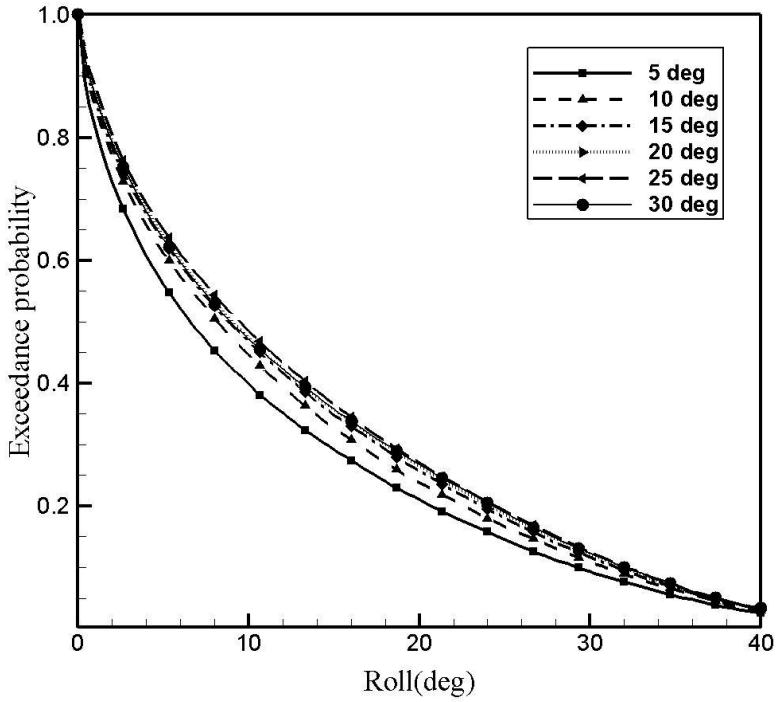


Figure 2.33 Exceedance probability for different initial roll angles

Run length, which is related to the number of realizations, is also an issue. The question is 'Which option is better, more realizations with a short run length or fewer realizations with a long run length?' Bulian [14] showed that the two options are equivalent. However, considering that more number of regular waves is needed to extend the run length, the first option would be preferable in a practical sense.

# Chapter 3. Theoretical Background

As already introduced in Section 1.2, there are several analytical and numerical approaches to parametric roll. In this section, theoretical backgrounds of those approaches are introduced from simple Mathieu equation to weakly nonlinear Rankine panel method.

## 3.1 1-DOF Mathieu equation

The linear roll equation of motion in longitudinal wave can be given by following equation.

$$(I_{44} + A_{44})\ddot{\phi} + \delta\dot{\phi} + \Delta \cdot g \cdot GZ(t) = 0 \tag{1}$$

where, $\phi$ is the roll angle, and $I_{44}$, $A_{44}$, $\Delta$ are the roll moment of inertia, the roll added moment inertia, and displacement, respectively. $\delta_1$ is linear damping coefficient. If we neglect higher order terms of GZ curve, GZ can be substituted by $GM(t) \cdot \phi$. The nonlinear terms take a very important role for lager roll angle but little role in initiation stage of parametric roll.

Time varying $GM(t)$ is modeled without higher order term as

$$GM(t) = GM_0 + GM_1 \cos(\omega t) \tag{2}$$

Then, Equation can be written as follows

$$\ddot{\phi} + \frac{\delta}{(I_{44} + A_{44})}\dot{\phi} + \frac{\Delta \cdot g}{(I_{44} + A_{44})}(GM_0 + GM_1 \cos(\omega t)\} = 0 \qquad (3)$$

We can define $\delta_n$, $\omega_n$ and $\omega_f$ as follows.

$$\delta_n = \frac{\delta}{(I_{44} + A_{44})}, \quad \omega_n = \sqrt{\frac{\Delta \cdot g \cdot GM_0}{(I_{44} + A_{44})}}, \quad \omega_f = \sqrt{\frac{\Delta \cdot g \cdot GM_1}{(I_{44} + A_{44})}} \qquad (4)$$

Substitution of theses definitions into equation and following transformation leads damped Mathieu equation.

$$\tau = \omega t, \quad '(\ )' = \frac{d}{d\tau}, \quad \mu = \frac{\delta_n}{\omega}, \quad p = \left(\frac{\omega_n}{\omega}\right)^2, \quad q = \left(\frac{\omega_f}{\omega}\right)^2 \qquad (5)$$

$$\phi'' + \mu\phi' + \{p + q\cos(\tau)\}\phi = 0 \qquad (6)$$

If $\mu$ is zero, Ince-Strutt diagram helps to determine stability regions.

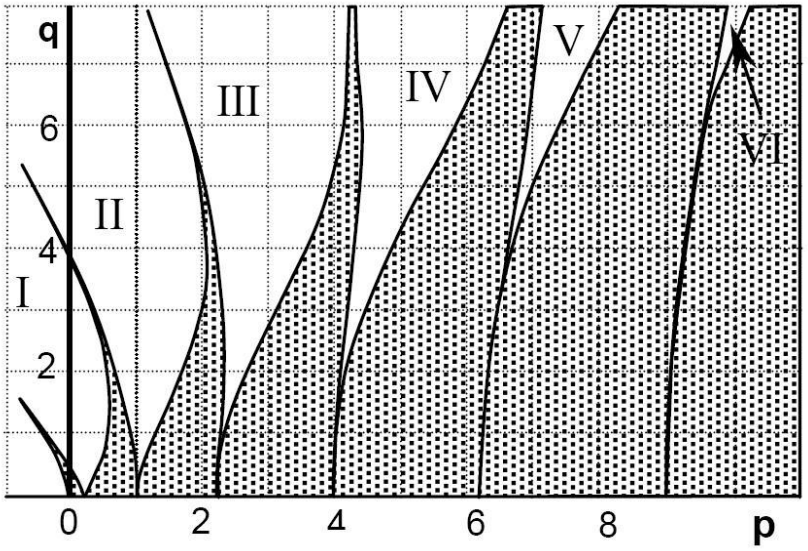


Figure 3.1 Ince-Strutt diagram

It is very easy and convenient to using Ince-Strutt diagram to identify parametric roll occurrence. However, it cannot give accurate results including steady state roll angle due to the lack of essential terms of restoring moment in this phenomenon.

## 3.2 1.5- DOF GM-GZ approximation

Let's consider the following 1-DOF equation of roll motion to describe parametric roll in longitudinal waves:

$$(I_{44} + A_{44})\ddot{\phi} + \delta_1\dot{\phi} + \delta_2\dot{\phi}|\dot{\phi}| + \Delta \cdot GZ(\phi, z, \theta, \zeta, t) = 0 \qquad (7)$$

The restoring lever GZ is affected mostly by the change of the water-plane area, which is a function of $\phi$, displacement of heave, $z$, pitch angle, $\theta$ and wave elevation $\zeta$. Considering the insignificant influence of roll motion on heave and pitch motions, it is not necessary to solve a fully coupled heave-roll-pitch equation, if 1-DOF roll motion can include explicitly the influence of heave and pitch motions. This means that pre-computed heave and pitch motions can be used to compute GZ. Therefore, the computational effort can be reduced significantly.

Better computational efficiency can be achieved if GZ can be properly approximated. In the analysis of above equation, GZ is an instantaneous quantity which can be obtained by the integration of the external pressure on the surface of a wetted ship. Such instantaneous direct pressure integration can require a significant computation time, particularly when a long simulation is considered for irregular waves. Therefore, if GZ can be

accurately and simply approximated, computation time can be significantly reduced.

### 3.2.1 GZ approximation

The shape of the GZ curve for still water is highly influenced by GM, which governs the slope of the curve for the upright condition or the zero roll angle. For many ship types, the GZ curve is very linear up to a certain roll angle before the side of a ship's deck is immersed into water. The linear region of the GZ curve reaches up to almost 30 degrees for container ships and to even larger degrees for tankers. This fact is still true for ships under motions in waves.

Figure 2.28 shows the fluctuations of actual GZ curves of a 10,000 TEU container ship when wave crests move the ship forward in head sea. Figure 2.28 (a), (b) and (c) show the GZ curves for wave lengths $\lambda$ of 2L, L and L/2. It shows that the GZ curves move up and down from the still water GZ curve according to wave condition, and the fluctuations are governed by the slope of the linear region. It also shows that the angles of the zero restoring moment are focused on a narrow range of angles where the still water GZ curve is zero regardless of the wave position or wave length.

From these observations, the GZ curve can be approximated as a function of the still water GZ curve and time variation of GM as follows.

$$GZ(\phi,t) = GZ_{still}(\phi) + \{GM(t) - GM_{still}\}\{\sin(\phi) - \sin^3(\phi)/\sin^2(\phi_{\max})\} \quad (8)$$

$\phi_{\max}$ is the angle where the still water GZ curve is zero. This equation enables the approximation of the GZ curve according to wave without the use of analytical functions, even when the shape is too complicated to be approximated properly. In the above equation, the only variable is the fluctuation of GM, which should be calculated considering the interaction among wave elevation, heave, pitch and hull shape.

Figure 3.2 shows GZ curves from direct calculation and approximated GZ curves by equation (8). It shows also approximated GZ curves proposed by US [23] and Japan [24] expressed by equation (9) and (10) respectively.

$$GZ(\phi,t) = \frac{GM(t)}{GM_{still}} GZ_{still}(\phi) \quad (9)$$

$$GZ(\phi,t) = GM_{still} + GM_0) \cdot \phi + \{GM_1 \cdot \cos(\omega t)\} \cdot \left\{1 - \left(\frac{\phi}{\pi}\right)^2\right\} \cdot \phi \quad (10)$$

Figure 3.3 to Figure 3.5 show GZ curves from direct calculation and approximated GZ curves for 5,500 TEU, 6,500 TEU and 8,000 TEU respectively, which show that the present method is very accurate compared to other methods.

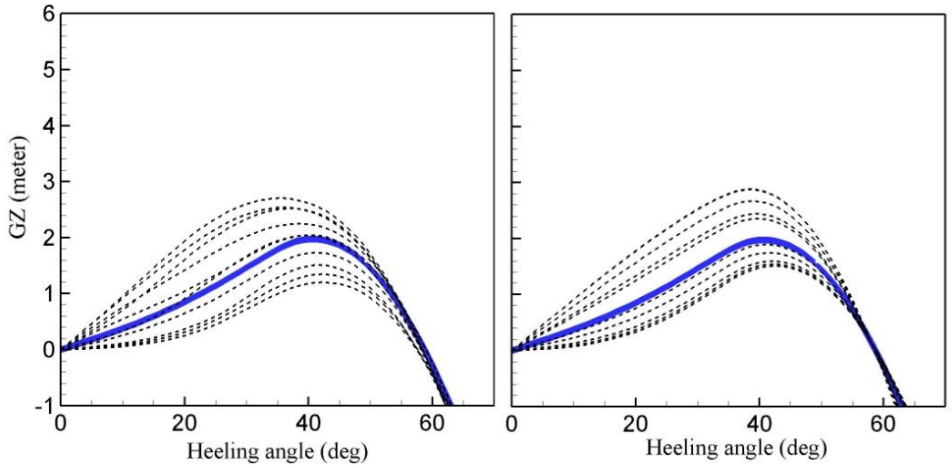


(a) Direct calculation (b) Proposed method

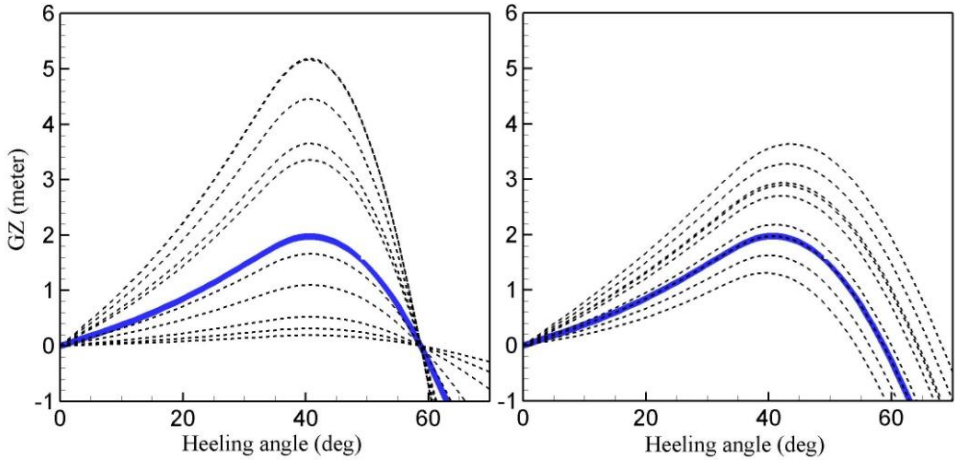


(c) Method 1 (d) Method 2

Figure 3.2 Comparison of GZ curves from direct calculation and several approximation methods for 10,000 TEU container ship ( $ka = 0.1$)

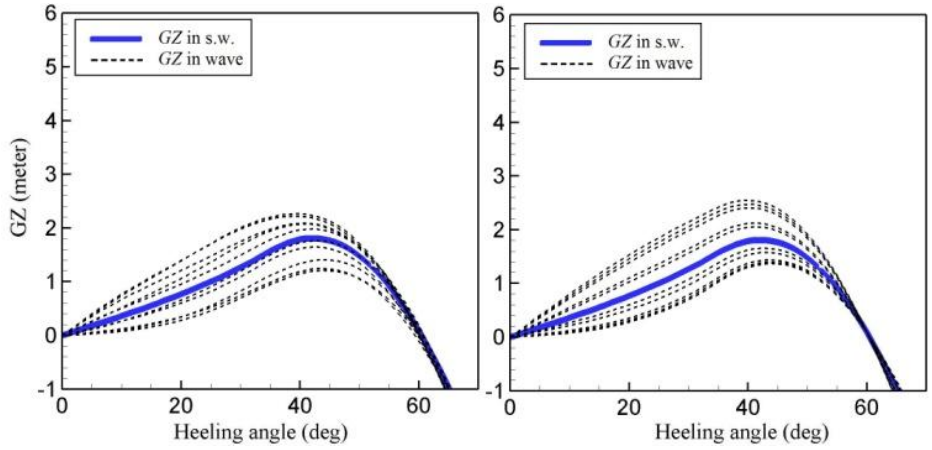


(a) Direct calculation (b) Proposed method

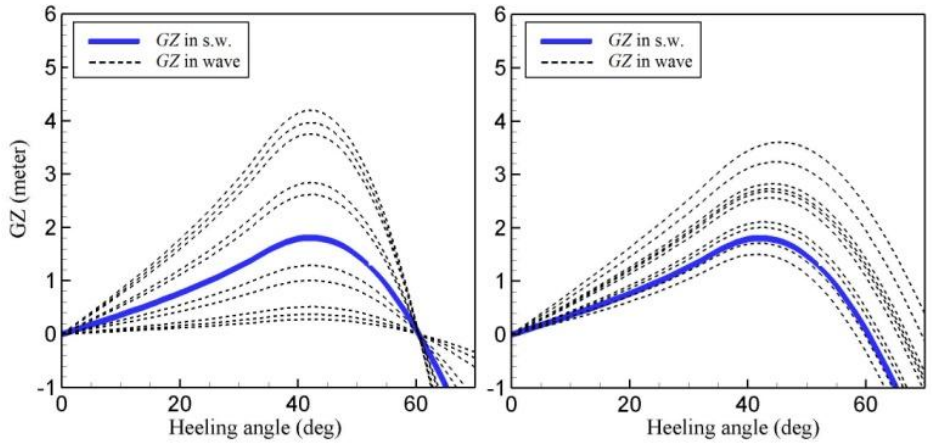


(c) Method 1 (d) Method 2

Figure 3.3 Comparison of GZ curves from direct calculation and several approximation methods for 5,500 TEU container ship ($ka = 0.1$)

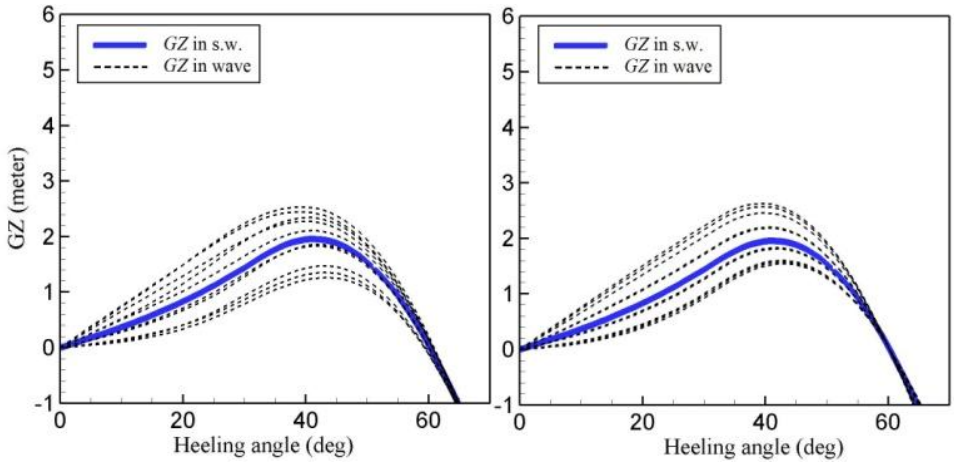


(a) Direct calculation (b) Proposed method

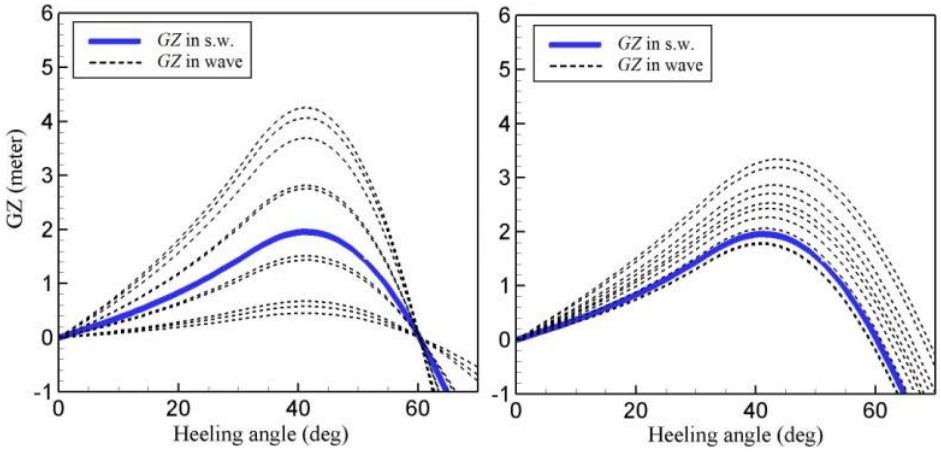


(c) Method 1 (d) Method 2

Figure 3.4 Comparison of GZ curves from direct calculation and several approximation methods for 6,500 TEU container ship ($ka = 0.1$)

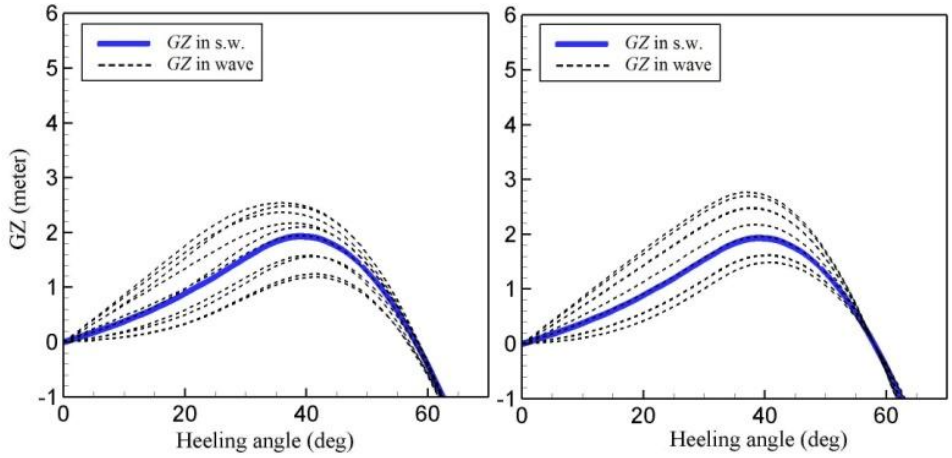


(a) Direct calculation (b) Proposed method

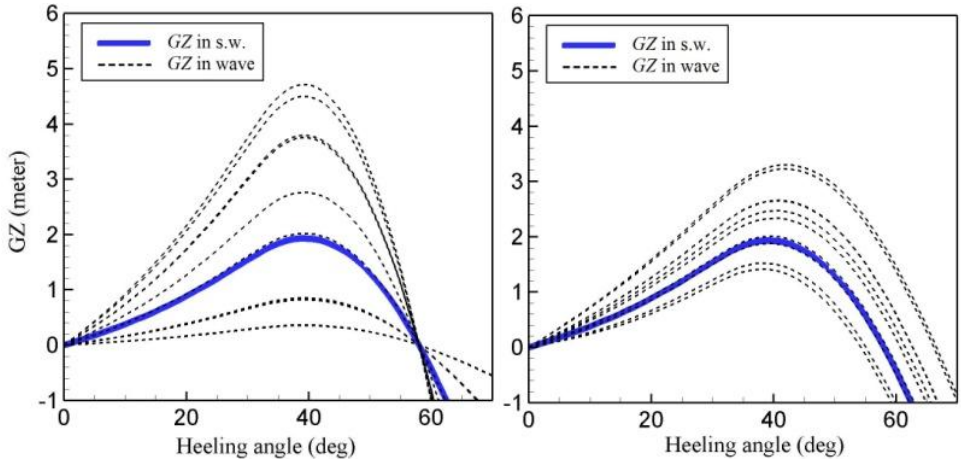


(c) Method 1 (d) Method 2

Figure 3.5 Comparison of GZ curves from direct calculation and several approximation methods for 8,000 TEU container ship ($ka = 0.1$)

### 3.2.2 Roll motion equation

The $GM(t)$ in (8) can be obtained for a regular wave with wave height $\zeta$, encounter frequency $\omega$ and phase angle $\alpha$ by equation (11) and for an irregular wave with significant wave height $Hs$ and zero crossing period $Tz$ by equation (12).

$$GM(t) = GM_{still} + \zeta \cdot RAO(GM_0, \omega) + \zeta \cdot RAO(GM_1, \omega) \cdot \cos(\omega t + \alpha) \quad (11)$$

$$\begin{aligned} GM(t) &= GM_{still} + GM_0(Hs, Tz) + \sum \zeta_i \cdot RAO(GM_1, \omega) \cdot \cos(\omega t + \alpha) \\ \zeta_i &= \sqrt{2 \cdot S(Hs, Tz, \omega_i d\omega} \end{aligned} \quad (12)$$

The substitution of (8) and (11) into (7) leads to the following roll equation for a regular wave.

$$\begin{aligned} &(I_{44} + A_{44})\ddot{\phi} + \delta_1\dot{\phi} + \delta_2\dot{\phi}|\dot{\phi}| + \Delta \cdot [GZ_{still}(\phi) + \zeta \cdot \{RAO\ (GM_{\ 0}, \omega) \\ &+ RAO\ (GM_{\ 1}, \omega) \cdot \cos(\omega t + \alpha)\} \cdot \{\sin(\phi) - \sin^3(\phi)/\sin^2(\phi_{\max})\}] = 0 \end{aligned} \quad (13)$$

The substitution of (8) and (12) in (7) leads to the following roll equation for an irregular wave.

$$\begin{aligned}&(I_{44}+A_{44})\ddot{\phi}+\delta_1\dot{\phi}+\delta_2\dot{\phi}\left|\dot{\phi}\right|+\Delta\cdot\left[GZ_{still}(\phi)+\left\{GM_0\left(Hs_0,Tz\right)\right.\right.\\&\left.\left.+\sum\zeta_i\cdot RAO\left(GM_1,\omega_t\right)\cdot\cos\left(\omega_i t+\alpha_i\right)\right\}\cdot\left\{\sin\left(\phi\right)-\sin^3(\phi)/\sin^2(\phi_{\max})\right\}\right]=0\end{aligned} \tag{14}$$

Lastly, transfer functions of $GM_0$ and $GM_1$ need to be obtained. Basically, the computation cost to obtain these transfer functions is not a critical problem because they will be computed only once before numerous numerical realizations are carried out by solving (13) or (14) to obtain a stable long-term result. Therefore, the transfer functions of $GM_0$ and $GM_1$ may be obtained by using any latest available tool, even if the tool requires time-consuming processing.

## 3.3 Impulse response function approach

This approach is basically the conversion of the frequency-domain solution into the time domain. Particularly, in this study, the conversion is limited to radiation force, and the excitation force includes the nonlinear Froude-Krylov force and restoring force on an instantaneous wetted surface as well as linear diffraction force. The wetted surface in the present computation is defined as the hull surface wetted by the body motion and incident wave (see Figure 3.6).

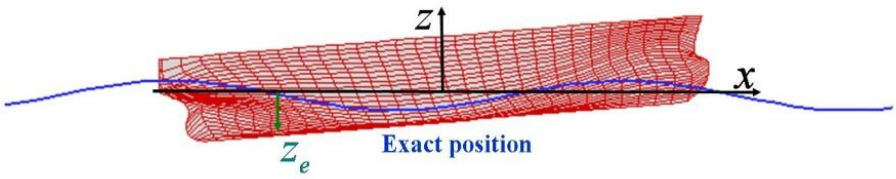


Figure 3.6 Definition of the wetted body surface

When the frequency-domain solution is known, the radiation force $F_{ROD}(t)$ can be calculated from the convolution integration of retardation function, $R(t)$, as follows:

$$F_{Rod}(t) = -M_{\infty}\ddot{\xi}(t) - \int_0^t R(t-\tau)\dot{\xi}(t)d\tau \tag{15}$$

The infinite-frequency added mass, $M_{\infty}$, and the retardation function can be obtained from pre-calculated hydrodynamic coefficients, as shown in equation (16) and (17). Either an added mass or damping coefficient can be used to obtain the retardation function. In the present study, the retardation function is obtained by using the damping coefficient.

$$M_{\infty} = M(\omega) + \frac{1}{\omega}\int_0^{\infty} R(t)\sin(\omega t)dt \tag{16}$$

$$R(t) = \frac{2}{\pi}\int_0^{\infty} b(\omega)\cos(\omega t)d\omega \tag{17}$$

Including the nonlinear Froude-Krylov and restoring forces, the equation of motion based on the IRF formulation can be written as follows:

$$\left(M+M_{\infty}\right)\zeta+\int_0^t R\left(t-\tau\right)\zeta\left(\tau\right)d\tau=\left(F_{F.K.}\right)_{nonlinear}+\left(F_{Diff}\right)+F_{Viscous}+F_{external} \quad (18)$$

where the force terms consist of Froude-Krylov, restoring, diffraction, viscous, and external forces. The diffraction force can be converted from the frequency-domain solution, and viscous force is added to the roll excitation component. In this study, an equivalent linear damping mechanism is applied. The external force includes the soft spring mechanism for non-restoring motions, but no such external force is needed for roll motion. Equation (18) can be solved by using a multi-step predictor-corrector method.

The amplitude of roll angle is sensitive to the viscous effect. In the actual physical problem, the viscous damping force is proportional to the quadratic of roll angular velocity, but the concept of an equivalent linear damping is popular for the ship motion analysis, e.g. Himeno. The equivalent damping coefficient is defined as follows:

$$F_{viscous}=-b_{equi\_viscous}\dot{\zeta} \quad (19)$$

$$b_{equi\_viscous}=b+\frac{8}{3\pi}\omega\phi_A b_{viscous} \quad (20)$$

$\phi_A$ and $\omega$ are the amplitude of roll motion and wave frequency, respectively. In addition, $b$ is the wave damping coefficient. The choice of the viscous damping coefficient would not be easy, because it is dependent on body shape, ship speed, wave frequency, and so on. For an easy numerical implementation, the equivalent linear viscous damping force defined in Equation (21) is adopted in this study. Here, $\gamma$ means the ratio with respect to the critical damping coefficient, and is generally in the range of 0.05~0.1. $C$ refers to the restoring coefficient of the considered motion, i.e. roll in this case.

$$b_{equi\_viscous} = b + 2\gamma\sqrt{(M + M_\infty)C} \tag{21}$$

The IRF approach requires a set of pre-computed hydrodynamic coefficients; however, when these are given, it has a strong advantage of fast computation time. This merit is important particularly for long-time prediction or many simulation cases.

## 3.4 3D Rankine panel method

A three-dimensional Rankine panel method is one of the most advanced methods to consider nonlinear effects. Recently, Kim et al. [31] introduced a new computer program based on a time-domain Rankine panel method, called WISH, under the support of several large shipbuilding companies. This program is used for the simulation of nonlinear ship motions in waves.

In this method, the total velocity potential is decomposed into three components as follows:

$$\phi(\vec{x},t) = \Phi(\vec{x},t) + \phi_{\mathrm{I}}(\vec{x},t) + \phi_d(\vec{x},t) \tag{22}$$

where $\Phi$, $\phi_I$, $\phi_D$ are the basis flow, incident wave, and disturbance velocity potentials, respectively. In the present weakly-nonlinear approach, the disturbed component of wave and velocity potential is assumed to be small. The kinematic, dynamic free surface boundary conditions and body boundary condition can then be linearized as follows:

$$\frac{\partial \zeta_d}{\partial t} - \left(\vec{U} - \nabla\Phi\right)\cdot\nabla\zeta_d = \frac{\partial \phi_d}{\partial z} - \nabla\Phi\cdot\nabla\zeta_{\mathrm{I}} + \frac{\partial^2\Phi}{\partial z^2}\left(\zeta_{\mathrm{I}} + \zeta_d\right) \; on \; z = 0 \tag{23}$$

$$\frac{\partial \zeta_d}{\partial t} - \left(\vec{U} - \nabla\Phi\right)\cdot\nabla\zeta_d = -g\zeta_d - \nabla\Phi\cdot\nabla\phi_I - \frac{\partial\Phi}{\partial t} + \left[\vec{U}\cdot\nabla\Phi - \frac{1}{2}\nabla\Phi\cdot\nabla\Phi\right] \qquad on\ z = 0 \tag{24}$$

$$\frac{\partial\Phi}{\partial n} = \vec{U}\cdot\vec{n} \qquad \text{on } S_B \tag{25}$$

$$\begin{aligned} \frac{\partial\phi_d}{\partial n} &= \sum_{j=1}^{6}\left(\frac{\partial\zeta_j}{\partial t}n_j + \zeta_j m_j\right) - \frac{\partial\phi_I}{\partial n} \qquad on\ S_B \\ \left(n_1,\ n_2,\ n_3\right) &= \vec{n} \\ \left(n_4,\ n_5,\ n_6\right) &= \vec{x}\times\vec{n} \\ \left(n_1,\ n_2,\ n_3\right) &= \left(\vec{n}\cdot\nabla\right)\left(\vec{U} - \nabla\Phi\right) \\ \left(n_4,\ n_5,\ n_6\right) &= \left(\vec{n}\cdot\nabla\right)\left(\vec{x}\times\left(\vec{U} - \nabla\Phi\right)\right) \end{aligned} \tag{26}$$

where the subscripts, I and d, refer to the incident wave and disturbance components, respectively. In addition, $\vec{n}$ indicates the normal velocity on the body surface. The m-terms in Equation (26), $m_j$, is hard to compute, since these require the second-order differentials of the basis flow. In this computation, the second-order differentials are converted to the first-order differentials by using Stoke's theorem.

The present study adopts the bi-quadratic B-spline basis function for physical variables, so that the variables can be written as follows:

$$\begin{bmatrix} \phi_d \\ \dfrac{\partial \phi_d}{\partial n} \\ \zeta_d \end{bmatrix}(\vec{x},t) = \sum_j \begin{bmatrix} (\phi_d)_j \\ \left(\dfrac{\partial \phi_d}{\partial n}\right)_j \\ (\zeta_d)_j \end{bmatrix}(t) B_j(\vec{x}) \tag{27}$$

where $B_j(\vec{x})$ is the B-spline basis function. By solving the Green second identity as well as the above boundary conditions, the solution of the boundary value problem can be obtained.

$$\phi_d + \iint_{S_B} \phi_d \frac{\partial G}{\partial n} dS - \iint_{S_F} \frac{\partial \phi_d}{\partial n} G dS = \iint_{S_B} \frac{\partial \phi_d}{\partial n} G dS - \iint_{S_F} \phi_d \frac{\partial G}{\partial n} dS \tag{28}$$

In time-marching, the instantaneous wave elevation can be obtained by the time integration of Equation (28), and the velocity potential on a free surface can be obtained from Equation (27). The hydrodynamic forces due to radiation and diffraction can be obtained by direct integration of pressure on the hull surface. Similarly to the IRF approach, the nonlinear Froude-Krylov and restoring forces are obtained by taking into account the actual wetted hull surface.

## 3.5 Comparison of different approaches

The parametric roll calculation results from this numerical model for a 6,500 TEU container ship are compared to the results from the 3D weakly nonlinear potential code called WISH [17] as shown in Figure 3.7. The wave slope is equal to $ka = 0.1$. Still water GM is 1meter.

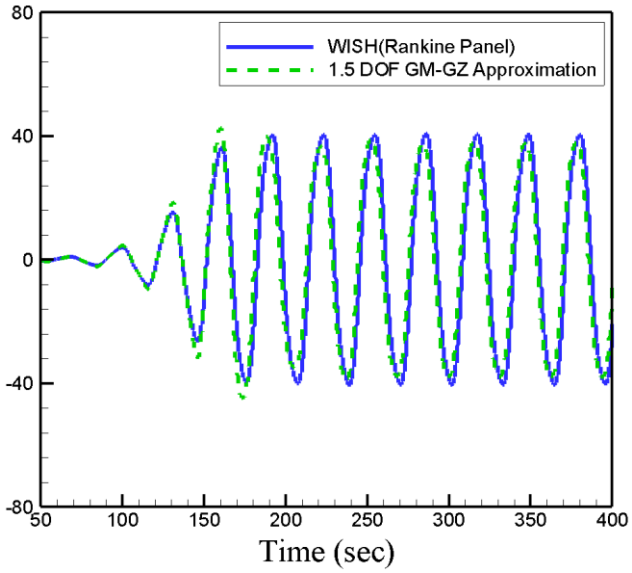


(a) $\lambda / L = 0.8$

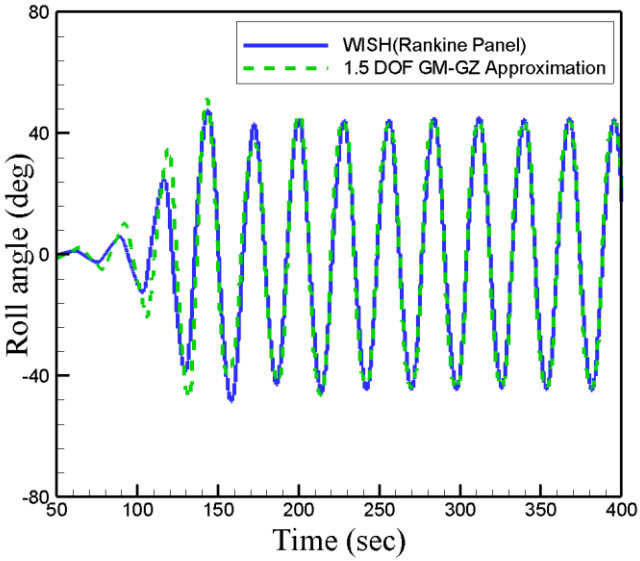


(b) $\lambda / L = 1.0$

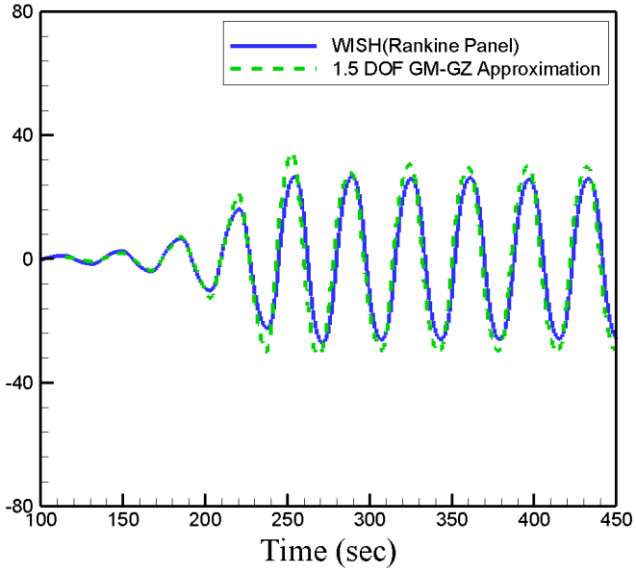


(c) $\lambda / L = 1.2$

Figure 3.7 Comparison of parametric roll results between 3D potential code and 1.5-DOF GM-GZ approximation approach

The results of Rankine panel method and 1.5-DOF GM-GZ approximation approach are carried out for three different waves. The steady roll angles are in good correspondence, but there are some discrepancies in the transient region. 1.5-DOF GM-GZ approximation gives unstable response in the transient region. The reason is assumed that the self-excitation energy can be transferred to other DOFs such as sway and yaw in 6-DOF Rankine panel method, while it acts only on roll motion in 1.5-DOF GM-GZ approximation approach.

# Chapter 4. A Multi-Level Approach for Evaluation of Parametric Roll

## 4.1 General

In this chapter, method to evaluate the vulnerability to parametric roll is provided. The method consists of multi-level approaches for efficient evaluation. Application of multi-level approach can reduce assessment time significantly. For example, tankers are hardly vulnerable to parametric roll because the geometrical nonlinearity of hull is very weak and the GM is always kept high. Therefore, it is not necessary to apply very high level and time-consuming approach to assess vulnerability of tankers to parametric roll. Just simple check of resonance can be enough.

The multi-level approaches in this paper consist of resonance check ($1^{st}$ level), regular wave check ($2^{nd}$ level), irregular wave check ($3^{rd}$ level) and operational guidance.

The environmental conditions is developed based on North Atlantic Wave Data from IACS because ships which are allowed to go anywhere on the globe without any restriction should be designed to survive in North Atlantic Sea which is known to be the most dangerous area.

## 4.2 Environmental conditions.

Table 4.1 shows North Atlantic Wave Data. The total observation number is 100,000. For irregular wave check ($3^{rd}$ level), the wave data can be directly used as it is. No process is necessary. In $3^{rd}$ level check, actual loading conditions, speeds and headings are also to be considered.

However, $1^{st}$ and $2^{nd}$ level checks are to be done for regular waves. Therefore reference regular waves are to be extracted from the wave data.

Table 4.1 IACS Standard Wave Data at North Atlantic Sea

| Hs\Tz | 3.5 | 4.5 | 5.5 | 6.5 | 7.5 | 8.5 | 9.5 | 10.5 | 11.5 | 12.5 | 13.5 | 14.5 | 15.5 | 16.5 | 17.5 | 18.5 | Sum |
|---|---|---|---|---|---|---|---|---|---|---|---|---|---|---|---|---|---|
| 0.5 | 1.3 | 133.7 | 865.6 | 1186 | 634.2 | 186.3 | 36.9 | 5.6 | 0.7 | 0.1 | 0 | 0 | 0 | 0 | 0 | 0 | 3050.4 |
| 1.5 | 0 | 29.3 | 986 | 4976 | 7738 | 5570 | 2376 | 703.5 | 160.7 | 30.5 | 5.1 | 0.8 | 0.1 | 0 | 0 | 0 | 22575.4 |
| 2.5 | 0 | 2.2 | 197.5 | 2159 | 6230 | 7450 | 4860 | 2066 | 644.5 | 160.2 | 33.7 | 6.3 | 1.1 | 0.2 | 0 | 0 | 23810.4 |
| 3.5 | 0 | 0.2 | 34.9 | 695.5 | 3227 | 5675 | 5099 | 2838 | 1114 | 337.7 | 84.3 | 18.2 | 3.5 | 0.6 | 0.1 | 0 | 19127.7 |
| 4.5 | 0 | 0 | 6 | 196.1 | 1354 | 3289 | 3858 | 2686 | 1275 | 455.1 | 130.9 | 31.9 | 6.9 | 1.3 | 0.2 | 0 | 13289.4 |
| 5.5 | 0 | 0 | 1 | 51 | 498.4 | 1603 | 2373 | 2008 | 1126 | 463.6 | 150.9 | 41 | 9.7 | 2.1 | 0.4 | 0.1 | 8328.1 |
| 6.5 | 0 | 0 | 0.2 | 12.6 | 167 | 690.3 | 1258 | 1269 | 825.9 | 386.8 | 140.8 | 42.2 | 10.9 | 2.5 | 0.5 | 0.1 | 4806.3 |
| 7.5 | 0 | 0 | 0 | 3 | 52.1 | 270.1 | 594.4 | 703.2 | 524.9 | 276.7 | 111.7 | 36.7 | 10.2 | 2.5 | 0.6 | 0.1 | 2586.2 |
| 8.5 | 0 | 0 | 0 | 0.7 | 15.4 | 97.9 | 255.9 | 350.6 | 296.9 | 174.6 | 77.6 | 27.7 | 8.4 | 2.2 | 0.5 | 0.1 | 1308.5 |

| Hs\Tz | 3.5 | 4.5 | 5.5 | 6.5 | 7.5 | 8.5 | 9.5 | 10.5 | 11.5 | 12.5 | 13.5 | 14.5 | 15.5 | 16.5 | 17.5 | 18.5 | Sum |
|---|---|---|---|---|---|---|---|---|---|---|---|---|---|---|---|---|---|
| 9.5 | 0 | 0 | 0 | 0.2 | 4.3 | 33.2 | 101.9 | 159.9 | 152.2 | 99.2 | 48.3 | 18.7 | 6.1 | 1.7 | 0.4 | 0.1 | 626.2 |
| 10.5 | 0 | 0 | 0 | 0 | 1.2 | 10.7 | 37.9 | 67.5 | 71.7 | 51.5 | 27.3 | 11.4 | 4 | 1.2 | 0.3 | 0.1 | 284.8 |
| 11.5 | 0 | 0 | 0 | 0 | 0.3 | 3.3 | 13.3 | 26.6 | 31.4 | 24.7 | 14.2 | 6.4 | 2.4 | 0.7 | 0.2 | 0.1 | 123.6 |
| 12.5 | 0 | 0 | 0 | 0 | 0.1 | 1 | 4.4 | 9.9 | 12.8 | 11 | 6.8 | 3.3 | 1.3 | 0.4 | 0.1 | 0 | 51.1 |
| 13.5 | 0 | 0 | 0 | 0 | 0 | 0.3 | 1.4 | 3.5 | 5 | 4.6 | 3.1 | 1.6 | 0.7 | 0.2 | 0.1 | 0 | 20.5 |
| 14.5 | 0 | 0 | 0 | 0 | 0 | 0.1 | 0.4 | 1.2 | 1.8 | 1.8 | 1.3 | 0.7 | 0.3 | 0.1 | 0 | 0 | 7.7 |
| 15.5 | 0 | 0 | 0 | 0 | 0 | 0 | 0.1 | 0.4 | 0.6 | 0.7 | 0.5 | 0.3 | 0.1 | 0.1 | 0 | 0 | 2.8 |
| 16.5 | 0 | 0 | 0 | 0 | 0 | 0 | 0 | 0.1 | 0.2 | 0.2 | 0.2 | 0.1 | 0.1 | 0 | 0 | 0 | 0.9 |
| Sum | 1.3 | 165.4 | 2091 | 9280 | 19922 | 24879 | 20870 | 12898 | 6245 | 2479 | 836.7 | 247.3 | 65.8 | 15.8 | 3.4 | 0.7 | 100000 |

The wave energy in actual irregular sea state is concentrated on the modal frequency. Therefore, the frequencies of reference waves are chosen by the modal frequency. The wave spectrum of North Atlantic is Pierson-Moscowitz spectrum. Then, the modal frequency $T_O$ can be converted from zero crossing period, $T_Z$ as follows.

$$T_O = 1.41 T_Z \tag{1}$$

The wave length $\lambda$ is determined as follows.

$$\lambda = \frac{g T_O}{2\pi} \tag{2}$$

If we define as $P_{ij}$ the probability associated with the short-term sea state $(T_{Z,i}, H_{1/3,j})$ characterized by period $T_{Z,i}$ and significant wave height $H_{1/3,j}$, the conditional average significant wave height $E\{H_{1/3,j} \mid T_{Z,i}\}$ is determined as follows.

$$E\left\{H_{1/3,j} \middle| T_{Z,i}\right\} = \frac{1}{W_i} \sum P_{ij} \cdot H_{1/3,j} \tag{3}$$

where, $W_i = \sum P_{ij}$

Then Table 4.2 shows the period, length, wave height and wave steepness of reference waves.

Table 4.2 Reference waves for regular wave test

| $T_Z$ | $T_O$ | $W_i$ | $\lambda$ | $E\{H_{1/3,j} \mid T_{Z,i}\}$ | Steepness |
|---|---|---|---|---|---|
| 3.5 | 4.94 | 1.3 | 38.04 | 0.500 | 0.0131 |
| 4.5 | 6.35 | 165.4 | 62.89 | 0.707 | 0.0112 |
| 5.5 | 7.76 | 2091.2 | 93.94 | 1.225 | 0.0130 |
| 6.5 | 9.17 | 9279.9 | 131.21 | 1.850 | 0.0141 |
| 7.5 | 10.58 | 19921.8 | 174.69 | 2.474 | 0.0142 |
| 8.5 | 11.99 | 24878.8 | 224.38 | 3.150 | 0.0140 |
| 9.5 | 13.40 | 20869.9 | 280.28 | 3.852 | 0.0137 |
| 10.5 | 14.81 | 12898.4 | 342.39 | 4.537 | 0.0132 |
| 11.5 | 16.22 | 6244.6 | 410.72 | 5.179 | 0.0126 |
| 12.5 | 17.63 | 2479 | 485.25 | 5.771 | 0.0119 |
| 13.5 | 19.04 | 836.7 | 566.00 | 6.315 | 0.0112 |
| 14.5 | 20.45 | 247.3 | 652.96 | 6.813 | 0.0104 |
| 15.5 | 21.86 | 65.8 | 746.12 | 7.281 | 0.0098 |
| 16.5 | 23.27 | 15.8 | 845.50 | 7.671 | 0.0091 |
| 17.5 | 24.68 | 3.4 | 951.09 | 8.029 | 0.0084 |
| 18.5 | 26.09 | 0.7 | 1062.90 | 8.500 | 0.0080 |

## 4.3 Development of a multi-level approach

### 4.3.1 Multi-level approach

A multi-level approach which consists of 3 levels and one operational guidance is proposed in this thesis. The 1st level is a simple resonance check for the reference waves. This level uses analytical forms and doesn't provide the steady roll angle but check whether parametric roll occurs or not. If a ship passes this level, it means the ship is conventional type. If the ship doesn't pass this level, the ship is unconventional and it may be vulnerable to parametric roll. Then 2nd level approach should be applied.

The 2nd level check is carried out for regular waves for the reference waves. In this level, the roll amplitude is obtained using 1-dof roll motion equation. The total probability that the roll exceeds certain reference value is used for the criteria. If the ship passes this level, it means the ship's vulnerability is not severe and the ship is safe. If the ship doesn't pass this level, quantity analysis should be done for irregular waves in North Atlantic Wave Data using 3rd level check.

If the ship doesn't pass the 3rd level, ship design should be changed or operational guidance should be provided to avoid dangerous situations.

Table 4.34 shows the specifications which all levels comply with. The most important requirement is to keep consistency through the whole approaches. The ship which doesn't pass lower level should not pass the higher levels.

Therefore, the standard of each level should be chosen carefully based on many sample results for various types of ships and all stake-holders such as ship owners, designers, Governments and Classifications should be joined to determine these values.

Table 4.3 Specifications of multi-level approach

| Level | Environment | Complexity | Safety Margin | Objective |
|---|---|---|---|---|
| 1st Level | Regular wave | Low | High | Identification of conventional ships (Tanker, Bulk carrier) |
| 2nd Level | Regular wave | Moderate | Moderate | Identification of less susceptible ships |
| 3rd Level | Irregular wave | High | Low | Evaluation of safety level based on ship performance |
| 4th Level | Real sea condition | Very High | Very Low | Operational Guidance for decision supporting to avoid parametric roll |

Figure 4.1 shows flow chart for application of the multi-level approach. The complexity or man-hour requirement are carefully calibrated according to the purpose and accuracy needed for each level.

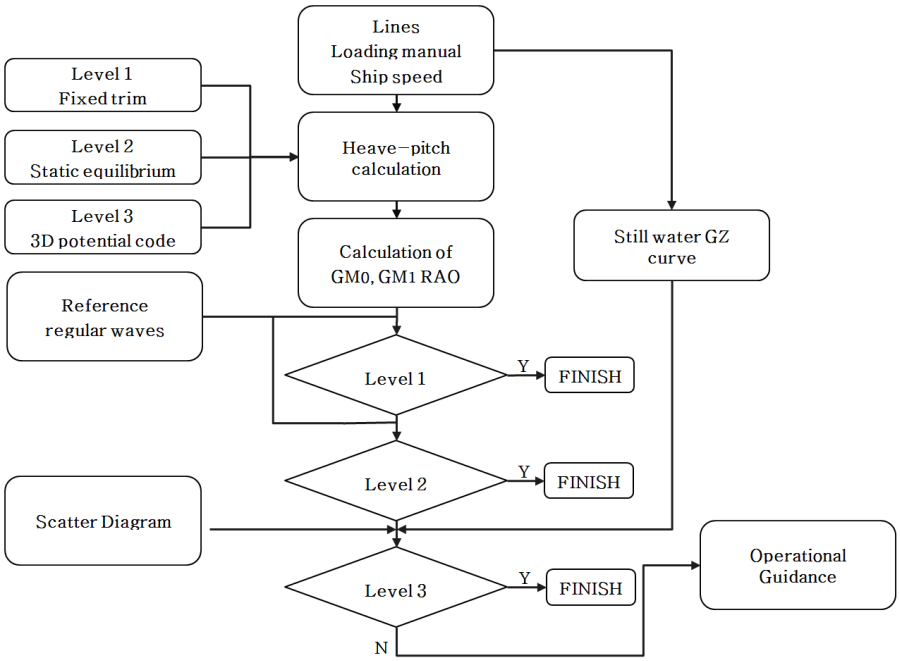


Figure 4. 1 Flow chart of the multi-level approach

### 4.3.2 1st level (resonance check)

The Mathieu equation in Section 3.1 is used for resonance check in this level according to following procedure.

a. $GM_0$ and $GM_1$ is calculated using ship shape information for reference waves.

b. The encounter frequency $\omega_e$ is calculated as follows

$$\omega_e = \omega_w + \frac{\omega_w^{\ 2}}{g} V \qquad in\ \ head\ \ sea$$
$$\omega_e = \omega_w - \frac{\omega_w^{\ 2}}{g} V \qquad in\ \ following\ \ sea \tag{4}$$

c. Following coefficients are calculated for the use of Mathieu equation according to Sec. 3.1

$$\mu = \frac{\delta_n}{\omega_e}, \quad p = \left(\frac{\omega_n}{\omega_e}\right)^2, \quad q = \left(\frac{\omega_f}{\omega_e}\right)^2$$
$$\delta_n = \frac{\delta}{\left(I_{44} + A_{44}\right)}, \quad \omega_n = \sqrt{\frac{\Delta \cdot g \cdot GM_0}{\left(I_{44} + A_{44}\right)}}, \quad \omega_f = \sqrt{\frac{\Delta \cdot g \cdot GM_1}{\left(I_{44} + A_{44}\right)}} \tag{5}$$

d. Using Ince-Strutt diagram or numerical method, following equation is solved. If the roll diverges, the parametric roll occurs.

$$\phi'' + \mu\phi' + \left\{p + q\cos(\tau)\right\}\phi = 0 \tag{6}$$

Three still water GM should be chosen as minimum value. The ship speed is chosen as zero speed for convenience.

### 4.3.3 2nd level (regular wave check)

The GZ approximation method is used to get the roll angle for the reference waves.

$$\begin{aligned}&(I_{44}+A_{44})\ddot{\phi}+\delta_1\dot{\phi}+\delta_2\dot{\phi}|\dot{\phi}|+\Delta\cdot\left[GZ_{still}(\phi)+\zeta\cdot\left\{RAO(GM_0,\,\omega)\right.\right.\\&\left.\left.+RAO(GM_1,\omega)\cdot\cos(\omega t+\alpha)\right\}\cdot\left\{\sin(\phi)-\sin^3(\phi)/\sin^2(\phi_{\max})\right\}\right]=0\end{aligned} \tag{7}$$

If the maximum roll is larger than reference roll angle $\phi_{ref}$ , the ship is judged to be vulnerable to parametric roll

### 4.3.4 3rd level (Irregular wave check)

The GZ approximation method is used to get the roll angle for the reference waves.

$$\begin{aligned}&(I_{44}+A_{44})\ddot{\phi}+\delta_1\dot{\phi}+\delta_2\dot{\phi}|\dot{\phi}|+\Delta\cdot\left[GZ_{still}(\phi)+\left\{GM_0(Hs,Tz)\right.\right.\\&\left.\left.+\sum\zeta_i\cdot RAO\ (GM_1,\omega_t)\cdot\cos(\omega_i t+\alpha_i)\right\}\cdot\left\{\sin(\phi)-\sin^3(\phi)/\sin^2(\phi_{\max})\right\}\right]=0\end{aligned} \tag{8}$$

The long-term predictions of parametric roll are carried out by applying Monte-Carlo simulation under following calculation condition.

- Wave data : North Atlantic

- Initial roll angle : 15 deg.
- Simulation time : 40 min, first 20 min cut off
- Simulation number : 1,000 times
- Still water GM : Minimum value. Maximum value, average value
- Ship speed : Zero speed, Maximum speed, Mean speed
- Heading angle, $\alpha$ : Head sea, Following sea

The probability of exceeding the roll angle $\phi$ is calculated by the following equations.

$$P(x>\phi)=\sum_{i}\sum_{j}\sum_{k}\sum_{l}\sum_{m}P\left(x>\phi,\ Hs_i,\ Tz_j,\ GM_k,\ V_l,\ \alpha_m\right) \cdot P\left(Hs_i,\ Tz_j\right)\cdot P(GM_k)\cdot P(V_l)\cdot P(\alpha_m) \tag{9}$$

### 4.3.5 Operational guidance

Ship designers and owners will face limitation in the design change for the purpose of mitigating parametric roll because any changes would increase shipbuilding cost and may sacrifice cargo capacity because such changes result in the reductions of the flare angle and the long transom stern. Increase of the $GM$ value results in excessive transverse acceleration and reinforcement of the cargo securing system. Installing roll damping devices may be effective but still expensive.

One of the best ways to solve this problem economically would be to provide operational guidance for the ship crews to avoid very dangerous situations. If the ship can be avoided severe environmental and operational conditions that can generate parametric roll, the occurrence probability can be reduced dramatically to be satisfied with criteria. Such an operational guidance can be implemented by using the latest advanced tools which can deal with 6-DOF ship motions, arbitrary heading angles and various ship speeds. However, to develop a precise operational guidance to support decision making, many cases dealing with several $GM_{steel}$ s, speeds, heading angles and sea states should be analyzed. In this level, the impulse-response-function (IRF) approach is used to develop operational guidance, keeping the accuracy of operational guidance and efficiency of numerical computation. Table 4.4 shows the calculation conditions for developing the operational guidance

Table 4.4 Calculation condition for operational guidance

| Parameter | Value |
|---|---|
| Hs(m) | 6, 7, 8 |
| Heading (deg.) | 0 ~ 360 (15 increment) |
| Tz(sec) | 25, 18, 14, 10, 8 |
| $GM_{steel}$ (m) | Max, Min, Ave |
| Speed(knots) | 0 ~ 10(1.0 increment) |

## 4.4 Comparison with ABS Guide

ABS has developed guide for parametric roll assessment in 2004 [1] and it's the only guideline for parametric roll. It consists of 'Susceptibility check', 'Severity check', 'Numerical simulation' and 'Operational guidance'. Table 4.5 shows comparison results between the proposed method and ABS method. The proposed approach method uses design wave sets on behalf of wave scatter diagram for 1st and 2nd level check, while ABS guide uses only one design wave of which has length is same to ship length. In 3rd level check, the proposed method uses probability level obtained from a number of numerical realizations to overcome non-ergodicity, while ABS guide uses 5 times realizations. ABS approach may give very unstable results because there is big deviation of maximum roll angles in 5 times realizations. ABS guide proposes just commercial software for 2nd level and 3rd level check but detailed specification of numerical schemes are proposed in this thesis.

Table 4.5 Comparison with ABS Guide

| Parameter | Proposed method | ABS Method |
|---|---|---|
| 1st Level check | Mathieu Equation<br>Resonance check<br>Design wave sets | Mathieu Equation<br>Resonance check<br>One design wave |
| 2nd Level check | Regular wave test<br>1.5-DOF GM-GZ approximation<br>Design wave sets | Regular wave test<br>Any commercial code<br>One design wave |
| 3rd Level Check | Irregular wave test<br>All sea states<br>1.5-DOF GM-GZ approximation<br>1,000 Times for each state<br>Safety level | Irregular wave test<br>All sea states<br>Potential cod<br>5 times for each state<br>Max Roll angle e |
| Operational Guidance | Most advanced tools<br>Polar diagram | Same to 3rd Level Check<br>Polar diagram |

# Chapter 5. Application to Real Ships

## 5.1 Sample ship selection

Ship types which are known to be most vulnerable to parametric roll are container ships, passenger ships and PCTCs. Therefore, 4 typical container ships, 3 PCTCs and 3 passenger ships with various ship lengths are selected as sample ships. One VLCC and S175 which are free from parametric roll are also added for reference. The dimensions are shown in Table 5.1 for container ships and VLCC and Table 5.2 for PCTCs and passenger ships. 'Pass' means passenger ships and the number is identification number of classification society.

Table 5.1 Main dimension of typical container ships and a VLCC

| | 5500 TEU | 6500 TEU | 8000 TEU | 10000 TEU | S175 | VLCC |
|---|---|---|---|---|---|---|
| L(m) | 263.0 | 286.3 | 309.2 | 334.0 | 175.0 | 322.0 |
| B(m) | 40.0 | 40.0 | 42.8 | 45.6 | 25.4 | 59.6 |
| D(m) | 24.2 | 24.2 | 24.6 | 27.3 | 17.5 | 30.5 |
| d(m) | 12.0 | 12.0 | 13.0 | 13.0 | 9.5 | 21.0 |
| s(kts.) | 25.0 | 25.0 | 25.0 | 25.0 | 20.0 | 15.0 |

Table 5.2 Main dimension of passenger ships and PCTC

| | PCTC 4800 | PCTC 6500 | PCTC 8100 | Pass 8754 | Pass 0254 | Pass 9051 |
|---|---|---|---|---|---|---|
| L(m) | 174.0 | 189.3 | 222.4 | 123.0 | 150.0 | 171.0 |
| B(m) | 30.6 | 32.3 | 32.3 | 23.0 | 23.6 | 24.8 |
| D(m) | 29.7 | 32.6 | 32.6 | 12.5 | 14.55 | 9.50 |
| d(m) | 8.2 | 9.0 | 9.0 | 5.467 | 5.60 | 6.92 |
| s(kts.) | 18.0 | 18.0 | 18.0 | 20.0 | 20.0 | 20.0 |

## 5.2 Multi-level vulnerability check

### 5.2.1 RAO of $GM_0$ and $GM_1$

The RAO of $GM_0$ and $GM_1$ is the base of all levels of vulnerability check. Those are dependent on ship length, hull shape, flare angle, transom stern and the length of parallel middle body. Therefore, those are very different according to the ship types, sizes and designs.

Figure 5.1 to Figure 5.6 show RAOs of various ship types and ship lengths.

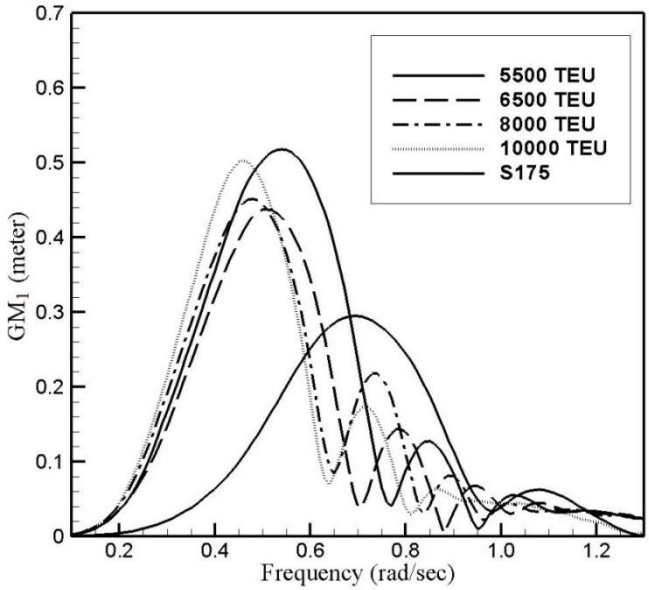


Figure 5. 1 RAO of $GM_1$ for container ships

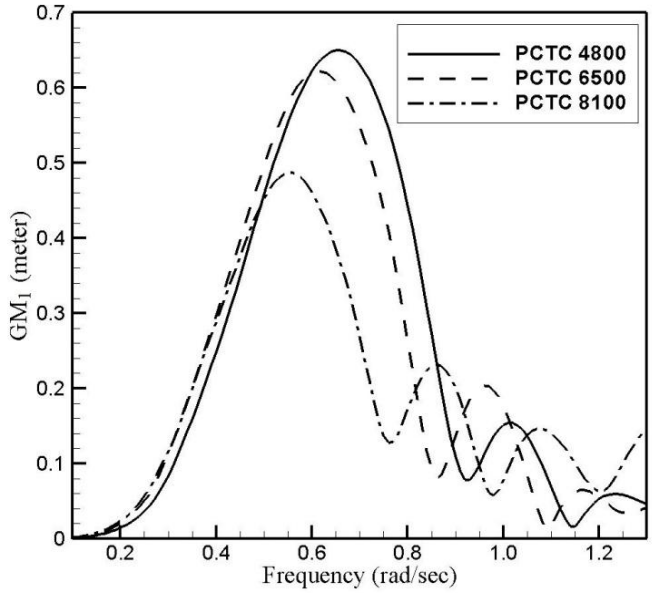


Figure 5. 2 RAO of $GM_1$ for PCTCs

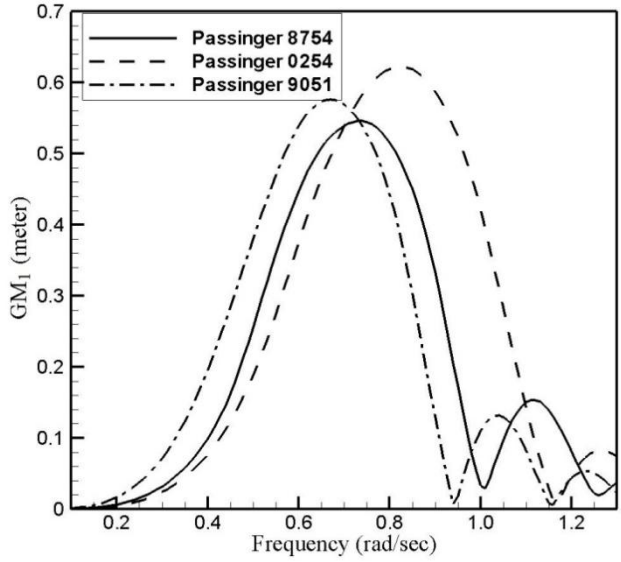


Figure 5. 3 RAO of $GM_1$ for passenger ships

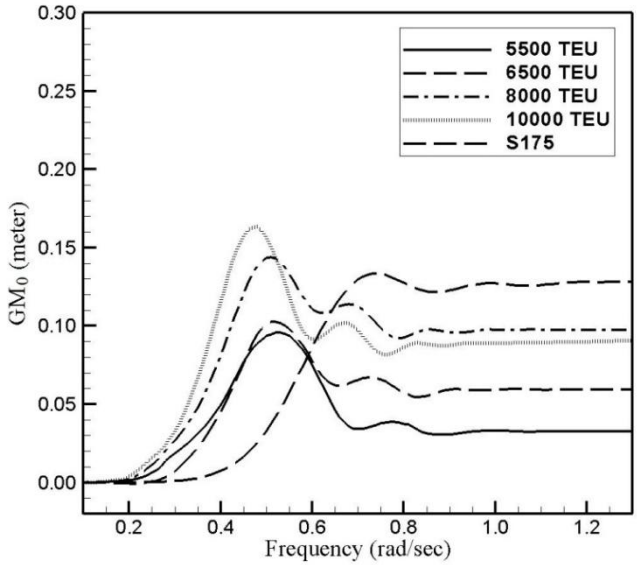


Figure 5. 4 RAO of $GM_0$ for container ships

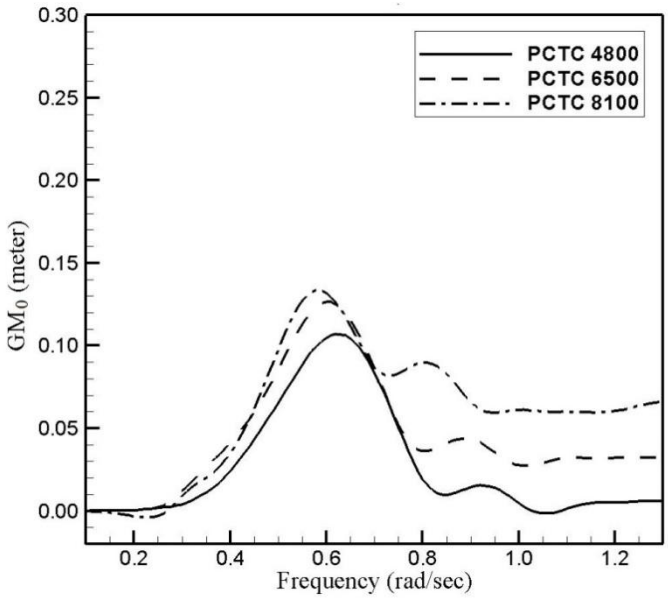


Figure 5. 5 RAO of $GM_0$ for PCTCs

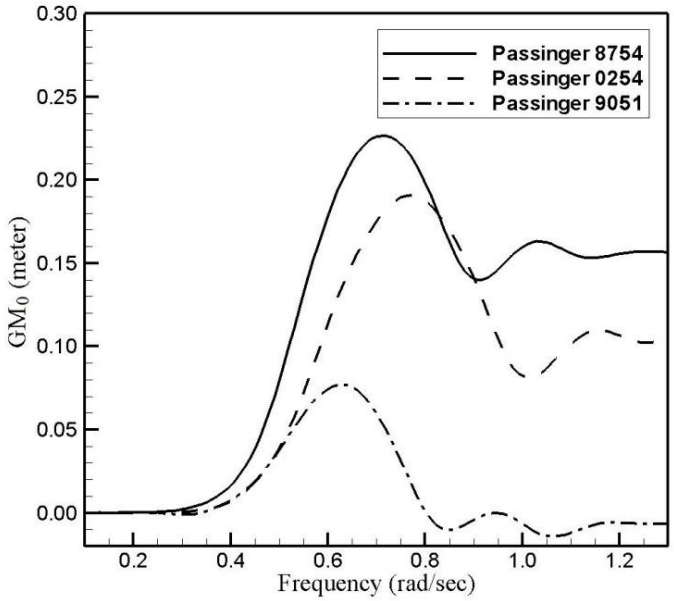


Figure 5. 6 RAO of $GM_0$ for passenger ships

The $GM_1$ RAO of container ships are not so high as PCTCs but the modal frequencies are near main wave zones of North Atlantic Sea because of long ship length. However, $GM_1$ RAO of S175 is small because it has no transom and the flare angle is small. The $GM_1$ RAO of PCTCs are quite high and the modal frequencies are near main wave zones. The $GM_1$ RAO of passenger ships are quite high but the modal frequencies are out of main energy zones because of short ship length.

The $GM_0$ RAO are quite different according to not only ship type but also ship length. It seems $GM_0$ RAO is dependent on average water plane area.

### 5.2.1 1st level (resonance check)

1st level check is carried out for reference waves shown in Table 4.2. Figure 5.7 to Figure 5.9 show the results for container ships, PCTCs, passenger ships and VLCC respectively. If damping effects are considered, S175 and VLCC are judged not to be vulnerable to parametric roll. All PCTCs and 5500 TEU and 6500 TEU are judged clearly to be vulnerable. In case of Passenger 8754, Passenger 0254, 8000 TEU and 10000 TEU are judged to be vulnerable but not clearly. 1st level check only indicates parametric roll is possible or not but 'how much vulnerable it is' cannot be evaluated.

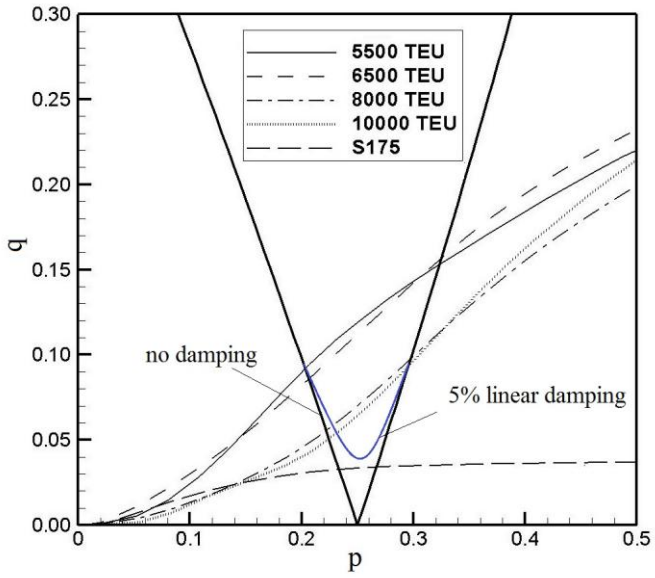


Figure 5. 7 1st level check for container ships

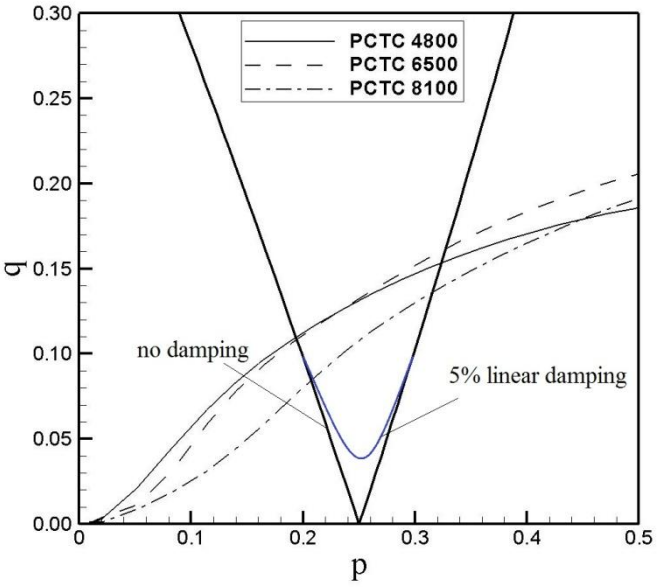


Figure 5. 8 1st level check for PCTCs

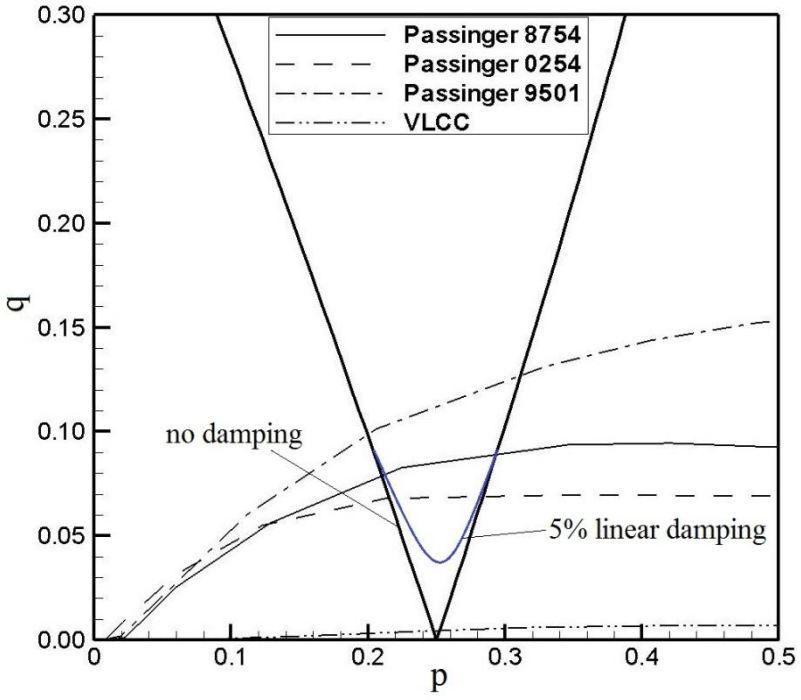


Figure 5. 9 1st level check for passenger ships and VLCC

### 5.2.2 2nd level (regular wave check)

2nd level check is carried out for reference waves shown in Table 4.2. Figure 5.10 to Figure 5.12 show the results for container ships, PCTCs, passenger ships and VLCC.

All container ships except S175 are judged to be vulnerable to parametric roll. The maximum roll angle is larger than 90 deg. Parametric roll never occurs for S175. All PCTCs are vulnerable to parametric roll but the maximum roll angle is smaller than 90 deg. It is because PCTC has a high free board and

enough reserve buoyancy. Passenger ships except Passenger 9051 are not vulnerable to parametric roll. If we determine the reference roll angle as 15 deg., all passenger ships except Passenger 9051 are not vulnerable. The $GM_1$ RAO of passenger ships is quite high but the wave energy or reference wave height is small. It means that small ships are less vulnerable to parametric roll than large ships. It can be confirmed for container ships. The $GM_1$ RAO of container ships are less or similar to that of passenger ships but they are judged to be vulnerable. As already expected, VLCC is never judged to be vulnerable.

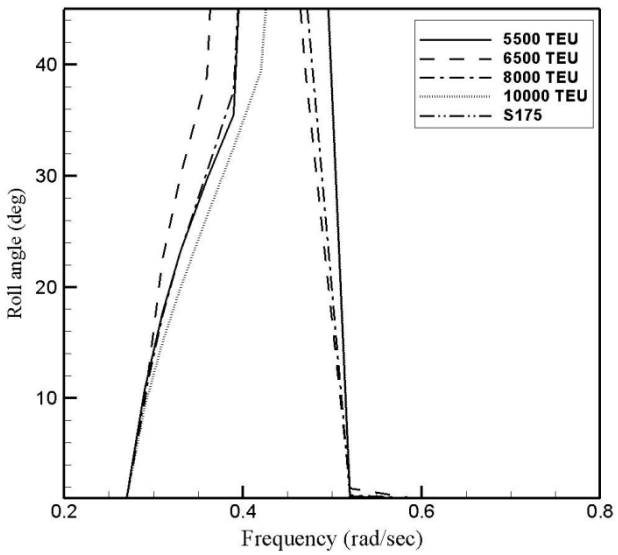


Figure 5. 10 2nd level check for container ships

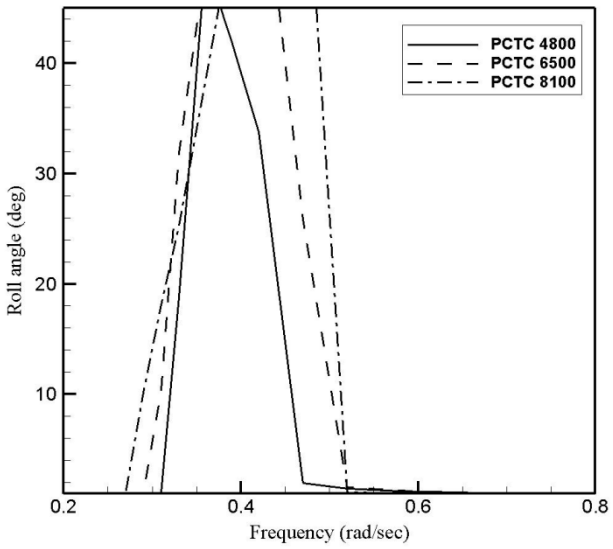


Figure 5. 11 2nd level check for PCTCs

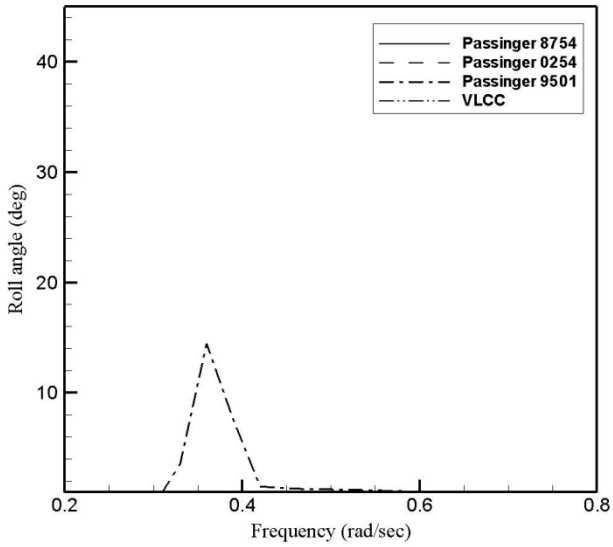


Figure 5. 12 2nd level check for passenger ships and VLCC

### 5.2.3 3rd level (Irregular wave check)

3rd level check is carried out considering all sea states of North Atlantic Sea shown in Table 4.1. Calculation conditions are as follows.

- Wave data : North Atlantic Sea
- Initial roll angle : 15 deg.
- Simulation time : 40 min, first 20 min cut off
- Simulation number : 1,000 times
- Still water GM : Minimum value. Maximum value, average value
- Ship speed : Zero speed, Maximum speed, Mean speed
- Heading angle, $\alpha$ : Head sea, Following sea

Figure 5.13 to Figure 5.15 show the results of 3rd level check. S 175 and VLCC are hardly vulnerable to parametric roll as already expected in 1st level check and 2nd level check. The PCTCs are most vulnerable because $GM_1$ RAO is highest and the modal frequency is near main energy zone. Container ships are also vulnerable but it is very difficult to grow up to 30 degrees.

All PCTCs and post-Panamax container ships are known to vulnerable to parametric roll. Therefore, the standard to identify vulnerability can be assigned using that information. If 20 degrees corresponding to $10^{-4.5}$ is assigned as standard, all PCTCs and post-Panamax container ships are judged

to be vulnerable. In case of passenger ships, Passenger 0254 and Passenger 9501 are not vulnerable and only Passenger 9501 is vulnerable to parametric roll.

When applying multi-level approaches to any kind of ships, keeping consistency is very important. If a ship is judged to be vulnerable to parametric roll by any level check, the ship should be judged to vulnerable in higher level check. While, if a ship is judged not to be vulnerable to parametric roll by any level check, the ship may be vulnerable in higher level check. This kind of consistency can be achieved by calibration of reference wave height or reference roll angle and corresponding probability level.

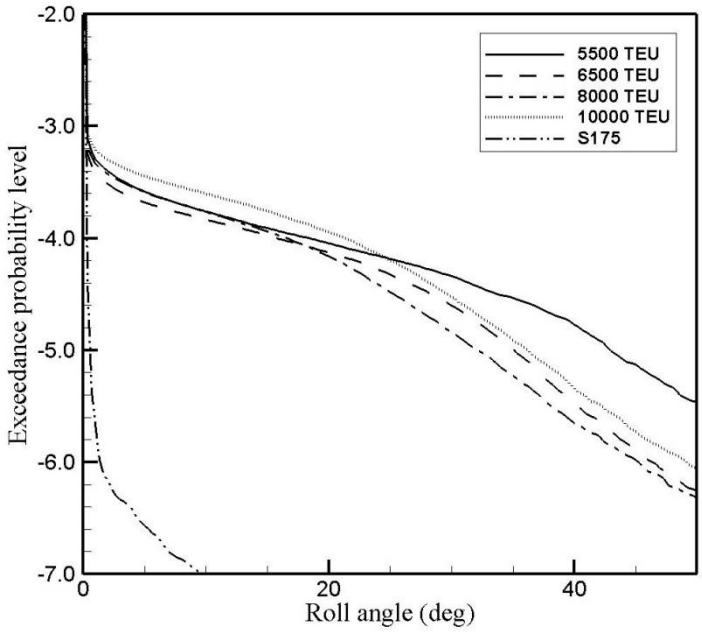


Figure 5. 13 3rd level check for container ships

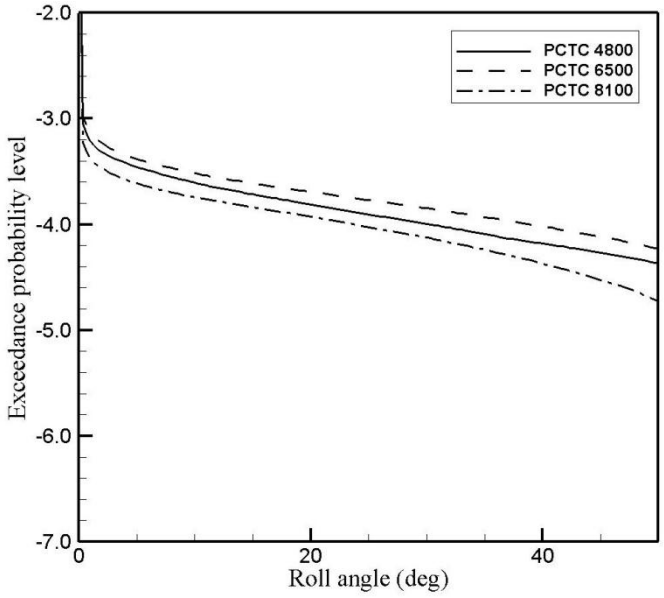


Figure 5. 14 3rd level check for PCTCs

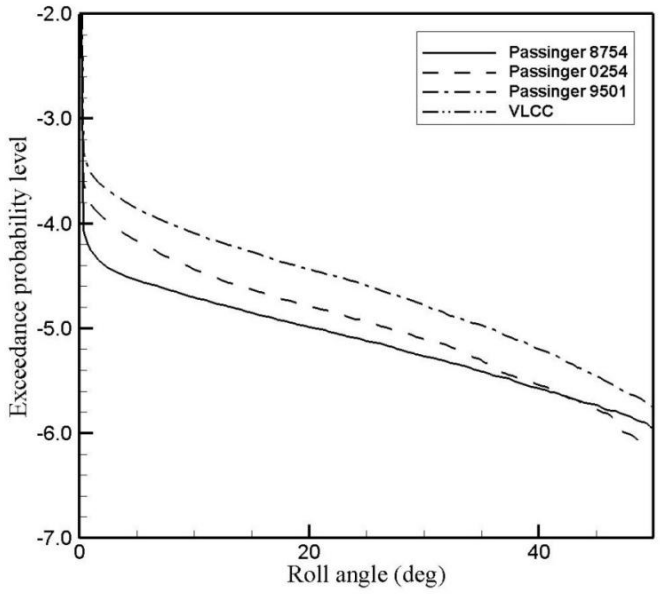


Figure 5. 15 3rd level check for passenger ships and VLCC

## 5.4 Operational Guidance for 8,800 TEU Container ships

The purpose of operational guidance is to help the crews to avoid severe roll motion induced by parametric roll. In this section, operational guidance for 8,000 TEU container ship is developed according to Section 4.

The ship crews may face harsh environmental condition which are expressed by significant wave height and mean zero crossing period for given loading condition or GM value. To avoid parametric roll, the ship crews can change heading angle and ship speed. Therefore, operational guidance should give roll angle for Hs, Tz and GM which are given, with respect to heading angle and ship speed which are controllable.

Based on Trim and Stability booklet, three GMs are chosen as calculation conditions which are 2.5m, 1.5m and 0.83m shown in Figure 5.16.

Three significant wave heights and five periods are considered as calculation condition. They are 6m, 7m, 8m for wave heights and 18 sec, 14 sec, 10 sec and 8sec for periods. The ship speeds from 0 knots to 10 knots are considered. Every 15 degree heading angles are considered. Table 5.3 shows summary of calculation condition for operational guidance.

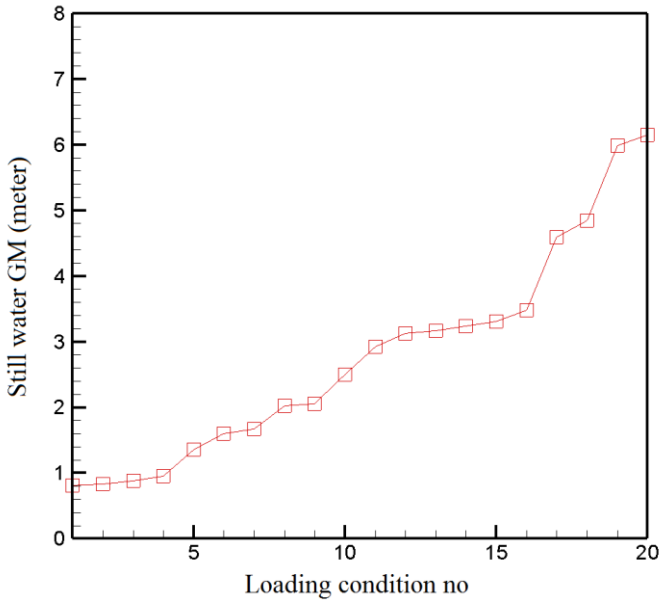


Figure 5. 16 Still water GM values in Trim and Stability booklet

Table 5. 3 Summary of Calculation condition

| Parameter | Value |
|---|---|
| Ship Type | 8,000 TEU Container carrier |
| Hs(m) | 6, 7, 8 |
| Heading (deg.) | 0 ~ 360 (15 increment) |
| Tz(sec) | 18, 14, 10, 8 |
| $\lambda_{modal} / L$ | 1.7, 1.0, 0.6, 0.33 |
| $GM$ (m) | 0.83, 1.5, 2.5 |
| Speed(knots) | 0 ~ 10(1.0 kts. increment) |

Figure 5.17 shows how to read occurrence map. It is expressed in polar coordinate where radius means ship speed and angle from center to downward means ship heading angle with respect to the wave direction. Therefore, inner circle is 0 kts. and outer circle is 10 kts., with 1 kts. increment between them. The downward direction means following sea and upward direction means head sea.

The red color means the roll angle more than 30 degrees may occur and blue color means parametric roll never occurs.

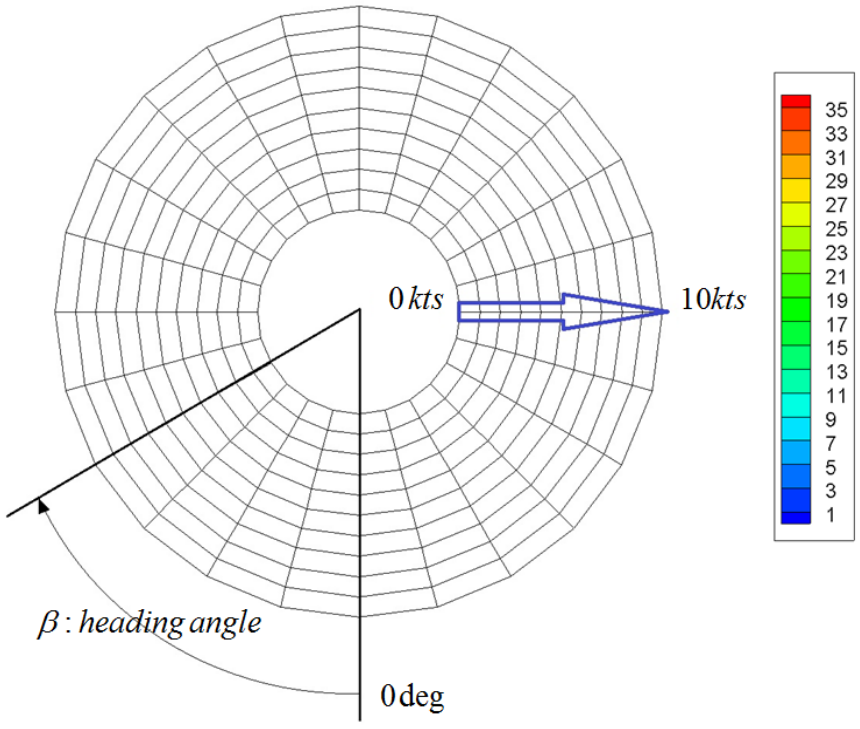


Figure 5. 17 Heading angle and speeds in polar diagram

From Section 5.4.1, 5.4.2 and 5.4.3 show the results for each GM and sea states

### 5.4.1 GM=2.5 m

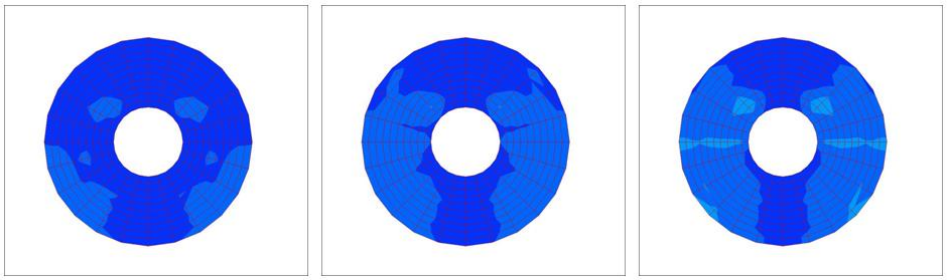

Figure 5.18 $\lambda_{modal} / L = 1.7$, T=18sec, Hs=6m, 7m, 8m

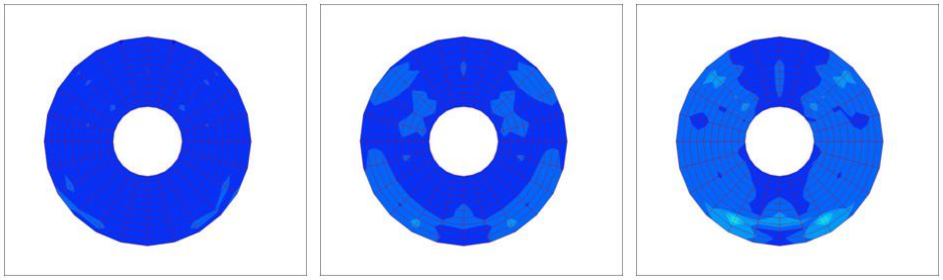

Figure 5. 19 $\lambda_{modal} / L = 1.0$, T=14sec, Hs=6m, 7m, 8m

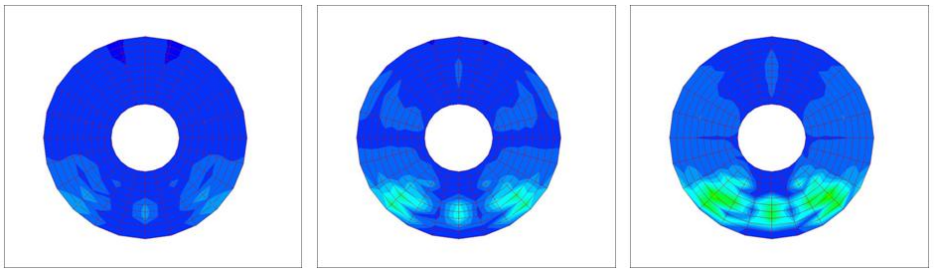

Figure 5.20 $\lambda_{modal} / L = 0.6$, T=10sec, Hs=6m, 7m, 8m

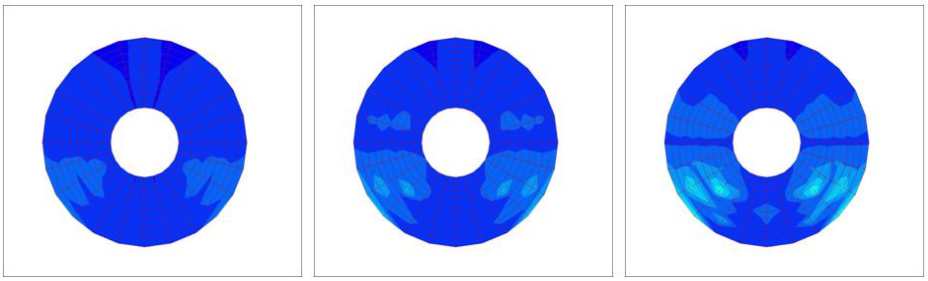

Figure 5.21 $\lambda_{modal} / L = 0.33$, T=8sec, Hs=6m, 7m, 8m

### 5.4.2 GM=1.5 m

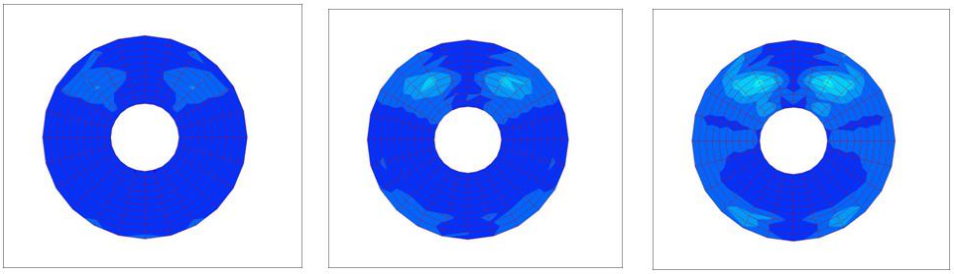

Figure 5.22 $\lambda_{modal} / L = 1.7$, T=18sec, Hs=6m, 7m, 8m

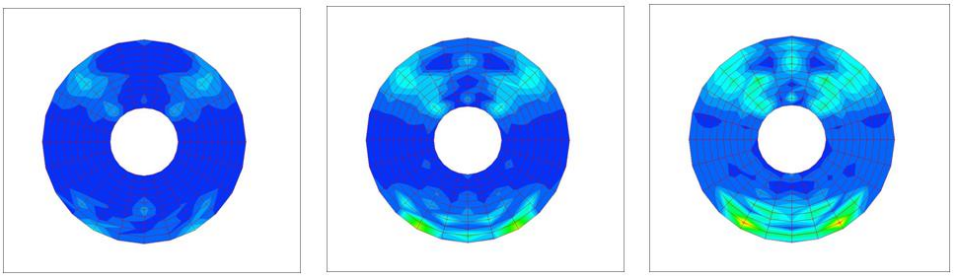

Figure 5.23 $\lambda_{modal} / L = 1.0$, T=14sec, Hs=6m, 7m, 8m

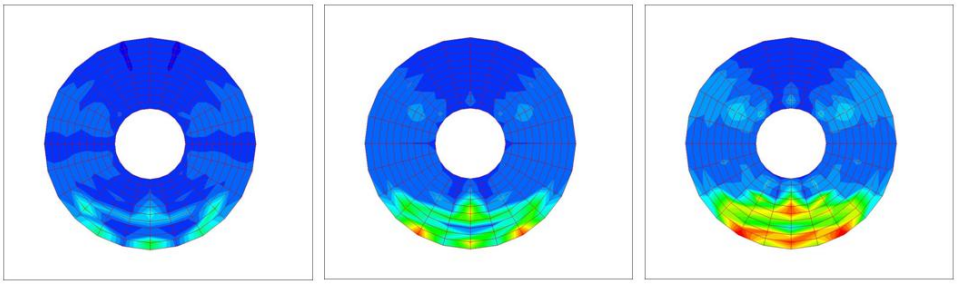

Figure 5.24 $\lambda_{modal} / L = 0.6$, T=10sec, Hs=6m, 7m, 8m

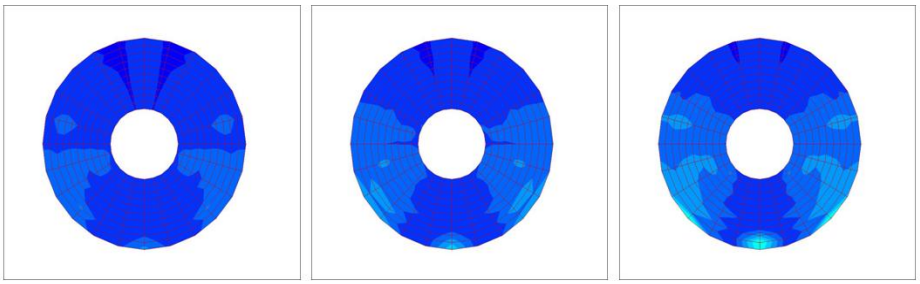

Figure 5.25 $\lambda_{modal} / L = 0.33$, T=8sec, Hs=6m, 7m, 8m

### 5.4.3 GM=0.83 m

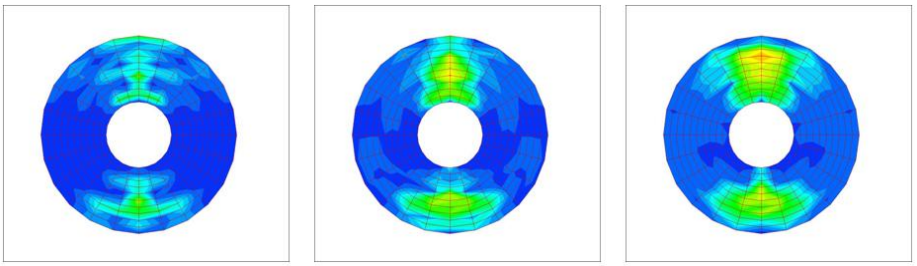

Figure 5.26 $\lambda_{modal} / L = 1.7$, T=18sec, Hs=6m, 7m, 8m

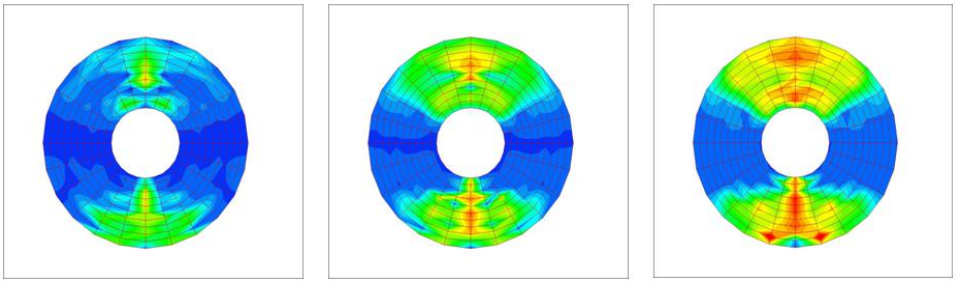

Figure 5.27 $\lambda_{modal} / L = 1.0$, T=14sec, Hs=6m, 7m, 8m

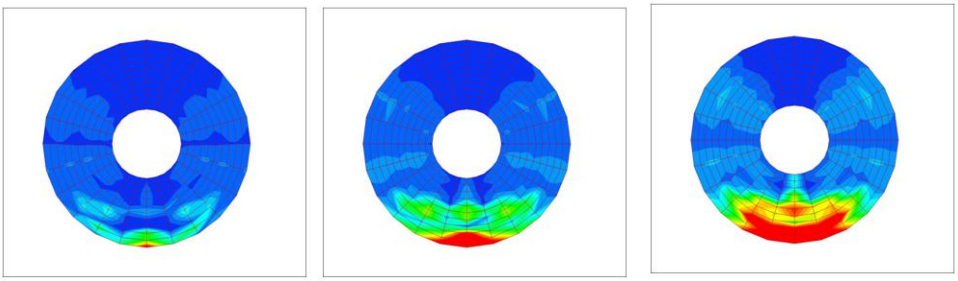

Figure 5.28 $\lambda_{modal} / L = 0.6$, T=10sec, Hs=6m, 7m, 8m

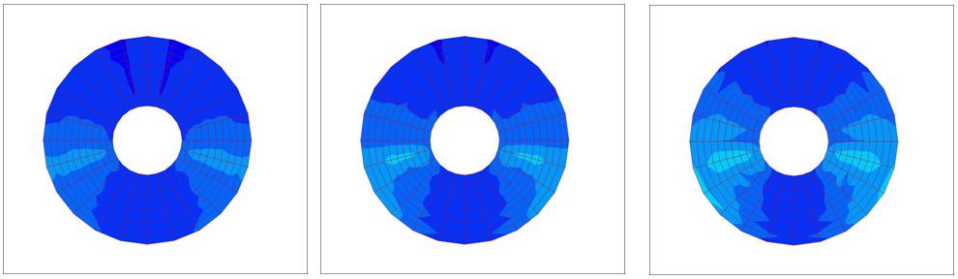

Figure 5.29 $\lambda_{modal} / L = 0.33$, T=8sec, Hs=6m, 7m, 8m

### 5.4.4 Review and summary of operational guidance

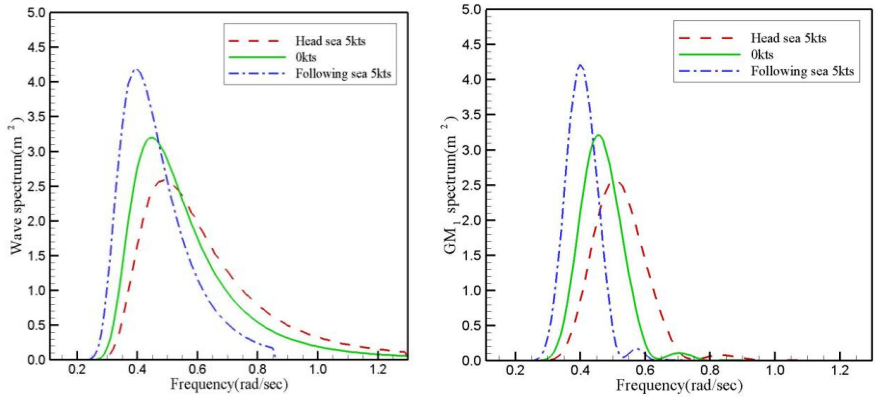


(a) Wave spectrum (b) response spectrum

Figure 5.30 Wave and response spectrum at $\lambda_{modal} / L = 1.0$, Hs=8m

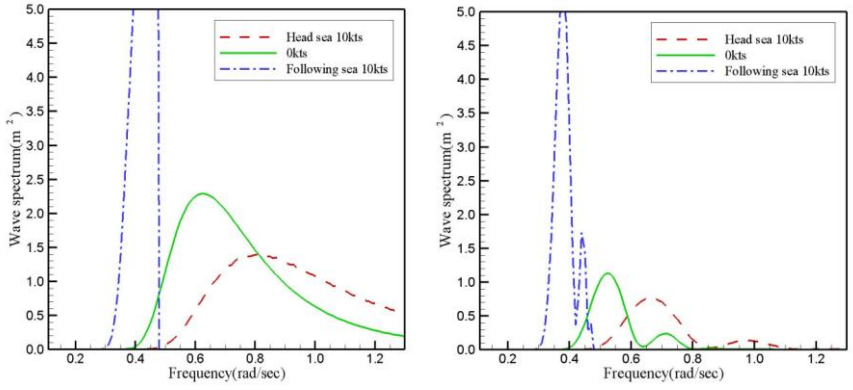


(a) Wave spectrum (b) response spectrum

Figure 5.31 Wave and response spectrum at $\lambda_{modal} / L = 0.6$, Hs=8m

In case of $\lambda_{modal} / L = 1.0$, parametric roll occurs all range of speeds as shown Figure 5.27. The response spectrum shown in Figure 5.30 has some amount of energy to generate parametric roll near the resonance frequency because the wave spectrums are large at the frequency and RAO of $GM_1$ is normally maximized if the wave length is equal to the ship length. Stern quartering sea (15 deg.) gives a peak value because the encountering frequency is shifted to the resonance frequency by combination of speed and wave heading angle. .

In case of $\lambda_{modal} / L = 0.6$, parametric roll occurs in only following sea over 5 kts. as shown in Figure 5.28. When the ship speed is near 10 kts., the wave energy shown in Figure 5.31 is concentrated on narrow band near the resonance frequency and the response spectrum of $GM_1$ is also maximized near the frequency.

In other hand, when the ship speed is 0kts. and 10 kts. in head sea, the wave spectrums are widely spread and the response spectrum is normally so low that parametric roll never occurs.

Normally the GM of container ships are kept about 1m ~ 2m to avoid synchronized roll by increase the natural roll frequency extremely long out of the main wave energy zone. The GM is 0.83m in this analysis and parametric roll is dominant source. If GM is quite large about 4m above, the

discrimination of parametric roll and synchronized Roll may be difficult. In this case, IPR(Index of Parametric Roll) proposed by Hong [20] can be useful.

The summary of operational guidance are as follows based on above calculation results

A. If GM is over 2.5 meter, parametric roll never occurs.

B. If GM is between 1.5 and 2.0, parametric roll parametric roll hardly occurs except wave period 10 sec (wave length is between 0.5L and 0.7L) in following sea. If the ship runs in following sea, the encounter wave spectrum gets narrow banded. When the modal period of this narrow banded spectrum is almost same as resonance period, parametric roll occur very severely.

C. If GM is between 0.8 and 1.5, it's safe in small wave height less than 6m or in short wave less than 8 sec or in long wave larger than 25 sec.

It's danger in both of following sea and head sea when the wave height is larger than 7m and wave period is near 14 sec(wave length is near L). In this case, the ship heading should be changed to oblique wave such as 30 deg. or more.

It's very danger in following sea when the wave height is larger than 7m and wave period is near 10 sec and ship speed is larger than 5 knots.

Table 5.4 shows dangerous situations which should be avoided and proper guidance for each situation. The most important thing the operators keep in mind is that the ship heading of head or following sea should be avoided in

low GM and rough sea. However, if the GM is larger than 2.5 meter, the ship heading should be kept in head sea, not beam sea to decrease the roll angle.
In urgent situation, ship crews have not enough time to make proper decision based on above huge information. Therefore following easy instruction can be useful.

**Parametric roll is a very rare event. It happens only in very rough sea (Hs>7m, Max Wave Height>14m).**

**However, if you meet Rough Sea in Low** *GM*

**Avoid [following waves with speed] definitely!!**

**Avoid [head waves]!!**

**Try to keep your heading to oblique sea (more than 30 deg.) or beam sea!!**

**Turn your ship slowly!!**

**If you meet Rough Sea in High** *GM* **more than 2.5m**

**Try to keep your heading to head sea!!**

Table 5. 4 Dangerous situations which are to be avoided

| Degree of danger | Condition | | Guidance |
|---|---|---|---|
| Most danger | GM | 0.8 ~ 1.0 | Best : Heading angle should be changed into oblique sea or beam sea smoothly Alternative : Speed down |
| | Environmental condition | rough sea(Hs>7m) | |
| | Wave period | about 10 sec | |
| | Wave length | about 160 m | |
| | Heading angle | following sea | |
| | Ship Speed | more than 5 kts. | |
| Danger 1 | GM | 0.8 ~ 1.0 | Best : Heading angle should be changed into oblique sea or beam sea smoothly |
| | Environmental condition | rough sea(Hs>7m) | |
| | Wave period | about 14 sec | |
| | Wave length | about 280 m | |
| | Heading angle | following sea head sea | |
| | Ship Speed | All speeds | |
| Danger 2 | GM | 1.0 ~ 2.0 | Best : Heading angle should be changed into oblique sea or beam sea smoothly Alternative : Speed down |
| | Environmental condition | rough sea(Hs>7m) | |
| | Wave period | about 10 sec | |
| | Wave length | about 160 m | |
| | Heading angle | following sea | |
| | Ship Speed | more than 5 kts. | |

# Chapter 6. Conclusions

In this study, a multi-level approach for the evaluation of parametric roll is developed and this approach is applied to modern commercial ships. For this purpose, physical and stochastic characteristics of parametric roll are investigated and theoretical backgrounds of each level are introduced. The application to modern ships is carried out and the results are provided for the purpose of ship design or ship operation. Based on what has been discussed, conclusions can be drawn as follows.

- Parametric roll is generated by self excitement induced by restoring moment change in head or following sea. It occurs when the wave period is half of natural roll period and the exciting energy is large enough to overcome energy loss by roll damping. It happens in modern container ships, PCTCs and passenger ships of which shape is nonlinear such as transom stern, large flare angle, etc.
- If the condition of parametric roll is satisfied, it is triggered by small disturbance and starts to grow up to steady state, when the energy gain from restoring moment change is balanced with energy loss. Steady state roll angle is independent from initial angle but large initial angle shortens the time to reach steady state. Roll damping doesn't take a critical roll to determine steady state roll because the energy is accumulated to the steady

state even if the energy gain is very small due to large roll damping. It means roll damping governs increasing rate but steady state roll angle.

- $GM$ fluctuation is induced by change of water plane area when the wave crest passes along the ship length. It can be expressed by Fourier series. The mean value of $GM$ fluctuation is always larger than still water $GM$ because the average of water plane area in wave is larger than that of still water condition. The first component of GM fluctuation is maximized when the wave length is 80% of ship length in case of container ships.
- $GM_0$ and $GM_1$ can be assumed to be linear to wave height practically and it is proved for container ships of which geometrical nonlinearlity is severe. This assumption can be useful to make simplified numerical formulation.
- Parametric roll is a highly non-ergodic process and conventional statistical approach is not valid because each realization gives different mean and variance for same irregular sea state. The occurrence of parametric roll is governed by response spectrum of RAO of $GM_0$ and $GM_1$.
- To get a stable probability density function of parametric roll, the only possible way is to collect enough sample data from huge number of numerical tests by Monte-Carlo simulation. More realizations give more stable prediction and the number of realizations is determined by confidence level and error bound of variance of variance.

- To quantify the vulnerability to parametric roll, 1.5-DOF roll motion equation is newly developed. It is based on assumption of linearity of $GM_0$ and $GM_1$. The GZ curve in wave is approximated by GZ variation and still water GZ curve from the observation of real physics. This approximation is compared to current ones in IMO and well proved to give quite good prediction. Using 1.5-DOF roll equation, huge number of numerical simulation can be carried out in practical time. The theoretical backgrounds of Mathieu equation, IRF method and Rankine panel method are also introduced.
- Based on above study, a multi-level approach is developed. It consist of resonance check by Mathieu equation ($1^{st}$ level check), regular wave check by 1.5-DOF roll equation($2^{nd}$ level check), irregular wave check($3^{rd}$ level check) and operational guidance by IRF method. Procedure to get environmental conditions for each level are developed and proposed for North Atlantic Sea. The present method is compared to ABS Guidance that it is more efficient and accurate than the guidance.
- The multi-level approach is applied to modern commercial ships such as 4 post-Panamax container ships, 3 PCTCs, 3 passenger ships which are known vulnerable to parametric roll and is applied to VLCC and S175 which are far from this phenomenon for reference. VLCC and S175 are judged not to be vulnerable to parametric roll in $1^{st}$ level check. Two

passenger ships, VLCC and S175 are judged not to be vulnerable in 2nd level check. In 3rd level, the vulnerability of all ships are evaluated quantitatively and the results are well consistent to the lower levels.

- The operational guidance for 8,000 TEU container ships is developed by IRF method. It is provided for ship crews to avoid severe parametric roll. Polar diagrams with respect to ship's speed and heading are provided for loading conditions and sea states because the formers are controllable and the later are given. Based on huge calculation, the summary and easy instruction is provided to help the ship crews to make decision effectively in harsh environmental conditions.

# Chapter 7. Discussions

Muti-level approach to evaluate the vulnerability to parametric roll is developed and it is applied current commercial ships. The remained issues are discussed in this chapter to be considered for the further study.

- The linearity of $GM_1$ should be theoretically investigated. It seems very hard to prove this linearity because it comes from real ship shape. However, it can be done through the simplification of ship shape. In same manner, the linearity or nonlinearity of $GM_0$ is expected to be proved. In this thesis, the linearity is proved in numerical way.
- More applications are to be carried out for small container ships, larger passenger ships naval ships and fishing vessels. Some naval ships with tumble home should be concerned because it will have opposite characteristics to normal ships.
- The standard to judge the vulnerability should be assigned based on statistics of real casualties. The consistency of each level should be achieved based on the results of more application and calibration of the standard.

- The results of this study have been reflected in IMO 2nd generation of intact stability criteria. More discussion should be done in IMO and the outcome of this study is expected to contribute to the ship design and operational guidance to improve the safety of the ship against this very dangerous phenomenon

# Bibliography

[1] American Bureau of Shipping : 2004, Guide for the Assessment of Parametric Roll Resonance in the Design of Container Carriers

[2] Reed AM., 26th ITTC Parametric Roll Benchmark Study, *Proceeding of the 12th International Workshop on Ship Stability and Operational Safety*, Washington DC., USA, 2011

[3] Ballard, EJ., Hudson, DA., Price, WG., et al. Time domain simulation of symmetric ship motions in waves, *Transactions of the Royal Institution of Naval Architects 2003, Part A: International Journal of Maritime Engineering*, 145 (A2), 89-103

[4] Belenky, VL. and Campbell B., Assessment of Short-Term Risk with Monte-Carlo Method, *Proceeding of the 11th International Workshop on Ship Stability and Operational Safety*, Wageningen, Netherlands, 2010

[5] Belenky, V.L, Degtyarev, AB., Boukhanovsky, AV., Probabilistic qualities of nonlinear stochastic rolling. *Ocean Engineering* 1998, 25(1), 1-25

[6] Belenky, VL., Suzuki, S. and Yamakoshi, Y. Preliminary results of experimental validation of practical non ergodicity of large amplitude roll motion, *Proceeding of the 5th International Workshop on Ship Stability and Operational Safety*, Trieste, Italy, 2001

[7] Belenky, VL. and Weems, KM., On the Distribution of Parametric Roll, *Proceeding of the 12th International Workshop on Ship Stability and Operational Safety*, Washington DC., USA, 2011

[8] Belenky, VL., Weems, KM., Pauling, JR. Probabilistic analysis of roll parametric resonance in head seas, *Proceeding of the 8th International Workshop on Ship Stability and Operational Safety*, Madrid, Spain, 2003

[9] Bulian, G. and Francescutto, A., Considerations on Parametric Roll and Dead Ship Conditions for the Development of Second Generation Intact Stability Criteria, *Proceeding of the 12th International Workshop on Ship Stability and Operational Safety*, Washington DC., USA, 2011

[10] Bulian, G., Francescutto, A. and Lugni, C. Theoretical, numerical and experimental study on the problem of ergodicity and 'practical ergodicity' with an application to parametric roll in longitudinal long crested irregular sea, *Ocean Engineering* 2006, 33, 1007-1043

[11] Bulian, G., Nonlinear parametric rolling in regular waves-a general procedure for the analytical approximation of the GZ curve and its use in time domain simulations, *Ocean Engineering* 2005, 309-330

[12] Cummins, WE. The impulse response function and ship motions, *Schiffstechnik* 1962, 47(9), 101-109

[13] Dunwoody, AB. Roll of a ship in astern Seas – Metacentric height spectra, *Journal of Ship Research* 1989, 33(3), 221-228

[14] Dunwoody, AB. Roll of a ship in astern Seas – Response to GM fluctuations, *Journal of Ship Research* 1989, 33(3), 284-290

[15] Fonseca, N. and Guedes Soares, C. Time-domain analysis of large-amplitude vertical ship motions and wave loads. *Journal of Ship Research* 1998, 42(2), 139-153

[16] France, WM., Levadou, M., Treakle, et al. An Investigation of Head-parametric rolling and its Influence on Container Lashing Systems, *Marine Technology* 2003, 40(1), 1-19

[17] Froude, W., Remarks on Mr. Scott-Russell's Paper on Rolling, *The Papers of William Froude*, Institution of Naval Architects, 1955

[18] Holden, C. Nonlinear Container Ship Model for the Study of Parametric Roll Resonance, *Modeling, Identification and Control* 2007, 28(4), 87-103

[19] Hong, SY., Nam, BW. and Yu HC., Investigation of Susceptibility of Parametric Roll in Regular and Irregular Waves, *Proceeding of the 12th International Workshop on Ship Stability and Operational Safety*, Washington DC., USA, 2011

[20] Hong, SY., Yu HC., Kim SE. and Sung HG., Investigation of Parametric Roll of a Container Ship in Irregular Seas by Numerical Simulation, *Proceeding of the 10th International Conference on Ships and Ocean Vehicles*, St. Petersburg, Russia, 2009

[21] IACS Recommendation 34: 2001. Standard Wave Data

[22] Ikeda, Y, et, al. Prediction methods for parametric rolling under drifting condition and their validation, *Report of SCAPE committee*, 2010

[23] IMO, SLF/52/INF.2 : 2010, Development of New Generation Intact Stability Criteria – Information collected by Correspondence Group

[24] IMO, SLF/53/INF.10 : 2011, Development of New Generation Intact Stability Criteria – Information collected by Correspondence Group

[25] IMO, SLF/54/INF.12 : 2012, Development of New Generation Intact Stability Criteria – Information collected by Correspondence Group

[26] IMO, SLF/52/WP.1 : 2010, Development of New Generation Intact Stability Criteria – Report of Working Group

[27] IMO, SLF/53/WP.1 : 2011, Development of New Generation Intact Stability Criteria – Report of Working Group

[28] IMO, SLF/53/WP.1 : 2012, Development of New Generation Intact Stability Criteria – Report of Working Group

[29] Jensen JJ., Efficient estimation of extreme non-linear roll motions using the first-order reliability method (FORM), *Journal of Marine Science and Technology*, 12, 191-202

[30] Katayama T., Miyamoto S., and Hashimoto H., An experimental study on characteristics of rolling in head waves for a vessel with non-linear GZ curve, *Proceedings of 11th International Workshop on Ship Stability*, September 2012, Athens, Greece

[31] Kim, YH. Time-domain analysis of nonlinear motion responses and structural loads on ships and offshore structures: development of WISH programs, *International Journal of Naval Architecture and Ocean Engineering* 2011, 3(1), 37-52

[32] Kim, TY. And Kim YH., Multi-level Approach of Parametric Roll Analysis, *ITTC*2010, Seoul, Korea

[33] Nayfeh, AH., Mook, DT, Nonlinear Oscillations, 1979, Wiley, New York

[34] Neves, MAS. On the excitation of combination modes associated with parametric resonance in waves, *Proceedings of 6th International Workshop on Ship Stability*, October 2002, Webb Institute, New York.

[35] Neves, MAS., Pe´rez, NA. and Lorca, OM. Experimental analysis of parametric resonance for two fishing vessels in head sea, *Proceedings of 6th International Workshop on Ship Stability*, October 2002, Webb Institute, New York.

[36] Oh, IG., Nayfeh, AH. and Mook, DT. A theoretical and experimental investigation of indirectly excited roll motion in ships, *Phil. Trans. R. Soc* 2002, 358, 1853–1881.

[37] Paulling, JR. and Rosenberg, RM. On Unstable Ship motions Resulting from Nonlinear Coupling, *Journal of Ship Research* 1959, 3, 36-46

[38] Ribeiro e Silva, S., Santos, TA., and Guedes Soares, C. Parametrically excited roll in regular and irregular head seas, *International Shipbuilding Progress* 2005, 52(1), 139-153

[39] Roberts, JB., Effect of parametric roll excitation of nonlinear rolling motion in random seas, Journal of Ship Research 1982, 26, 246-253

[40] Shin, YS., Belenky, VL., Paulling, JR. et al. Criteria for parametric roll of large container ships in head seas, *Transactions of SNAME* 2004, 112, 14-47

[41] Spanos, D. Numerical simulation of parametric roll in head seas, *International Shipbuilding Progress* 2007, 54, 249-267

[42] Umeda, N. Nonlinear dynamics on parametric roll resonance with realistic numerical modeling. *International Shipbuilding Progress* 2004, 51, 205-220

[43] Umeda, N. Recent developments of Theoretical prediction on capsizes of intact ships in waves, *Proceedings of 8$^{th}$ International Workshop on Ship Stability*, October 2005, Turkey, Istanbul.

[44] Umeda, N. and Hashimoto, H. An investigation of different methods for the prevention of parametric rolling, *Journal of Marine Science and Technology* 2008, 13

[45] Shigunov V., Themelis N. and Spyrou KJ., Critical wave groups vs. direct Monte-Carlo simulations for typical stability failure modes of a container ship, *Proceedings of 11th International Workshop on Ship Stability*, September 2012, Athens, Greece

[46] Vidic-Perunovic, J. Influence of the GZ calculation method on parametric roll prediction, *Ocean Engineering* 2011, 38, 295-303.

[47] Vidic-Perunovic, J., Jensen, J., Parametric roll due to hull instantaneous volume changes and speed variations, *Ocean Engineering* 2009, 36, 891-899

# 초 록

본 논문은 파라메트릭 롤에 대응하기 위한 해석, 평가, 운항지침 개발 등 선박 설계에서부터 운항에 이르기 까지 조선소 및 선사에서 필요한 실제적인 기술 개발 및 적용 결과를 다루고 있다.

파라메트릭 롤에 대한 과거의 수 많은 연구에도 불구하고, 대양을 항행하는 선박에 대하여 이 현상의 발생 가능성을 정량적으로 예측하는 것은 매우 어려운 실정이다. 따라서 본 논문에서는 파라메트릭 롤의 물리적 통계적 특성을 깊이 있게 고찰하고 이를 바탕으로 불규칙 해상에서 정량적으로 예측할 수 있는 새로운 수치 모델을 개발하였다.

파라메트릭 롤의 non-ergodic 한 특성으로 인하여 안정적인 장기 확률분포를 구하기 위해서는 가능한 한 많은 수의 수치 시뮬레이션이 필요하다. 이를 위해 근사 GZ 곡선을 사용한 1.5 자유도 GM-GZ 수치모델이 개발하였다. 이 모델에서는 GM 의 전달함수라는 개념을 도입하여 평균값 및 1 차 하모닉 성분을 이용함으로써 GM 값을 구하였으며 계산된 GM 과 정수 중 GZ 곡선으로 파랑중 GZ 곡선을 근사하였다. 이 수치모델 계산 결과는 3 차원 비선형 퍼텐셜 프로그램과의 비교를 통하여

검증하였다. 개발된 수치모델을 통해 몬테카를로 시뮬레이션을 수행함으로써 장기 확률 분포를 구하였으며 가장 적절한 초기값, 해석 시간 및 시뮬레이션 횟수 등을 제안하였다.

또한 본 논문에서는 파라멕트릭 롤을 해석하기 위한 다양한 수치모델 즉 가장 단순한 매튜 방정식으로부터 IRF 기법 및 Rankine Panel 방법 등 가장 진보된 수치해석 툴을 소개 하고 본 논문에서 새롭게 개발된 1.5 자유도 GM-GZ 수치모델을 포함하여 파라메트릭 롤을 평가하기 위한 단계별 해석방법을 개발하였다. 본 방법은 1 단계 매튜 방정식에 의한 공진체크, 2 단계 1.5 자유도 GM-GZ 수치모델에 의한 규칙파 해석, 3 단계 1.5 자유도 GM-GZ 수치모델에 의한 불규칙파 해석 및 4 단계 최신 수치해석 툴을 이용한 운항지침 개발로 구성되어 있다.

개발된 단계별 해석방법은 4 척의 대형 컨테이너선, 3 척의 자동차 운반선, 3 척의 여객선, 1 척의 초대형 유조선 및 S175 컨테이너선에 대하여 북대서양 항해 기준으로 파라메트릭 롤을 해석하였다. 실선적용 결과를 통하여 본 논문에서 제시하는 단계별 해석 방법은 일관되고 효과적으로 파라메트릭 롤을 평가하며 각 선종 및 길이별로 이 현상의 발현 확률을 명확히 정량적으로 구분할 수 있음을 보여 주었다.

어떤 선박이 단계별 해석방법을 통하여 파라메트릭 롤에 의해 심각한 피해를 입을 수가 있다고 판단된다면 선원의 판단을 지원할 수 있는 운항지침 개발이 필수적이다. 본 논문에서는 IRF 방법을 통한 운항지침 개발방법을 제안하였으며 제안된 방법에 따라 8,000TEU 컨테이너에 대한 해석을 수행하였다. 모든 해석 결과는 본 논문에 포함되어 있으며 선원이 효과적인 판단을 통하여 파라메트릭 롤을 회피하기 위하여 간략화한 안내서 예제를 제공하였다.

**주요어: 파라메트릭 롤, 단계별 해석 방법, 정량적 해석, 1.5 자유도 GM-GZ 수치 모델, 2세대 비손상 복원성 기준, 운항지침**

**학 번:** 2006-30809